Coordination Chemistry Reviews 555 (2026) 217604

Contents lists available at ScienceDirect

Coordination Chemistry Reviews

journal homepage: www.elsevier.com/locate/ccr

Unveiling the versatility and reactivity of N-heterocyclic carbene complexes with metal and non-metal fluorides: a comprehensive review☆

Evelin Gruden, Gašper Tavčar *

Jožef Stefan Institute, Jamova cesta 39, 1000 Ljubljana, Slovenia

ARTICLE INFO

Dedicated to Professor Resnati, celebrating a career in chemical bonds on the occasion of his 70th birthday.

Keywords:
N-heterocyclic carbenes
Metal fluorides
Main-group fluorides
Coordination compounds
Cyclic alkyl(amino)carbenes
Crystal structures

ABSTRACT

N-Heterocyclic carbenes (NHCs) have become cornerstone ligands in modern coordination and main-group chemistry, yet their interactions with metal and non-metal fluorides have long remained underexplored because many fluorides are poorly soluble and often difficult to handle. This review surveys the synthesis, structures, and reactivity of all structurally characterized NHC complexes and adducts containing the NHC-M-F fragment reported from the advent of isolable NHCs (1991) through mid-2025. Across 33 elements spanning the s-, p-, d-, and f-blocks, we compile 458 reported compounds, including 277 crystallographically authenticated species, and organize the field by element group and oxidation state. Emphasis is placed on practical synthetic entry points: direct coordination to soluble fluoride sources, transmetalation and synthon strategies, dehydrofluorination routes from fluoride salts, fluorination of pre-formed halide, hydride, or organo precursors, and redox-driven fluoride formation. We highlight how ligand sterics and electronics (including CAAC and related carbenes) govern stability and speciation. Comparative analysis of NHC–M and M–F metrics, typical geometries, and ^{19}F NMR ranges reveals periodic trends and recurring structural motifs, providing a unified reference framework for designing new NHC-stabilized fluoride compounds and leveraging their distinctive reactivity.

1. Introduction

Since the discovery, isolation, and characterization of the first "bottleable" NHC carbene in 1991 [1], carbene chemistry has expanded tremendously, quickly becoming indispensable in various research areas and applications. In main group and transition metal chemistry, NHCs have become popular ligands due to their strong donor ability. Historically, NHCs were considered phosphine mimics, as both are monodentate two-electron ligands [2]. In many cases, the geometries of donor-acceptor complexes with phosphines and NHCs exhibit similar

Abbreviations: 6-Dipp, 1,3-bis(2,6-diisopropylphenyl)-3,4,5,6-tetrahydropyrimidin-2-ylidene; 6-^{i}Pr, 1,3-bis(isopropyl)-3,4,5,6-tetrahydropyrimidin-2-ylidene; 6-Mes, 1,3-bis(2,4,6-trimethylphenyl)-3,4,5,6-tetrahydropyrimidin-2-ylidene; 7-Dipp, 1,3-bis(2,6-diisopropylphenyl)-4,5,6,7-tetrahydro-1,3-diazepin-2-ylidene; aIDipp, 1,3-bis-(2,6-di-iso-propylphenyl)-imidazol-4-ylidene; aIMe, 1,3-dimethyl-imidazol-4-ylidene; aI^{t}Bu, 1,3-di-*tert*-butyl-imidazol-4-ylidene; BICAAC, Bicyclic (alkyl)(amino)carbene; CAAC, Cyclic (alkyl)(amino)carbene; ^{Cl2}IDipp, 4,5-dichloro-1,3-bis-(2,6-di-iso-propylphenyl)-imidazolin-2-ylidene; ^{Cl2}IMes, 4,5-dichloro-1,3-bis-(2,4,6-trimethylphenyl)-imidazolin-2-ylidene; ^{Cl2}I^{t}Bu, 4,5-dichloro-1,3-di-tert-butyl-imidazolin-2-ylidene; cod, 1,5-cyclooctadiene; Cp, Cyclopentadienyl; Cp*, Pentamethylcyclopentadienyl; Cy, Cyclohexyl; DAC, *N,N'*-Diaminocarbene; DCM, Dichloromethane; DMAP, 4-(Dimethylamino)pyridine; DMF, Dimethylformamide; dppp, 1,3-Bis(diphenylphosphino)propane; ICy, 1,3-dicyclohexylimidazol-2-ylidene; IDD, 1,3-dicyclododecylimidazol-2-ylidene; IDipp, 1,3-bis-(2,6-di-iso-propylphenyl)-imidazol-2-ylidene; I^{i}Pr, 1,3-di-iso-propyl-imidazol-2-ylidene; I^{i}PrMe, 1-iso-propyl-3-methyl-imidazol-2-ylidene; IMe, 1,3-dimethyl-imidazol-2-ylidene; IMes, 1,3-bis-(2,4,6-trimethylphenyl)-imidazol-2-ylidene; I^{n}Pr, 1,3-di-*n*-propyl-imidazol-2-ylidene; I^{t}Bu, 1,3-di-*tert*-butyl-imidazol-2-ylidene; I^{t}BuMe, 1-*tert*-butyl-3-methyl-imidazol-2-ylidene; KHMDS, Potassium bis(trimethylsilyl)amide; LDA, Lithium diisopropylamide; LiHMDS, Lithium bis(trimethylsilyl)amide; ^{Me2}IEtMe, 1-ethyl-3,4,5-trimethyl-imidazol-2-ylidene; ^{Me2}I^{i}Pr, 1,3-di-*iso*-propyl-4,5-dimethyl-imidazol-2-ylidene; ^{Me2}IMe, 1,3,4,5-tetramethyl-imidazol-2-ylidene; ^{Me2}I^{n}Pr, 1,3-di-*n*-propyl-4,5-dimethyl-imidazol-2-ylidene; ^{Me2}I^{t}Bu, 1,3-di-*tert*-butyl-4,5-dimethyl-imidazol-2-ylidene; ^{Me}CAAC, 1-(2,6-di-*iso*-propylphenyl)-3,3,5,5-tetramethyl-pyrrolidin-2-ylidene; MeCN, Acetonitrile; Mes, Mesitylene; NHC, N-heterocyclic carbene; NFSI, N-Fluorobenzenesulfonimide; pin, Pinacolato; py, Pyridine; Selectfluor, 1-chloromethyl-4-fluoro-1,4-diazonia-bicyclo[2.2.2]octane bis(tetrafluoroborate); SIDipp, 1,3-bis-(2,6-di-*iso*-propylphenyl)-imidazolidin-2-ylidene; SIMe, 1,3-dimethyl-imidazolidin-2-ylidene; SIMes, 1,3-bis-(2,4,6-trimethylphenyl)-imidazolidin-2-ylidene; TBAF, Tetrabutylammonium fluoride; THF, Tetrahydrofuran; TMAF, Tetramethylammonium fluoride; tmen, *N,N,N',N'*-Tetramethylethane-1,2-diamine; TMS, Tetramethylsilane.

☆ This article is part of a Special issue entitled: 'Chemical Bonds' published in Coordination Chemistry Reviews.

* Corresponding author.
E-mail address: gasper.tavcar@ijs.si (G. Tavčar).

https://doi.org/10.1016/j.ccr.2026.217604
Received 29 October 2025; Received in revised form 2 January 2026; Accepted 13 January 2026
Available online 31 January 2026

features, with some exceptions attributed to differences in ligand donor strength [3]. Among these, NHCs are typically considered much stronger net donors [2,4]. Quantum chemical calculations on SiF_4 and $SiCl_4$ have suggested that NHC complexes are more stable than those with amines and phosphines [5]. This was also confirmed experimentally by the stabilization of penta- and octacoordinated SiF_4 with NHCs, while identification of phosphine or thioether counterparts was unsuccessful [6]. Compared with hard N- or O- donor ligands, NHCs, phosphines, and thioethers form softer donor-acceptor adducts with high oxidation state d- and p-block fluorides [7]. Nevertheless, NHC chemistry has developed into a useful and complex field distinct from other ligands. A major advantage of using NHCs is the easy modification of their steric and electronic properties through simple variations of the starting materials [4].

By definition, NHCs are neutral heterocyclic compounds that contain at least one nitrogen atom within the heterocyclic ring and a divalent carbon atom with only six electrons in its valence shell. Because the ring size, functionalization, and number of nitrogen atoms are not specified, many different NHC classes exist within these criteria, each with distinct properties [4]. Their synthesis, structure, and electronic properties have been extensively studied and reviewed [4,8–14]. The most common classes of NHCs discussed in this review are shown in **Fig. 1**. They are derived from imidazole (NHC and aNHC), imidazoline (SNHC), and pyrrolidine (CAAC). Other classes are also becoming increasingly popular.

Strongly donating ligands, such as CAACs, are now being extensively studied. The presence of a quaternary carbon in the position α to the carbene center distinguishes CAACs from NHCs by influencing their electronic and steric properties. Consequently, CAACs are more electron-rich than NHCs and phosphines. This makes them more nucleophilic, more electrophilic, and more basic than NHCs [9,11]. These features enable the synthesis of otherwise unstable intermediates and unusual d- and p-block complexes [4,9]. In a recent study, the steric properties of CAACs enabled the synthesis of the first transition metal hexafluoride complex with a pentagonal bipyramidal geometry, $[WF_6(CAAC)]$ [15]. In contrast, the same reactions using NHCs resulted in seven-coordinate complexes in the form of distorted capped trigonal prisms, which are more common [15]. In addition, the unique properties of CAACs allow the stabilization of unusual low-valent transition metal and main group complexes, which are not found with NHCs [11]. For example, the Si(II) adduct $[SiF_2(CAAC)_2]$ was obtained by the reduction of $[SiF_4(CAAC)]$, while the same reaction with NHC did not yield the reduced compound [16]. Similarly, the B(I) adduct $[BF(CAAC)_2]$ was also obtained [17].

Coordination of NHCs to transition metals and the formation of transition metal complexes typically involve the formation of strong NHC–M bonds. Similarly, NHC carbenes form adducts with main group species, which can be highly stable and non-labile due to strong dative coordination. The synthesis, structure, and application of many NHC complexes and adducts have already been extensively studied and reviewed [18–24]. NHC transition metal complexes, including fluorides,

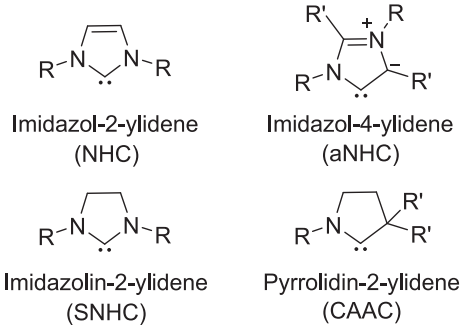

Fig. 1. Common types of NHC carbenes.

are the most widely used in homogeneous catalysis and organic transformations [4]. For example, the broad utility of [CuF(NHC)] complexes has been demonstrated in several reactions with organosilicon compounds and in cross-coupling reactions [25]. The strong NHC-metal binding increases the stability and, consequently, the catalytic stability of complexes due to low rates of catalyst decomposition [4]. Compared to other ligands, NHC complexes exhibit higher reactivity, improved selectivity, efficiency, and versatility, allowing access to unprecedented reactivity pathways [4]. For example, fluoride complexes with late transition metals such as Au are usually labile and reactive. However, using NHCs prevented reduction to Au metal, enabling the synthesis of the first [AuF(NHC)] complex [26]. Another significant advantage is the solubility of these complexes in aprotic solvents, compared to the often insoluble nature of the corresponding metal fluoride [25]. However, a drawback of such complexes is their sensitivity to moisture. In Cu chemistry, this was addressed by using more stable bifluoride adducts [25].

It is worth noting that many recent reviews of NHC transition metal complexes and main group element adducts do not focus on NHC-stabilized fluoride species. One reason is that the chemistry of fluorides was traditionally developed separately from that of other halides. Working with fluorine-containing molecules sometimes requires specialized equipment and skills, which are rarely available in most laboratories [7]. Fortunately, with the development of adequate experimental techniques, equipment, characterization methods, and fluorination reagents, interest in this area has grown enormously.

The synthesis of NHC-stabilized metal and non-metal fluorides can be accomplished using various methods, as shown in **Scheme 1**. The most commonly used method is the free carbene route. For many elements, complexes with NHC-M-F fragments have been prepared by directly combining a fluoride with a free NHC. This procedure is straightforward but requires a fluoride with good solubility in the chosen solvent, a free carbene, and anhydrous conditions. To avoid the need for anhydrous conditions, transmetalation procedures can be used. In this method, a carbene-transfer reagent is combined with a metal or non-metal fluoride source to produce the desired NHC fluoride. To increase the solubility of fluorides, synthons (e.g. $[MF_n(L)]$, where L is a neutral ligand) can be used. In this approach, a neutral ligand of a synthon is displaced by an NHC ligand to form the desired NHC fluoride.

Sometimes, dehydrofluorination of the corresponding fluoride salts leads to the formation of NHC-stabilized fluorides. For example, thermolytic decomposition of $[(NHC)H][MF_{(n+1)}]$ salts or their *in-situ* deprotonation can directly yield $[MF_n(NHC)]$ complexes.

NHC-stabilized fluorides can also be obtained by fluorinating preformed $[MX_n(NHC)]$ complexes. Depending on the selectivity of the fluorinating reagent, the starting substituents on the metal or non-metal center can be partially or completely replaced with fluorides. Various reagents can be used for this purpose, such as inorganic fluorinating compounds (KF, AgF, AgF_2, Me_3SnF, SF_4, SF_6, KHF_2, etc.), organic fluorinating reagents (Selectfluor, NFSI, NH_4F, NR_4F, $Et_3N{\cdot}3HF$, etc.), or fluorinated organic compounds (C_6F_6, benzyl fluoride, etc.).

The $[MF_n(NHC)]$ complexes can be further functionalized to form new species. Functionalization can occur at the metal or non-metal center by exchanging fluorides with other substituents to form derivatives of the type $[MF_{(n-m)}R_m(NHC)]$, or at the NHC scaffold to form derivatives of the type $[MF_n(NHC\text{-}R)]$, where R is a C-, N-, O-substituent, or halide.

Reductions and oxidations of existing complexes can also lead to the formation of new NHC-stabilized metal fluorides. For example, reduction of $[MF_n(NHC)]$ with KC_8 yields complexes in a low oxidation state. Conversely, oxidation of compounds in a lower oxidation state with XeF_2 or 2,2-difluoroimidazolidine produces NHC-stabilized fluorides in a high oxidation state.

Over the past 25 years, extensive study in metal and non-metal fluoride chemistry has led to the synthesis and characterization of many NHC complexes and adducts. Their chemistry has been partially

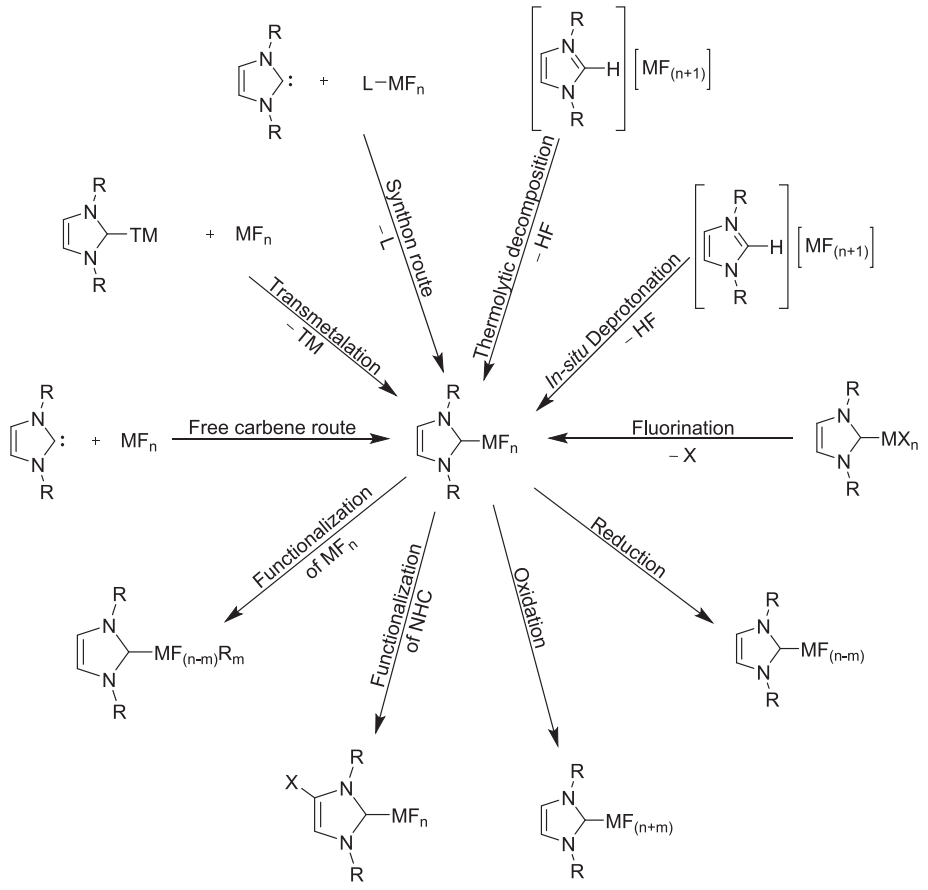

Scheme 1. Methods for the synthesis of NHC-stabilized metal and non-metal fluorides. TM = transmetalation group.

covered in several review articles [7,26–32].

This article reviews the synthetic and structural aspects of NHC transition metal complexes and main group element adducts. In this review, we focus exclusively on compounds containing NHC-M-F fragments, prepared from the discovery of stable NHCs in 1991 through mid-2025. To the best of our knowledge, 33 elements form such fragments, as

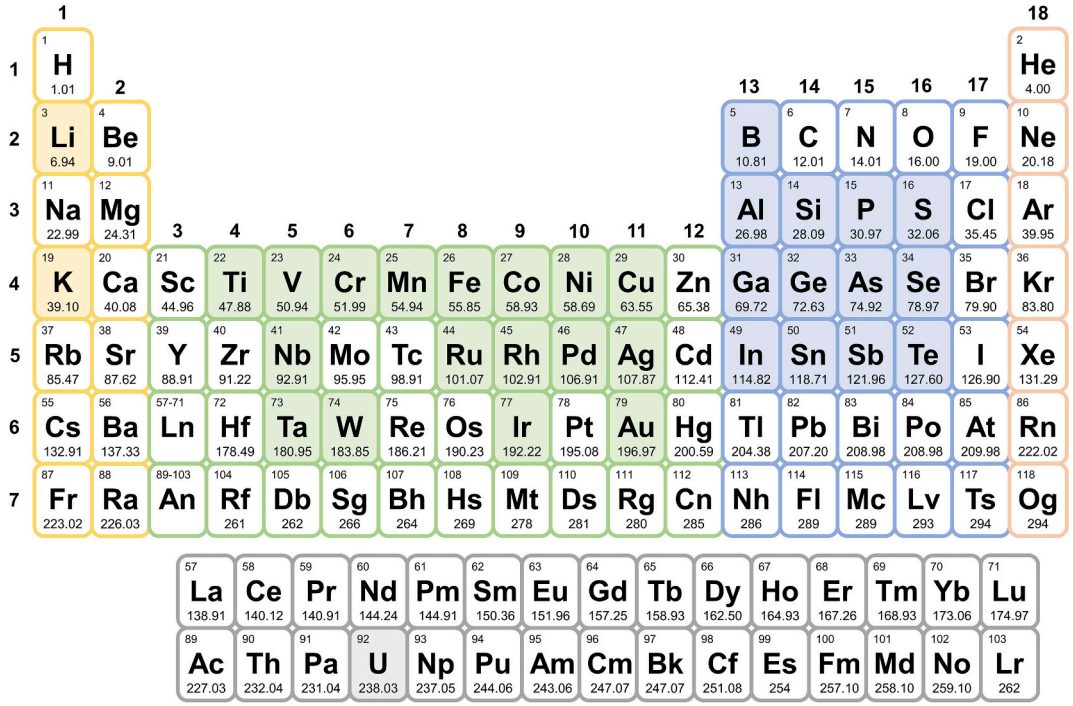

Fig. 2. Elements forming NHC-M-F fragments.

indicated on the periodic table in Fig. 2. Among the 458 compounds included in this review, B is by far the most extensively studied element, followed by P, Ni, Ru, Au, and Cu. Fig. 3 shows the proportions of known compounds with NHC-M-F fragments for each element.

A detailed search of The Cambridge Structural Database identified 277 unique structurally characterized compounds [33]. In analyzing their structural features, we focused on their NHC–M and M–F bond lengths. Because this information may be useful to a broad audience, we compiled the typical bond lengths, geometries, and ^{19}F NMR data of the structurally characterized neutral NHC-stabilized metal and non-metal fluorides in Table 1. Note that not all elements discussed in this review form neutral complexes. All data collected for the 277 structurally characterized complexes are provided in the Supporting Information.

2. s-block complexes

S-block metal fluorides stabilized with NHC ligands are not known. In the literature, only a few structures are reported in which NHC-stabilized metals are coordinated to weakly coordinating anions. More information about s-block metal complexes with NHC ligands in available in ref. [18].

2. GROUP I

2.1.1. Lithium & Potassium

Stable Li-containing products were obtained by deprotonating the corresponding imidazolium phosphate salts with Li-containing reagents. The formation of complexes **1** and **2** (Fig. 4) was confirmed by single-crystal structure analysis. Both structures exhibit tetrahedral coordination at the Li center and a bridging fluorine bond to $[PF_6]^-$ anions [34,35]. In both cases, using an excess of LiHMDS reagent in THF was a key factor in forming the complexes [35]. The NHC–Li bond lengths in known complexes range from 2.22 to 2.23 Å, while the Li–F bond lengths are between 1.90 and 1.93 Å, which is significantly shorter than in $LiPF_6$ [36].

Similarly, deprotonation of phosphorane-substituted NHC precursors carrying one or two weakly coordinating anionic $PF_2(C_2F_5)_3$ groups with K bases led to the formation of K-containing salts, which upon crystallization produced structures **3** and **4**. In both structures, K does not form

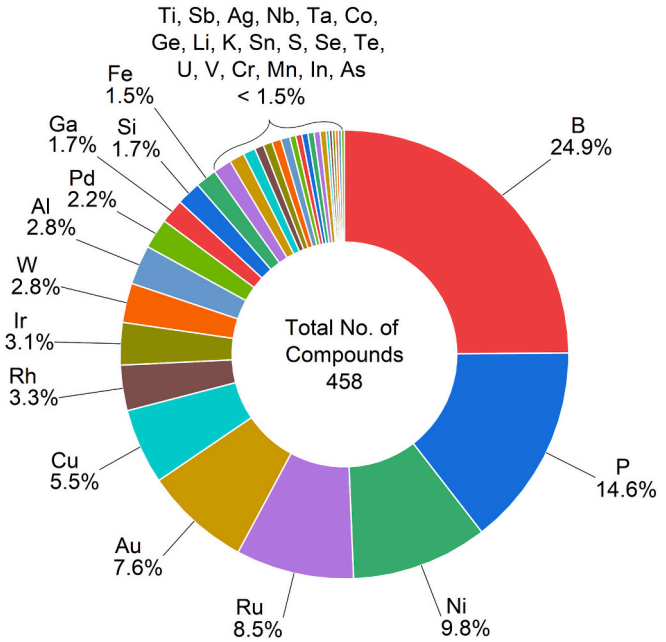

Fig. 3. Proportions of complexes with NHC-M-F fragments per element.

Table 1
Typical geometries, bond lengths, and ^{19}F NMR data for neutral NHC-stabilized metal and non-metal fluorides of the following elements. All data were collected from known crystal structures.

Element	Typical geometry	d(NHC–M) / Å	d(M–F) / Å	^{19}F NMR / ppm
Li	Tetrahedral	2.22–2.23	1.90–1.93	NA
K*	7- or 9-coordinate	2.94–2.96	2.75–2.99**	NA
U	Trigonal bipyramidal	2.09	2.65	NA
Ti	Octahedral	2.24–2.28	1.84–1.90	122–197
V	Square pyramidal	2.14	1.78–1.80	174–178
Nb	Octahedral	2.32–2.35	1.87–1.93	153
Ta	Octahedral	2.31–2.43	1.88–1.92	0–82
Cr	Square planar	2.17	1.91	NA
W	Seven-coordinate, Octahedral	2.19–2.28	1.86–1.93	140–152
Mn*	Octahedral	2.04	1.90	−325
Fe	Tetrahedral	2.09–2.12	1.85–1.89	−158
Ru	Octahedral	2.07–2.20	1.95–2.27 *cis*; 2.18–2.38 *trans*	(−302)–(−405)
Ru	Square pyramidal	2.05–2.10	2.02–2.04 *cis*	(−208)–(−239)
Co	Tetrahedral	1.95–2.15	1.87–1.89	−460*
Rh	Square planar	1.97–2.06	2.02–2.15	(−254)–(−327)
Ir	Square planar	2.02–2.05	2.01–2.07	(−221)–(−227) (−314)–(−376)
Ni	Square planar	1.84–1.96	1.83–1.94	Ni*F*R −560 NiF_2
Pd	Square planar	1.94–2.07	1.96–2.01	(−236)–(−400)
Cu	Linear	1.85–1.96	1.78–1.87	(−213)–(−254)
Ag*	Linear	2.05	2.07**	−243*
Au(I)	Linear	1.94–1.96	2.03–2.06	−247
Au(III)	Square planar	1.97–2.05	1.91–1.94	(−311)–(−341)
B	Tetrahedral	1.53–1.73	1.32–1.46	(−130)–(−181)
Al	Tetrahedral	1.99–2.11	1.67–1.71	(−147)–(−171)
Ga	Tetrahedral	1.99–2.05	1.79–1.84	(−151)–(−212)
In	Tetrahedral	2.18	2.19**	−124**
Si	Octahedral	1.80–2.03	1.58–1.69	(−103)–(−120)
Ge	Trigonal pyramidal, Trigonal bipyramidal	1.98–2.12	1.78–1.83	(−112)–(−116)
Sn	Octahedral	1.97–1.98	1.97–1.98	−121
P	Octahedral	1.87–1.99	1.53–1.66	(−43)–(−102)
As	Octahedral	2.00	1.72	(−45.97)–(−68.06)
Sb	Octahedral	2.14–2.18	1.86–1.90	(−99.47)–(−122.28)
S	T-shape	1.73	1.82	−97
Se(II)	T-shape	1.88	1.94	−158
Se(IV)	Square pyramidal	1.97	1.85	3.6
Te	Square pyramidal	2.12–2.29	1.94–1.98	−47

* marks the elements, where no neutral compounds are structurally characterized. In this case, values of ionic compounds are given.
** marks the M–F bond lengths where the only structurally characterized compound has bridging bonds.

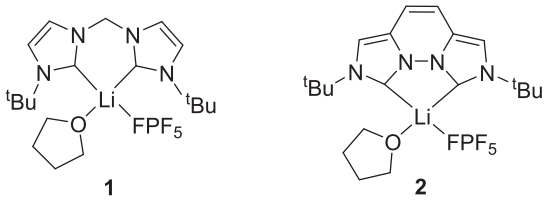

Fig. 4. Schematic representation of **1** and **2**.

direct bonds with F but is weakly coordinated to F atoms of the $PF_2(C_2F_5)_3$ group (Fig. 5) [37]. The NHC–K bond lengths in known complexes range from 2.94 to 2.96 Å, while the bridging K–F bond lengths are between 2.75 and 2.99 Å.

3. f-block complexes

Lanthanide fluoride compounds do not form neutral simple complexes with neutral electron-donating ligands. This is due to their insolubility in water and common organic solvents. Some lanthanide fluorides are also strong fluorinating agents, which further hinders complex formation. The coordination chemistry of actinide fluorides is more extensive but remains limited. Most research has focused on uranium, partly because access to actinide elements is restricted outside specialized nuclear facilities [7,28]. Consequently, NHC-stabilized f-block metal fluoride complexes are extremely rare, as are other NHC-stabilized halide complexes. To the best of our knowledge, only one such compound is known in the literature.

3.1. Actinides

3.1.1. Uranium

Only one structure with the NHC-U-F motif is known, and it was formed accidentally. During investigations of the reactivity of the U complex, its reaction with Me_3SiCF_3 led to the formation of an isolable red-brown U fluoride complex **5** in 69% yield. The structure of this compound is shown in Fig. 6. It displays a 5-coordinate geometry at the U center, with F in the axial position. The structure has an NHC–U bond distance of 2.09 Å and a U–F bond distance of 2.65 Å [38].

4. d-block complexes

The chemistry of d-block NHC-stabilized metal fluorides is discussed in the following chapters, with each group of elements covered separately. Notably, almost all groups of d-block elements form complexes with the NHC-M-F motif, except for group III and group XII.

4.1. GROUP IV

Within group IV, only NHC-stabilized Ti fluoride complexes are known, most of which are derived from TiF_4.

4.1.1. Titanium

The coordination chemistry of TiF_4 with neutral electron-donating ligands is well studied, due to its solubility in organic solvents. Its synthesis, reactivity, and applications are thoroughly summarized in the review by Nikiforov [27].

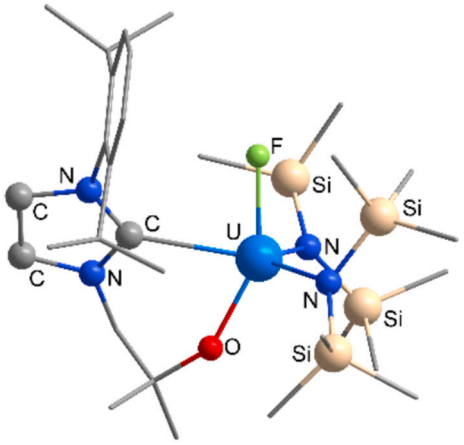

Fig. 6. View of the structure of **5**, redrawn from ref. [38].

TiF_4 reacts with NHC carbenes in THF in a 1:2 ratio to form $[TiF_4(NHC)_2]$ complexes **6** [39], **7**, and **8** [40], as shown in Fig. 7. Complex **6** forms whether one or two equiv of NHC are used. It is stable in the solid state under an inert atmosphere at room temperature but tends to slowly decompose in solution or upon contact with moisture [39]. Degradation of complexes in solution also occurs with **7** and **8**. The latter converts to the corresponding $[(^{Me2}I^iPr)H][TiF_5(^{Me2}I^iPr)]$ salt **9** in C_6D_6 and MeCN within a few hours [40].

The three $[TiF_4(NHC)_2]$ complexes **6**, **7**, and **8** were also structurally characterized. Their structures display octahedral coordination at the Ti center, with the two NHC ligands in *trans* positions (Fig. 8) [39,40]. The *trans* arrangement is attributed to the bulkiness of the ligands [40].

Compound **7** was also used to test the properties of $[TiF_4(NHC)_2]$ complexes (Scheme 2). It reacted with $Ti(NEt_2)_4$ to form dimer **10**, whose composition was confirmed by crystal structure analysis.

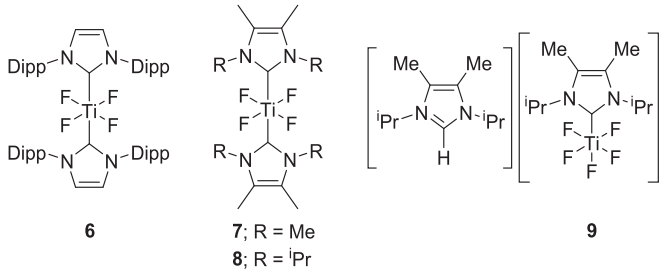

6 **7**; R = Me **8**; R = ^{i}Pr **9**

Fig. 7. Schematic representation of complexes **6**–**9**.

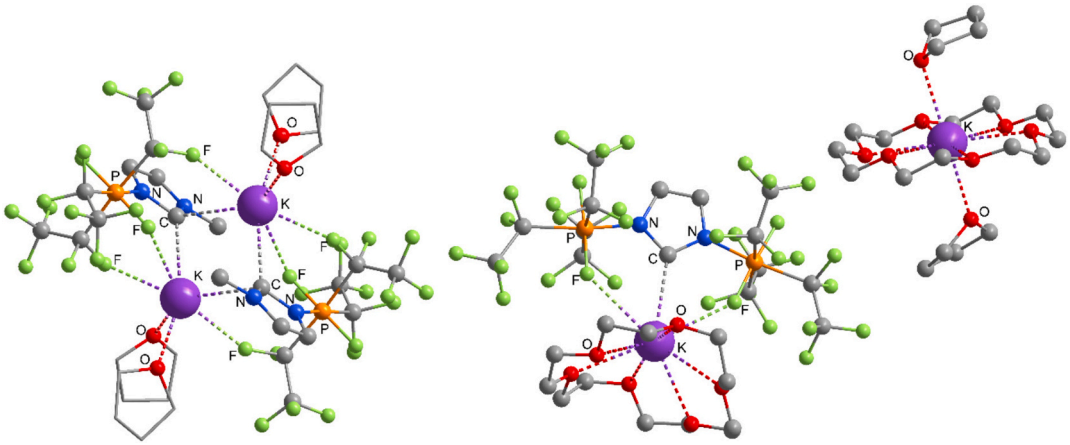

Fig. 5. View of the structures of **3** (left) and **4** (right), redrawn from ref. [37].

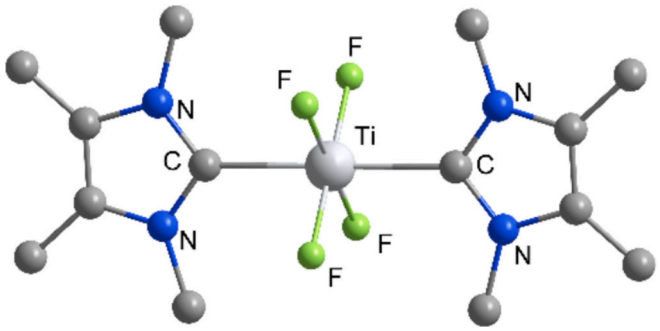

Fig. 8. View of the structure of **7**, redrawn from ref. [40].

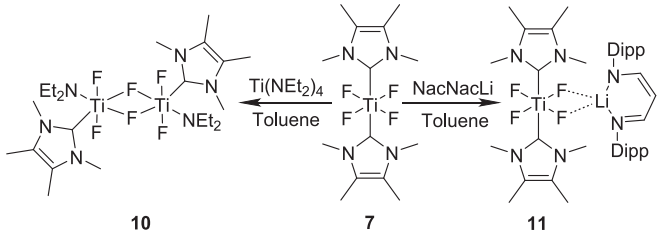

Scheme 2. Synthesis of dimer **10** and adduct **11**.

Alternatively, dimer **10** was formed directly by reacting of $Ti(NEt_2)_4$ with 3 equiv of TiF_4 and 4 equiv of NHC in toluene. Complex **7** also reacted with NacNacLi to form a 1:1 adduct **11**, whose composition was deduced from NMR, mass spectrometry, and elemental analysis data [40].

Based on the known structures of NHC-stabilized Ti fluorides, the NHC–Ti bond lengths in neutral complexes are typically between 2.24 and 2.28 Å. The only anionic species, $[TiF_5(NHC)]^-$ in the structure of **9**, has a slightly longer NHC–Ti bond of 2.31 Å [40]. In contrast, the average Ti–F bond lengths in all reported structures range from 1.90 to 1.84 Å. Only the complex with bridging fluorine bonds shows a longer Ti–F bridging bond of 2.05 Å [40].

4.1.2. Zirconium & Hafnium

The chemistry of ZrF_4 and HfF_4 is less explored than that of TiF_4, due to their inert polymeric nature, which prevents dissolution in common organic solvents. Nevertheless, the structures of their fluoride complexes with neutral electron-donating ligands have been comprehensively reviewed by Davidovich [41]. To the best of our knowledge, there is only one report on the reactivity of ZrF_4 and HfF_4 compounds with NHC carbenes. Levason's group attempted to synthesize $[MF_4(NHC)_2]$ (M = Zr, Hf) complexes by displacing DMF in the corresponding $[MF_4(DMF)_2]$ synthons with IDipp carbene. The reaction was unsuccessful and resulted in the formation of [(IDipp)H][Cl] in DCM, indicating a tendency toward protonation rather than adduct formation. In THF, salts of the type $[IDippH]_3[M_3F_{15}]\cdot 4THF$ (M = Zr, Hf) were obtained and structurally characterized [42].

4.2. GROUP V

Within Group V, only a limited number of NHC-stabilized complexes of vanadium oxyfluorides, niobium fluorides, and tantalum fluorides in high oxidation states have been reported.

4.2.1. Vanadium

In general, the chemistry of VOF_3 and VO_2F with neutral electron-donating ligands is well established, while the chemistry of high-valent V fluorides is unusual and limited to a few reports. An overview of their chemistry can be found in ref. [28].

To date, only one neutral complex of VOF_3 with an NHC carbene has been prepared and structurally characterized. $[VOF_3(IDipp)]$ (**12**) was obtained by reacting VOF_3 with free IDipp carbene in ethers (THF or Et_2O) [43]. Structural characterization revealed a distorted square pyramidal coordination at the V center, with the oxygen atom in the apical position, as shown in **Fig. 9**. The structure features an NHC–V bond length of 2.14 Å and V–F bond lengths in the range of 1.78–1.80 Å [43].

The group also attempted to prepare molecular VO_2F by reacting **12** with $(Me_3Si)_2O$, following the procedure for preparing known neutral N-complexes [44], but was unsuccessful. Complex **12** hydrolyzed in the presence of moisture, forming $[(IDipp)H][VOF_4]$ and $[(IDipp)H][VO_2F_2]$ salts. Alternatively, $[(IDipp)H][VOF_4]$ could be obtained in pure form by reacting VOF_3 with the [(IDipp)H][F] fluorinating reagent [43].

4.2.2. Niobium & Tantalum

Nb and Ta pentafluorides are very hygroscopic powders that dissolve easily in organic solvents, enabling their use in coordination chemistry. A comprehensive review of various Nb and Ta fluoride complexes with neutral electron-donating ligands can be found in references [7, 28].

The first $[MF_5(NHC)]$ (M = Nb, Ta) complexes were prepared by the group of Marchetti in 2016 [45]. NbF_5 and TaF_5 reacted in a 1:1 ratio with IDipp carbene in toluene or benzene to afford the corresponding $[NbF_5(IDipp)]$ (**13**) and $[TaF_5(IDipp)]$ (**14**) in moderate yields (**Fig. 10**). The complexes were characterized by NMR spectroscopy, IR spectroscopy and elemental analysis.

Three years later, Tavčar's group prepared complexes **13** and **14** using a similar procedure and structurally characterized both [46]. Structural analysis of **13** and **14** revealed that they are isostructural, with octahedral geometry around the metal center (**Fig. 11**). Interestingly, in **13** and **14**, the MF_5 group is oriented in a staggered position relative to the plane of the NHC ring, which was attributed to interactions between the fluorine atoms and the "wingtips" of the ligand [46]. Unfortunately, the complexes are very susceptible to moisture, degrading in the presence of traces of water [45]. In polar solvents such as MeCN and DCM, conversion to imidazolium salts $[(IDipp)H][NbF_6]$ and $[(IDipp)H][TaF_6]$ occurs [46]. Alternatively, the two hexafluorometalate salts can be prepared in pure form by reacting NbF_5 and TaF_5 with the [(IDipp)H][F] fluorination reagent [46].

The group led by Marchetti observed that compound **13** shows moderate air stability when isolated but is significantly more sensitive to moisture in toluene solution. Slow crystallization of **13** in toluene under moist air led to gradual hydrolysis of the complex, resulting in the formation of the $[NbOF_3(IDipp)]_2$ dimer (**15**) [47]. This binuclear complex consists of two distorted octahedral Nb units that share one edge. The

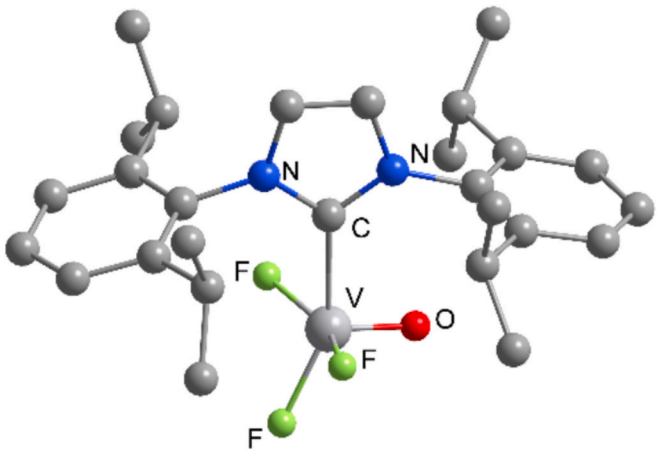

Fig. 9. View of the structure of $[VOF_3(IDipp)]$ (**12**), redrawn from ref. [43].

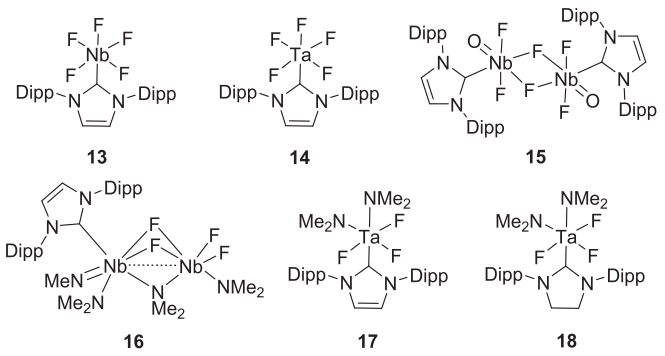

Fig. 10. Schematic representation of complexes **13**–**18**.

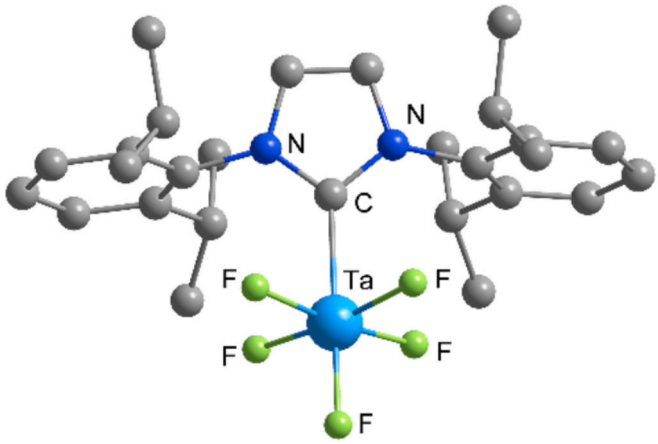

Fig. 11. View of the structure of $[TaF_5(IDipp)]$ (**14**), redrawn from ref. [46].

terminal oxygen atom and the NHC ligand occupy equatorial positions relative to the $Nb_2(\mu\text{-}F)_2$ ring, as shown in Fig. 12 [47].

A binuclear Nb complex, **16** (Fig. 10), was prepared by reacting $Nb(NMe_2)_5$ with $[(IDipp)H][BF_4]$. Calculation of its formal oxidation state confirmed the formation of a mixed-valent Nb(IV,V) complex with one unpaired electron [48]. Presumably, Nb is reduced to Nb(IV) due to elimination of a methyl group from the dimethylamide substituent, forming methylimide. The yield was very low, indicating the occurrence of various parallel reactions in the mixture. In contrast, the same reaction of $Nb(NMe_2)_5$ with $[(IMes)H][BF_4]$ afforded the $[(IMes)H][NbF_6]$ salt instead. Both compounds were structurally characterized [48].

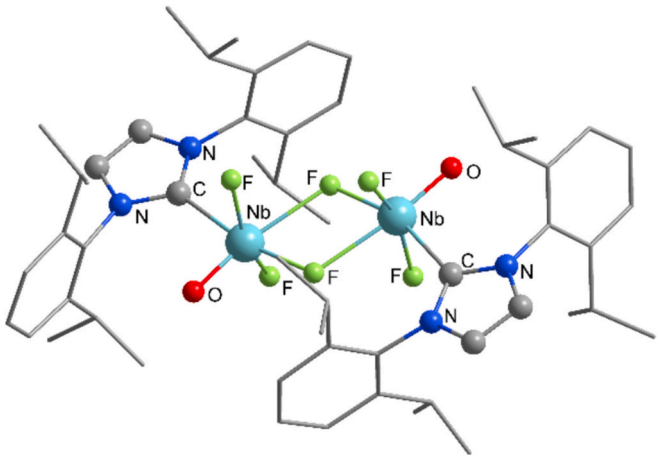

Fig. 12. View of the structure of the $[NbOF_3(IDipp)]_2$ dimer (**15**), redrawn from ref. [47].

Similar experiments were conducted with the Ta counterpart, $Ta(NMe_2)_5$, which reacted with $[(NHC)H][BF_4]$ (NHC = IMes and SIMes) to form Ta amidofluoride complexes $[TaF_3(NHC)(NMe_2)_2]$ (NHC = IMes **17**, SIMes **18**) (Fig. 10). Structural analysis revealed that **17** and **18** are isostructural. Both complexes exhibit octahedral coordination at the Ta center, with all fluoride substituents in *cis* positions relative to the NHC ligand [49].

Based on the known structures of NHC-stabilized Nb and Ta fluorides, the NHC–M and M–F bonds are very similar for both elements. The NHC–Nb bond lengths in neutral complexes are usually between 2.32 and 2.35 Å, while the NHC–Ta bonds range from 2.31 to 2.43 Å. The average Nb–F bond lengths are between 1.87 and 1.93 Å, while the Ta–F bonds range from 1.88 to 1.92 Å. Only complex **15**, with bridging F atoms, exhibits longer Nb–F bridging bonds in the range of 2.13–2.34 Å [48].

4.3. GROUP VI

Group VI metal fluorides stabilized with NHC ligands are rare. To date, only one Cr compound and several W compounds have been reported.

4.3.1. *Chromium*

A Cr silylamido complex, $Cr(N(SiMe_2Ph)_2)_2(THF)_2$, reacts with $[(IMes)H][FHF]$ in the presence of IMes carbene to form $[CrF_2(IMes)_2]$ (**19**). This compound is only the second structurally characterized organometallic Cr(II) fluoride known. It adopts a square planar geometry at the Cr center, with a *trans* arrangement of the NHC ligands, as shown in Fig. 13. The structure features an average NHC–Cr bond length of 2.17 Å and an average Cr–F bond length of 1.91 Å [50].

4.3.2. *Tungsten*

Recently, the first W fluoride complexes stabilized by NHCs have been prepared. Stoichiometric reactions of WF_6 with different carbenes in hexane led to the formation of complexes **20**–**25** (Fig. 14) [15]. All W(VI) complexes exhibit 7-coordinate metal centers. The geometry of the structurally characterized NHC complexes **21** and **22** is best described as distorted mono-capped trigonal prismatic, with the carbene in the capping position, while the CAAC complex **25** adopts a pentagonal bipyramidal geometry, with the CAAC ligand in the pentagonal plane, as shown in Fig. 15. This represents the first example of a transition metal hexafluoride adduct with that geometry [15].

Treatment of the NHC-stabilized WF_6 complexes **20**–**25** with 0.5 equiv of the non-metallic reducing agent 2,3,5,6-tetramethyl-1,4-bis

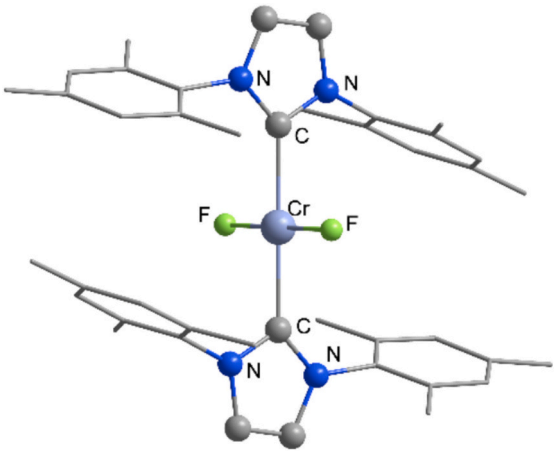

Fig. 13. View of the structure of $[CrF_2(IMes)_2]$ (**19**), redrawn from ref. [50].

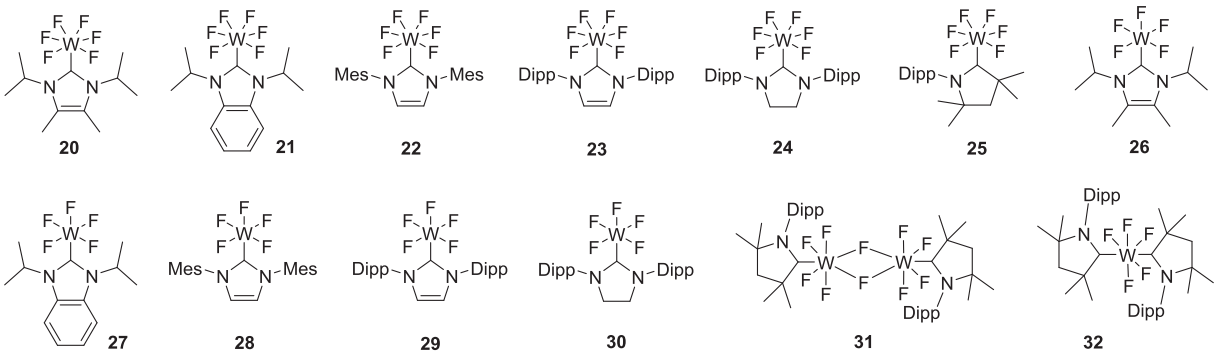

Fig. 14. Schematic presentation of **20**–**32**.

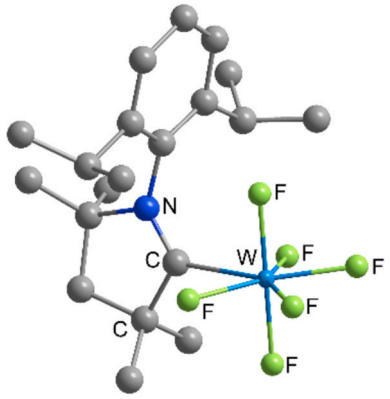

Fig. 15. View of the structure of [WF_6(^{Me}CAAC)] (**25**), redrawn from ref. [15].

(trimethylsilyl)-1,4-dihydropyrazine resulted in formation of W(V) complexes **26**–**30** [15]. Under the same conditions, the CAAC counterpart **25** remained unaffected. Its reduction was achieved using a more reactive derivative, 1,4-bis(trimethylsilyl)-1,4-dihydropyrazine, which upon crystallization revealed the formation of the fluoride-bridged dimeric complex [WF_5(^{Me}CAAC)]$_2$ (**31**) [15]. Furthermore, the dimeric complex was converted to the bis-CAAC complex [WF_5(^{Me}CAAC)$_2$] (**32**) by treatment of **31** with 2 equiv of ^{Me}CAAC carbene. Complexes **31** and **32** were structurally characterized, revealing a pentagonal bipyramidal geometry at the metal centers with CAAC carbenes in equatorial positions [15].

Based on known structures of NHC-stabilized W fluorides, the NHC–W bond lengths are usually between 2.19 and 2.28 Å, while the average W–F bond lengths are usually between 1.86 and 1.93 Å. Notably, the W–F bonds in trans position to NHCs are slightly longer. Only complex **31**, with bridging F atoms, exhibits longer W–F bridging bonds of 2.10 Å [15].

4.4. GROUP VII

Group VII metal fluorides stabilized with NHC ligands are also extremely rare. To date, only one Mn compound has been reported. The absence of Tc and Re fluorides is likely due to the challenges in accessing the corresponding metal fluorides.

4.4.1. Manganese

Oxidation of the Mn(IV) nitride complex with AgF led to the formation of the NHC-stabilized Mn fluoride **33**. The cationic complex adopts an octahedral geometry at the Mn center, with the trimeric NHC ligand and the fluoride coordinated in the equatorial plane, as shown in

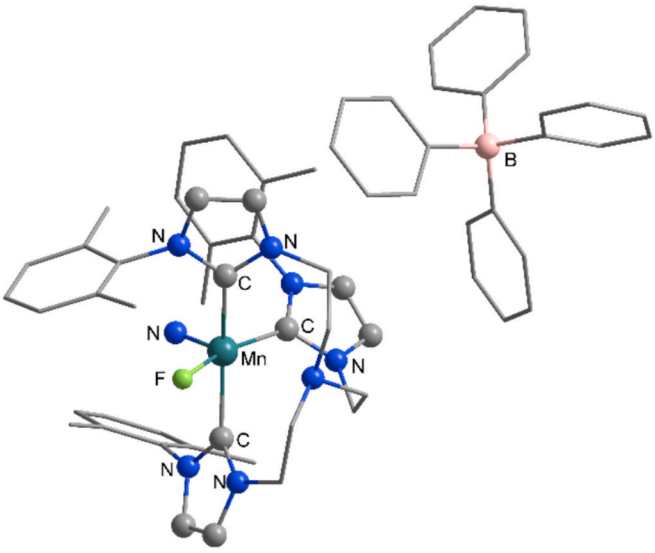

Fig. 16. View of the structure of **33**, redrawn from ref. [51].

Fig. 16. The structure features an NHC–Mn bond length of 2.04 Å and a Mn–F bond length of 1.90 Å [51].

4.5. GROUP VIII

NHC-stabilized Group VIII metal fluoride compounds are limited to those of Fe and Ru. Fe compounds are mainly found in the +3 and +2 oxidation states, while Ru compounds are restricted to the +2 oxidation state. Both elements have been extensively studied for their favorable catalytic properties.

4.5.1. Iron

The first NHC-stabilized Fe fluoride complexes were prepared by oxidizing the dimer complex [Fe(^{Me2}I^{i}Pr)(μ-NDipp)]$_2$ with 1 or 2 equiv of [Cp_2Fe][BF_4]. The reaction yielded the paramagnetic complexes **34** and **35**, respectively, as shown in Scheme 3 [52]. Both complexes were structurally characterized and feature a rhombic [Fe(μ^2-NDipp)$_2$Fe] core with tetrahedral coordination at the Fe center and NHC ligands in *trans* orientation [52].

The first mononuclear NHC-stabilized iron fluoride complex **36** was synthesized from the corresponding methoxide by reaction with TMS-CF_3. The structure of the tris-NHC complex features a tetrahedrally coordinated Fe center, as shown in Fig. 17 [53]. Using a similar route, the group also prepared and structurally characterized the related tris-NHC complex **37** by fluorinating the FeCl complex with Me_4NF (Fig. 18) [54].

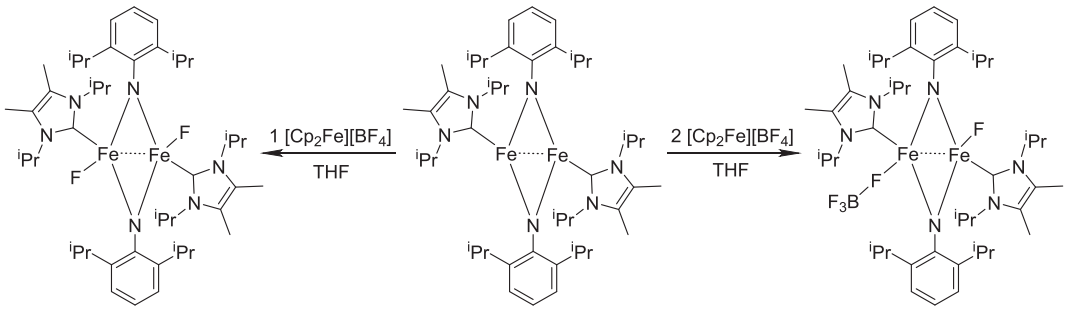

Scheme 3. Synthesis of the binuclear complexes **34** and **35**.

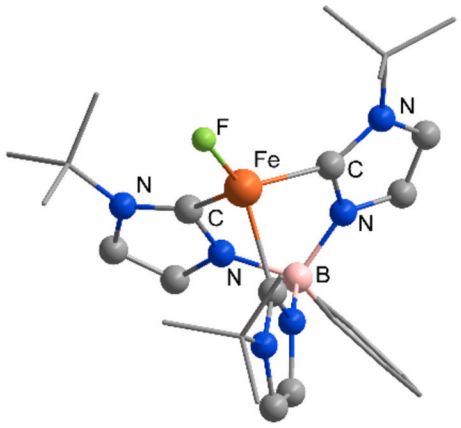

Fig. 17. View of the structure of **36**, redrawn from ref. [53].

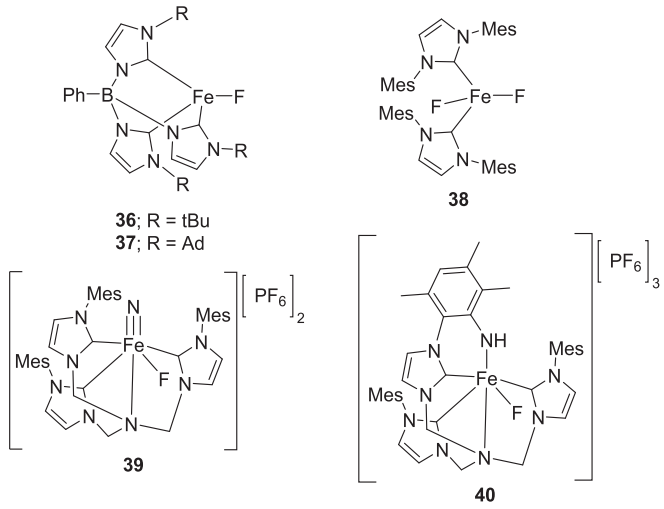

Fig. 18. Schematic presentation of **36**–**40**.

A rare example of an NHC-stabilized FeF_2 complex was prepared by reacting the iron silylamido complex $Fe(N(SiMe_2Ph)_2)_2(THF)_2$ with [(IMes)H][FHF] in the presence of IMes carbene. The resulting $[FeF_2(IMes)_2]$ (**38**) was obtained using the same procedure as for the Cr(II) complex [50]. Structurally, the Fe counterpart, which features a tetrahedral geometry at the Fe center, differs from the Cr complex, which has a square planar geometry [50]. Recently, a dicationic hexavalent Fe nitrido fluoride complex was prepared by oxidizing the corresponding dicationic nitrido complex with AgF_2. The molecular structure of **39** revealed octahedral coordination at the Fe(VI) center with an equatorially coordinated F substituent [55]. The complex can be further oxidized with 1 equiv of a strong oxidizing agent (ReF_6, MoF_6, or XeF^+ cations) to form a one-electron oxidized Fe(VII) nitride, which undergoes rearrangement above −50 °C *via* intramolecular amination to form a cyclic Fe(V) imido complex [55]. In one instance, crystallization of the nitrido fluoride complex yielded single crystals of the intermediate **40**, in which the mesityl group bonds to the nitrido substituent [55]. All complexes are shown schematically in **Fig. 18**.

Based on known structures of NHC-stabilized Fe fluorides, the NHC–Fe bond lengths in neutral complexes are typically between 2.09 and 2.12 Å, while cationic complexes have shorter NHC–Fe bonds (dicationic **39**: 1.98 Å; tricationic **40**: 1.91 Å) [55]. The average Fe–F bond lengths are usually between 1.85 and 1.89 Å, although longer bonds are observed in cationic complexes (**40**: 2.06 Å) or in structures with bridging bonds (**35**: 2.06 Å) [52,55].

4.5.2. *Ruthenium*

A wide range of NHC-stabilized Ru fluoride compounds is known. These have been extensively studied due to their favourable catalytic properties.

The first complex in this category was the 16-electron hydride fluoride complex [RuFH(IMes)$_2$(CO)] (**41**), prepared by adding $Et_3N{\cdot}3HF$ to [RuH_2(IMes)$_2$($AsPh_3$)(CO)], as shown in **Scheme 4** [56]. The hydride fluoride complex is converted to the 18-electron dicarbonyl complex [RuFH(IMes)$_2$(CO)$_2$] (**42**) upon exposure to 1 atm CO at room temperature. In the crystal structure, both complexes exhibit octahedral coordination at the metal center, with the NHC ligands in a *trans* arrangement [56].

A few years later, the same group extended their research on coordinatively unsaturated Ru complexes. RuFH(PPh_3)$_3$(CO) reacted with the NHC pentafluorobenzene adducts SIMes(C_6F_5)H, SIDipp(C_6F_5)H, IMes, IDipp, and 6-Mes to form [RuFH(NHC)(PPh_3)(CO)] (NHC = SIMes **43**, SIDipp **44**, IMes **45**, IDipp **46**, 6-Mes **47**), as shown in **Fig. 19** [57,58]. The structure of **43** is shown in **Fig. 20**. It features square planar coordination at the Ru center, with the H atom in the apical position and the NHC and phosphine ligands in a *trans* arrangement [59]. Upon cooling the reaction mixtures of **43**–**46** to −59 °C, the unsaturated complexes formed the 18-electron bis-phosphine complexes [RuFH

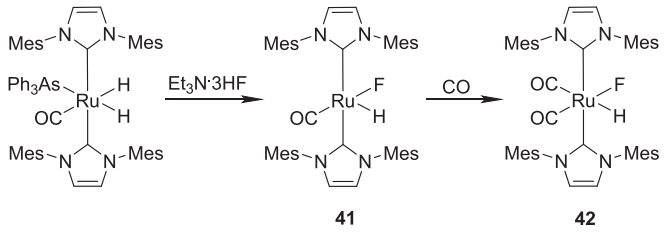

Scheme 4. Synthesis of **41** and **42**.

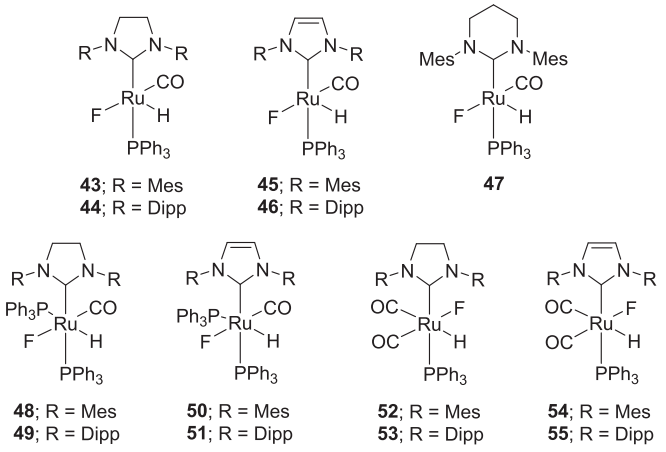

Fig. 19. Schematic presentation of **43**–**55**.

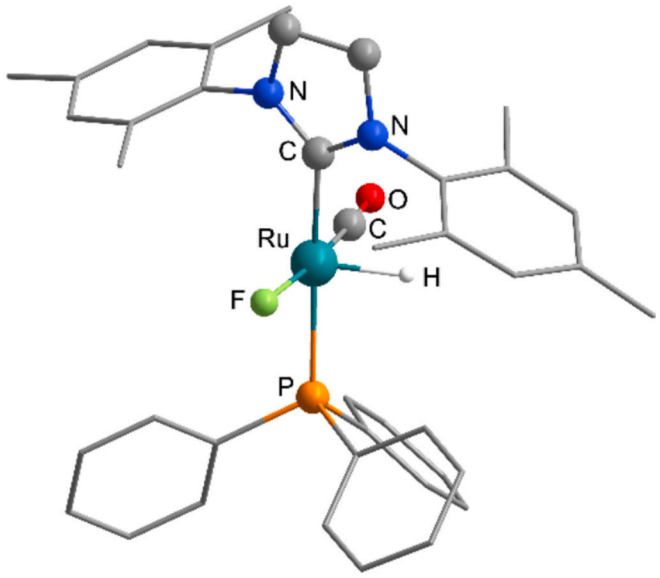

Fig. 20. View of the structure of the complex [RuFH(SIMes)(PPh_3)(CO)] (**43**), redrawn from ref. [60].

(NHC)(PPh_3)$_2$(CO)] (NHC = SIMes **48**, SIDipp **49**, IMes **50**, IDipp **51**), respectively (Fig. 19). The coordinatively unsaturated **43**–**46** were also trapped with CO to give the corresponding [RuFH(NHC)(PPh_3)(CO)$_2$] (NHC = SIMes **52**, SIDipp **53**, IMes **54**, IDipp **55**) [57].

A series of mono-substituted NHC complexes [RuFH(NHC)(PPh_3)$_2$(CO)] (NHC = ^{Me2}IMe **56**, ^{Me2}IEt **57**, ^{Me2}I^{i}Pr **58**, ICy **59**), shown in Fig. 21, was prepared by ligand exchange from the corresponding hydride fluoride phosphine complexes [RuFH(PPh_3)$_3$(CO)]. The phosphine complexes were obtained by fluorination of the [RuH_2(PPh_3)$_3$(CO)] precursors with Et_3N·3HF [60]. Complexes **56**–**59** exhibit octahedral coordination at the Ru center with a *trans* arrangement of the two phosphine ligands. However, isomerization from *trans*- to *cis*-phosphine isomers occurred when the samples were stored in THF-d_8 at ambient temperature for 1–2 weeks [60].

The same ligand exchange reaction was used to prepare [RuFH(IMes)(dppp)(CO)] (**60**) from the corresponding phosphine complex [RuFH(PPh_3)(dppp)(CO)], while [RuFH(ICy)(dppp)(CO)] (**61**) was obtained by fluorination of the corresponding RuH_2 complex with Et_3N·3HF [59]. This fluorination method proved highly effective, yielding three unprecedented complexes, **62**, **63**, and **64** (Fig. 21). Of these, only the last was structurally characterized. Its structure features a *trans* arrangement of the NHC-Ru-P ligands and a *trans* arrangement of the F-Ru-CO

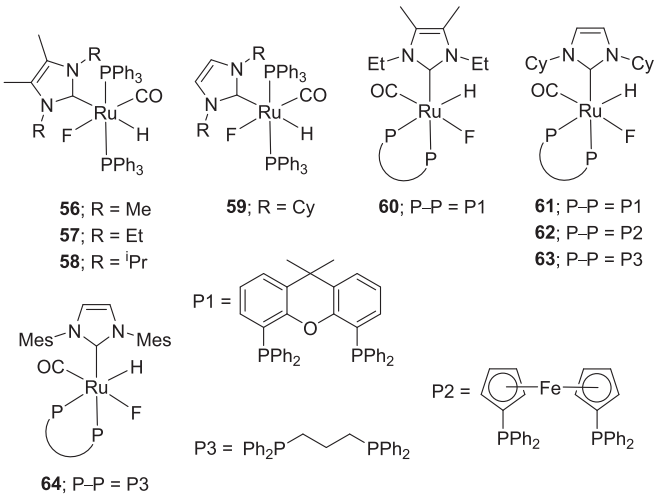

Fig. 21. Schematic presentation of **56**–**64**.

substituents [61].

Fluorination of RuH_2 complexes can also be achieved using fluorinated aromatic compounds. This procedure was first used to fluorinate [RuH_2(^{Me2}IEt)$_2$(PPh_3)$_2$] with C_6F_6 or C_6F_5H, resulting in a mixture of the *trans* hydride fluoride complex [RuFH(^{Me2}IEt)$_2$(PPh_3)$_2$] (**65**) (Fig. 22) and the hydride pentafluorophenyl species [RuH(C_6F_5)(^{Me2}IEt)$_2$(PPh_3)$_2$] [62]. A more convenient route to the hydride fluoride complex remains the use of Et_3N·3HF. However, using excess reagent led to the formation of the [RuH(^{Me2}IEt)(PPh_3)$_2$][H_2F_3] salt [62]. Later, [RuFH(^{Me2}IMe)$_2$(PPh_3)$_2$] (**66**) was prepared using C_6F_5H [63], while [RuFH(^{Me2}IMe)$_4$] (**67**) and [RuFH(IMe)$_4$] (**68**) were prepared using C_6F_6 [64]. Complex **66** was also used as a precursor for the synthesis of complexes with chelating phosphine ligands, [RuFH(^{Me2}IMe)$_2$(P-P)] (**69**–**71**) and [RuFH(^{Me2}IEt)$_2$(P-P)] (**72**), by direct substitution of the two phosphines with a chelating ligand [63].

The first Ru difluoride NHC complexes, [RuF_2(NHC)$_2$(CO)$_2$] (NHC = IMes **73**, IDipp **74**), shown in Fig. 22, were prepared from the [RuF(μ-F)(CO)$_3$]$_4$ tetramer by reaction with 8 equiv of NHC. Structural characterization of the IDipp complex **74** revealed a *trans* arrangement of the two NHC ligands and a *cis* arrangement of the two F and CO substituents [65]. The IMes-stabilized difluoride **73** subsequently reacted with BF_3, which, after carbonylation, allowed isolation of [Ru(BF_4)(IMes)$_2$(CO)$_3$][BF_4] (**75**). In contrast, the IDipp complex **74** reacted directly with BF_3 to form the [Ru_2(μ-Cl)$_3$(IDipp)$_2$(CO)$_4$](BF_4)/(F) salt [65]. The reactivity of the IDipp-stabilized RuF_2 complex **74** was further tested with the Lewis acid B(C_6F_5)$_3$. This reaction yielded the 16-electron cationic complex [RuF(IDipp)$_2$(CO)$_2$][FB(C_6F_5)$_3$] (**76**), which can be further carbonylated to the 18-electron cationic complex [RuF(IDipp)$_2$(CO)$_3$][FB(C_6F_5)$_3$] (**77**) [66].

Fluorination of a commercially available NHC-stabilized $RuCl_2$ complex with AgF in 1:1 and 1:2 ratios selectively afforded the mixed fluoride chloride **78** and the difluoride complex **79**. The structures of both complexes feature a distorted square pyramidal geometry with the indenylide unit at the apical position, as shown in Fig. 23 [67].

Based on known structures of NHC-stabilized Ru fluorides, the NHC–Ru bond lengths in these complexes are typically between 2.05 and 2.20 Å. The Ru–F bond lengths, however, can vary significantly depending on their configuration. When F is in a *cis* position relative to NHC, the bond lengths are generally in the range of 1.98–2.26 Å. A *trans* arrangement usually results in longer Ru–F bond lengths, ranging from 2.18 to 2.38 Å.

4.6. GROUP IX

Group IX chemistry is widely studied due to its catalytic properties

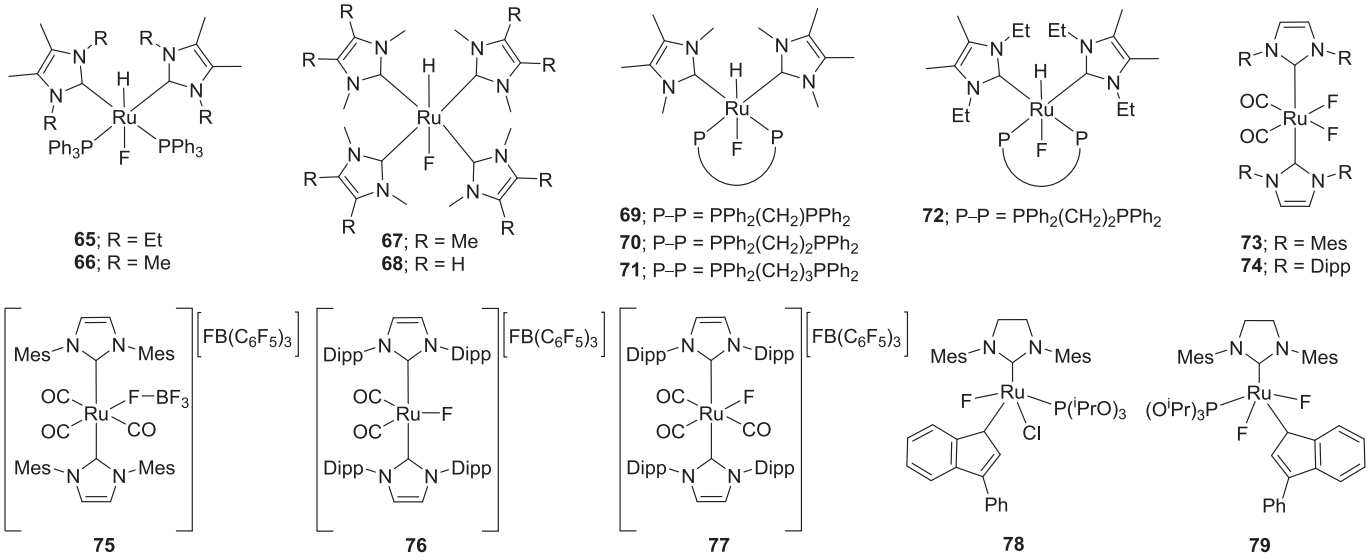

Fig. 22. Schematic representation of **65**–**79**.

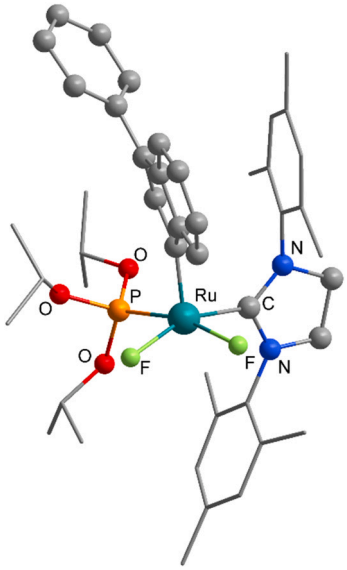

Fig. 23. View of the structure of complex **79**, redrawn from ref. [67].

[68–70]. The chemistry of NHC-stabilized Co compounds has been reviewed in Ref. [29]. Rh(I) complexes with neutral donors and their applications in catalysis have been comprehensively reviewed in Ref. [70], while the chemistry of Ir compounds with NHC carbenes has been reviewed in Ref. [71].

The few NHC-stabilized Co fluorides are found in +3 and +2 oxidation states, while Rh and Ir complexes are found predominantly in the +1 oxidation state.

4.6.1. Cobalt

The only neutral NHC-stabilized CoF_2 complex, $[CoF_2(IMes)_2]$ (**80**), was prepared by reacting the cobalt silylamido complex $Co(N(SiMe_2Ph)_2)_2(THF)_2$ with [(IMes)H][FHF] in the presence of IMes carbene. Compound **80** was prepared using the same procedure as for the CrF_2 and FeF_2 fluorides. The CoF_2 complex adopts a tetrahedral arrangement, as shown in Fig. 24. Structurally, it is similar to the FeF_2 counterpart [50].

A diamagnetic dicationic Co(III) fluorido complex stabilized by a

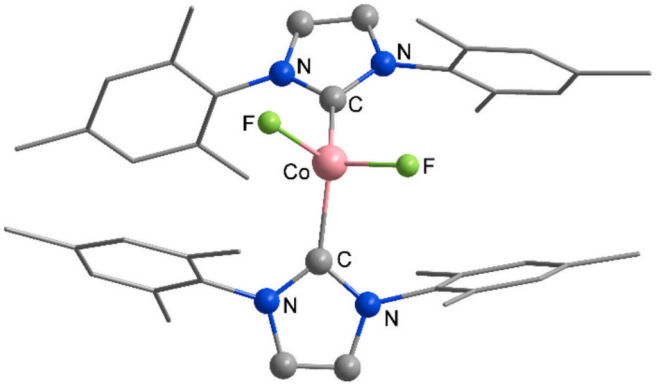

Fig. 24. View of the structure of $[CoF_2(IMes)_2]$ (**80**), redrawn from ref. [50].

trimeric NHC ligand, **81**, was formed by hydrolysis of the corresponding tricationic salt [72], while another dicationic Co(III) fluorido complex stabilized by a chelating NHC ligand, **82**, was prepared from the

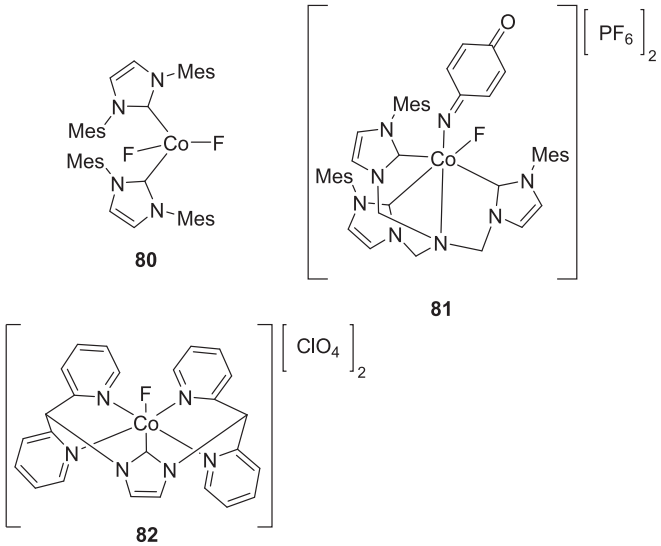

Fig. 25. Schematic representation of **80**–**82**.

corresponding aqua complex in water by fluorination with NaF [73]. The structures of these two cationic complexes are schematically shown in Fig. 25.

Based on the known structures of NHC-stabilized Co fluorides, the NHC–Co bond lengths are typically between 1.95 and 2.15 Å, while the cationic complex **82** features a shorter NHC–Co bond (1.83 Å) [73]. The average Co–F bond lengths are usually between 1.87 and 1.89 Å.

4.6.2. Rhodium

The Whittlesey group began research on NHC-stabilized Rh fluoride catalysts using the same methods as for Ru compounds. Fluorination of [RhH(NHC)(PPh_3)$_2$] (NHC = 6-^{i}Pr, 6-Me, 6-Et) with $Et_3N{\cdot}3HF$ produced the bifluoride complexes *cis*-[Rh(FHF)(6-^{i}Pr)(PPh_3)$_2$] (**83**), *trans*-[Rh(FHF)(6-Me)(PPh_3)$_2$] (**84**), and *cis*- and *trans*-[Rh(FHF)(6-Et)(PPh_3)$_2$] (**85**), as shown in Fig. 26 [74,75]. Subsequent abstraction of HF from **83** with anhydrous Me_4NF yielded the Rh fluoride complex [RhF(6-^{i}Pr)(PPh_3)$_2$] (**86**). Both 6-^{i}Pr complexes **83** and **86** adopt square planar coordination at the metal center, with the two phosphines in a *cis* arrangement, as shown in Fig. 27 [74].

The Rh fluoride complexes can also be synthesized by hydrodefluorination reactions of [RhH(NHC)(PPh_3)$_2$] with fluorinated organic compounds. C–F activation of C_6F_6 leads to the formation of [RhF(6-^{i}Pr)(PPh_3)$_2$] (**86**), while activation of $CF_3CF{=}CF_2$ results in the formation of *cis*-[RhF(6-Me)(PPh_3)$_2$] (**87**) and *cis*-/*trans*-[RhF(6-Et)(PPh_3)$_2$] (**88**) [74,75]. Activation of $C_6F_5CF_3$ and 2-$C_6F_4HCF_3$ yields a *cis*-/*trans*-[RhF(6-^{i}Pr)(PPh_3)$_2$] (**86**) mixture, with predominant formation of the *trans* product [76]. In addition, [RhF(6-^{i}Pr)(PPh_3)$_2$] (**86**) rapidly reacts with CO at room temperature to form [RhF(6-^{i}Pr)(PPh_3)(CO)] (**89**). Its formation was determined only by spectroscopic methods [75].

Treatment of Rh hydroxide complexes [Rh(OH)(NHC)(cod)] with KHF_2 or $Et_3N{\cdot}3HF$ resulted in ligand exchange and the formation of [RhF(NHC)(cod)] (NHC = IDipp **90**, ICy **91**) complexes (Fig. 26). However, in one instance, when excess $Et_3N{\cdot}3HF$ was used, the bifluoride complex [Rh(FHF)(IDipp)(cod)] (**92**) was formed [77].

The rhodium(I) fluoride complex *trans*-[RhF($IMes$)$_2$(CO)] (**93**) was prepared by reacting *trans*-[RhCl($IMes$)$_2$(CO)] with Me_4NF, as shown in Scheme 5 [78]. Both the chloride and fluoride complexes were used in further reactions with SF_5Cl, yielding *trans*,*trans*-[Rh(Cl)$_2$($IMes$)$_2$(CO)][SF_5] and *trans*-[Rh(Cl)(F)($IMes$)$_2$(CO)][SF_5] (**94**), respectively. These were then converted to the fluorido complexes *trans*,*trans*-[Rh(Cl)$_2$(F)(CO)($IMes$)$_2$] (**95**) and *cis*,*trans*-[Rh(Cl)(F)$_2$($IMes$)$_2$(CO)] (**96**) (Scheme 5), respectively. The formation of these complexes was determined only spectroscopically [78].

Based on the known structures of NHC-stabilized Rh fluorides,

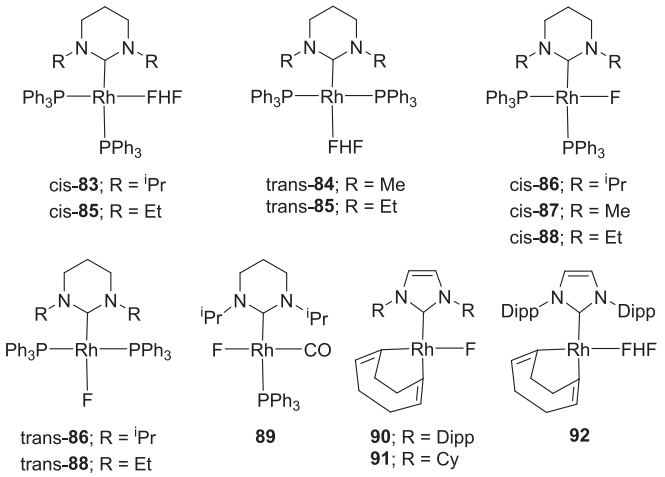

Fig. 26. Schematic representation of **83**–**92**.

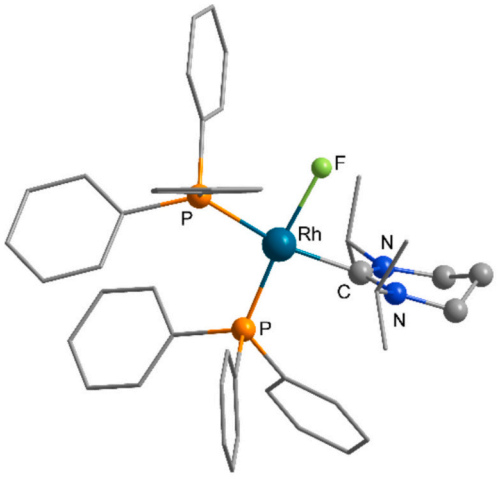

Fig. 27. View of the structure of *cis*-[RhF(6-^{i}Pr)(PPh_3)$_2$] (**86**), redrawn from ref. [74].

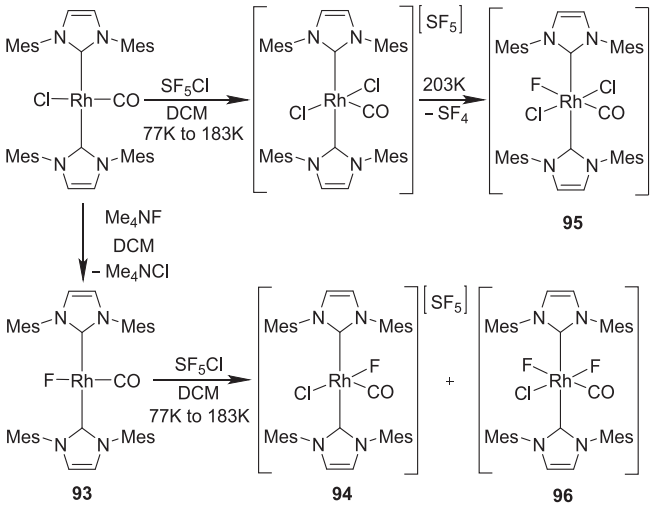

Scheme 5. Reactivity of *trans*-[RhCl($IMes$)$_2$(CO)] and *trans*-[RhF($IMes$)$_2$(CO)] (**93**) with SF_5Cl.

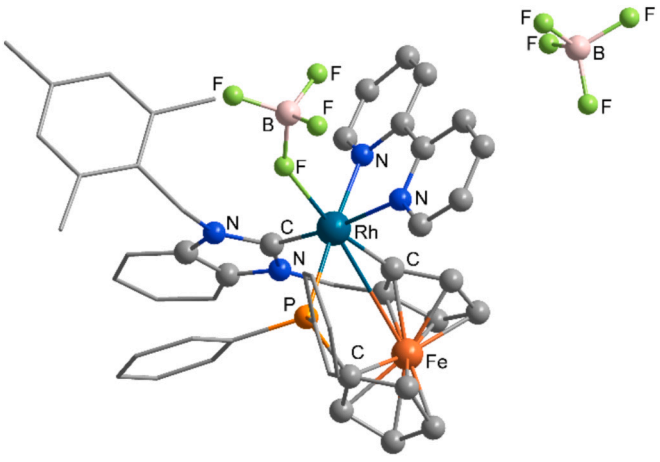

Fig. 28. View of the structure of **97**, redrawn from ref. [79].

including the crystal structure of the ionic compound **97** (Fig. 28), the NHC–Rh bond lengths are typically between 1.97 and 2.06 Å, while the

Rh–F bond lengths generally range from 2.02 to 2.15 Å. As observed for Ru, the Rh–F bond lengths also depend slightly on their configuration. The *cis* arrangement of F and NHC ligands usually results in shorter bond lengths than the *trans* arrangement.

4.6.3. Iridium

Treatment of Ir chloride complexes [IrCl(NHC)(cod)] with AgF, or the hydroxide complex [Ir(OH)(NHC)(cod)] with KHF_2 or $Et_3N{\cdot}3HF$, resulted in ligand exchange and the formation of [IrF(NHC)(cod)] (NHC = IDipp **98**, IDD **99**, I^iPr **100**, ICy **101**) complexes (**Fig. 29**) [77].

However, when excess $Et_3N{\cdot}3HF$ was used, the bifluoride complexes [Rh(FHF)(NHC)(cod)] (NHC = IDipp **102**, I^iPr **103**) were formed. Many of these complexes were structurally characterized. An example of a fluoride and a bifluoride complex is shown in **Fig. 30** [77].

Neutral Ir(I) NHC-chloride complexes [IrCl(NHC)$(CO)_2$] and [IrCl(NHC)(cod)] can be oxidized by XeF_2 at low temperature to yield Ir(III) NHC-fluoride complexes [IrF_2Cl(NHC)(CO)] (NHC = IMes **104**, IDipp **105**) and [IrF_2Cl(NHC)(cod)] (NHC = IMes **106**, IDipp **107**), respectively (**Fig. 29**) [80]. Similarly, the Ir(I) carbonyl cations [Ir(IMes)$(CO)_2$L][BF_4] and [Ir(NHC)$(CO)_2$py][BF_4] react with XeF_2 to produce a mixture of two isomeric difluoride complexes, [IrF_2(IMes)$(CO)_2$L][BF_4] (L = PPh_2Et **108**, PPh_2CCPh **109**) and [IrF_2(NHC)$(CO)_2$py][BF_4] (NHC = IMes **110**, IDipp **111**), in approximately a 1:1 ratio. The reduced stability of cod-containing carbonyl cations hampered the studies, as these compounds rapidly decompose in the presence of XeF_2. All complexes were characterized only spectroscopically, due to their high instability and rapid decomposition in solution during crystallization [80].

Based on known structures of NHC-stabilized Ir fluorides, the NHC–Ir bond lengths in these complexes are typically between 2.02 and 2.05 Å, while average Ir–F bond lengths are usually between 2.01 and 2.07 Å.

4.7. GROUP X

The NHC-stabilized Group X metal fluoride compounds are limited to Ni and Pd. These compounds are found predominantly in the +2 oxidation state. Typically, the complexes are 4-coordinated with square planar geometry. Currently, the NHC complexes of both elements are being extensively studied due to their favorable catalytic properties [81].

4.7.1. Nickel

A comprehensive review of various NHC-stabilized Ni complexes can be found in Ref. [29].

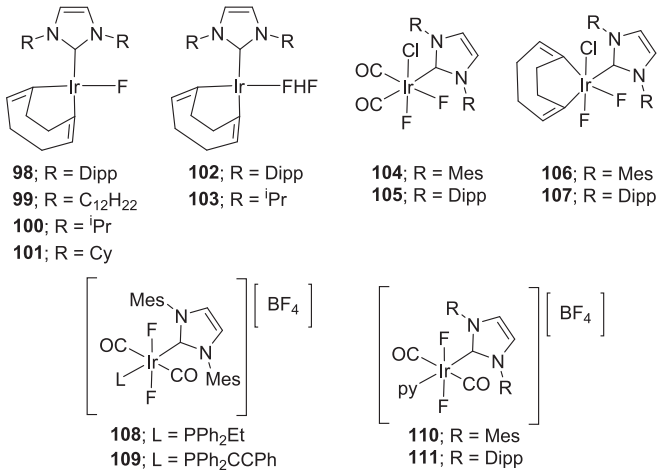

Fig. 29. Schematic representation of **98**–**111**.

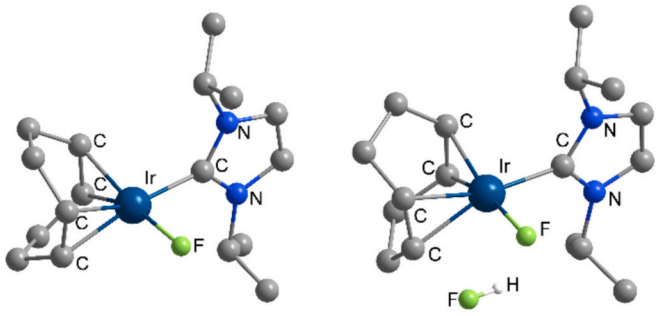

Fig. 30. View of the structures of [IrF(I^iPr)(cod)] (**100**) (left) and [Ir(FHF)(I^iPr)(cod)] (**103**) (right), redrawn from ref. [77].

The Radius group initiated research on NHC-stabilized Ni fluorides. In 2005, the group observed C–F bond activation of C_6F_6 with the NHC-stabilized Ni complex [$Ni_2(I^iPr)_4$(cod)]. The reaction efficiently produced *trans*-[NiF(I^iPr)$_2$(C_6F_5)] (**112**), which was initially characterized only spectroscopically [82]. Its crystal structure was published three years later by the same group, confirming the square planar coordination at the metal center with a *trans* arrangement of NHC ligands (**Fig. 31**) [83]. Alternatively, compound **112** can be synthesized directly by reacting [Ni(cod)$_2$] with I^iPr and C_6F_6 in THF [84].

Encouraged by these results, the group investigated C–F bond activation of other fluorinated arenes. The reactions of [$Ni_2(I^iPr)_4$(cod)] with octafluorotoluene and decafluorobiphenyl in various solvents (THF, benzene, or toluene) proceed with high chemo- and regioselectivity to give *trans*-[NiF(I^iPr)$_2$(4-(CF_3)C_6F_4)] (**113**) and *trans*-[NiF(I^iPr)$_2$(4-(C_6F_5)C_6F_4)] (**114**) (**Fig. 32**). Complex **113** was also structurally characterized, showing the same arrangement as **112** [85]. The same procedure worked very well for other polyfluorinated and partially fluorinated aromatics, yielding to products **115**–**122**. For aromatics of the type C_6F_5R, C–F activation selectively occurs at the *para* position to the R group, affording *trans* products [83]. Next, the group tested [Ni(I^iPr)$_2$(η^2-C_2H_4)] in reactions with previously used fluorinated aromatic compounds. In general, the same products were obtained as with [$Ni_2(I^iPr)_4$(cod)] when the temperature was kept low. However, at room temperature, there were two exceptions. [Ni(I^iPr)$_2$(η^2-C_2H_4)] reacted with pentafluoropyridine to give a mixture of insertion products at positions 4 and 2, forming complexes **122** and **123**, respectively. The same reaction with octafluoronaphthalene at room temperature also yielded a mixture of two isomers, **116** and **124** [83]. Treating complexes **112** or **113** with 1 equiv of [$Ni_2(I^iPr)_4$(cod)] at elevated temperature (60 °C) enabled a second C–F activation of the polyfluoroarene to give dinuclear metal complexes **125** and **126**, respectively. Alternatively, these complexes can be obtained directly from [$Ni_2(I^iPr)_4$(cod)] with 1 equiv of

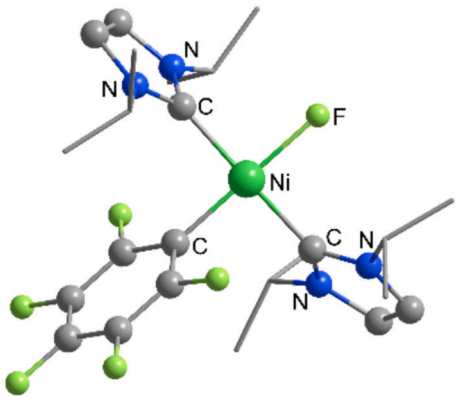

Fig. 31. View of the structures of *trans*-[NiF(I^iPr)$_2$(C_6F_5)] (**112**), redrawn from ref. [83].

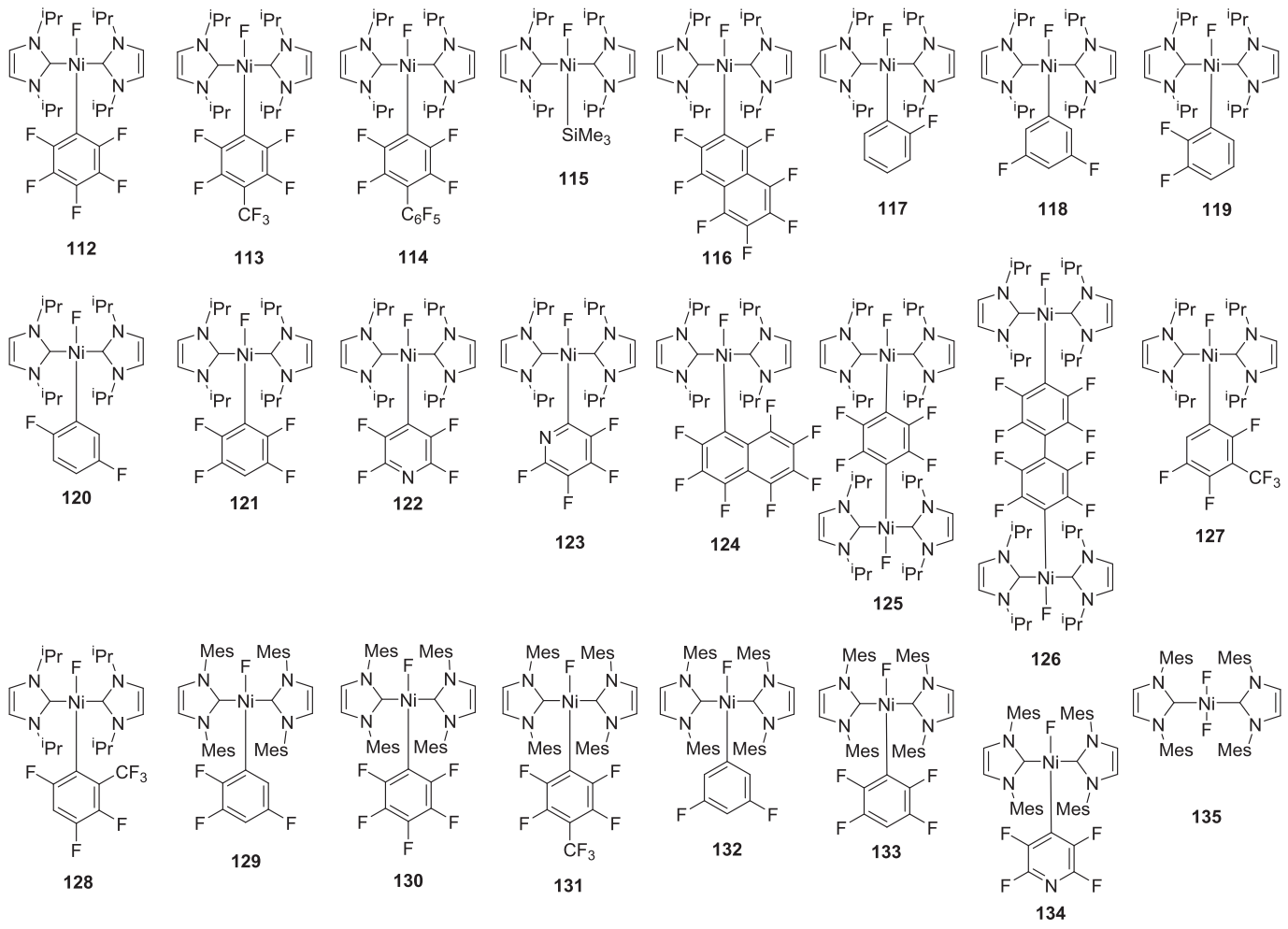

Fig. 32. Schematic representation of **112**–**135**.

C_6F_6 and $C_{12}F_{10}$ at 60 °C in almost quantitative yield [86].

The C–F activation compounds **112** and **113** react with silanes $PhSiH_3$ and Ph_2SiH_2 to form the corresponding hydride complexes [NiH(I^iPr)$_2$(R)]. Both complexes rearrange in solution at room temperature within a few days, or within a few hours at 60 °C. Complex **112** rearranges to compound **121**, which was previously prepared, while complex **113** rearranges to a mixture of isomers **127** and **128** in an approximately 4:1 ratio [87]. The C–F bond activation of arene 1,2,3,5-$C_6F_4H_2$ also proceeds with [Ni(IMes)$_2$], yielding compound **129** in good yield [88]. Similarly, activation of other fluorinated organic compounds with [Ni(IMes)$_2$] leads to the formation of compounds **130**–**134** [89]. During the formation of **130** with C_6F_6, small amounts of a side product were obtained, which turned out to be the NiF_2 compound *trans*-[NiF_2(IMes)$_2$] (**135**). However, when the reaction mixture was stored in solution for 3 days at –30 °C, a one-electron oxidative addition reaction may occur, leading to the formation of the Ni(I) compound *trans*-[Ni^I(C_6F_5)(IMes)$_2$] and the Ni(I) radical species [Ni^IF(IMes)$_2$]. Alternatively, compound **135** was prepared by fluorination of the corresponding diiodo complex with 2 equiv of AgF in DCM [89], and by the reaction of nickelocene with [(IMes)H][F] [90].

[NiF(I^iPr)$_2$(C_6F_5)] (**112**) forms adducts with $C_6F_4I_2$ and indole by forming halogen or hydrogen bonds with ligands in compounds **136** and **137** (Fig. 33). In the crystal structure of **136**, compound **112** coordinates to two $C_6F_4I_2$ ligands, forming a zigzag chain structure as shown in Fig. 34. In contrast, the formation of **137** was confirmed only in solution [91]. The scope of research was then extended to other NHC-stabilized Ni fluorides. [NiF($^{Me2}I^iPr$)$_2$(C_6F_5)] (**138**) coordinates one

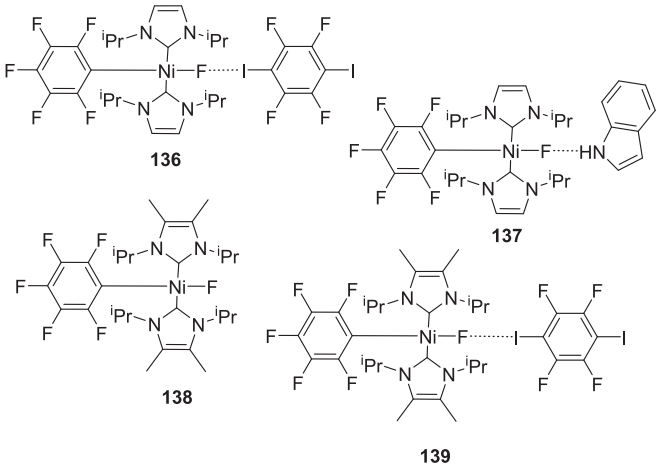

Fig. 33. Schematic representation of **136**–**139**.

$C_6F_4I_2$ ligand to form **139** (Fig. 33). The formation of only one halogen bond in **139** was attributed to steric hindrance from the bulkier carbene. Moreover, the even more sterically encumbered complex [NiF(IMes)$_2$(C_6F_5)] (**130**) does not form an adduct with $C_6F_4I_2$ [91].

The *trans*-[NiF(ICy)$_2$(Ar)] (**140**) (Fig. 35) was obtained directly in a one-pot reaction starting from Ni(cod)$_2$ and an ammonium triflate in the presence of [(ICy)H][BF_4] and CsF as a deprotonation agent. The

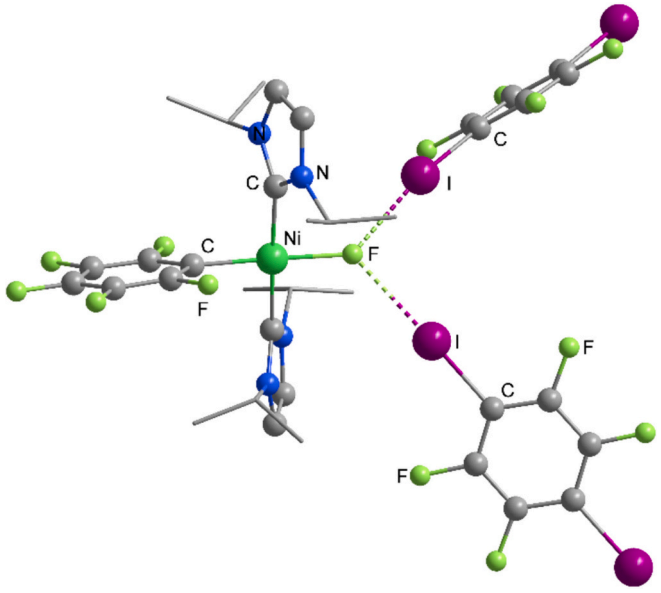

Fig. 34. View of the structures of **136**, redrawn from ref. [91].

reaction proceeded in higher yields at elevated temperature (80 °C). The structure of **140** agrees well with previously determined related compounds. It features a square planar geometry with a *trans* arrangement of the NHC ligands at the Ni(II) center [92]. A similar result was observed by the oxidative addition of a Ni(0) compound, Ni(6-Mes)$(PPh_3)_2$, with C_6F_6, which resulted in the formation of *trans*-[NiF(6-Mes)$(PPh_3)(C_6F_5)$] (**141**) [93].

The Ni(0) NHC-stabilized complexes [Ni$(NHC)_2$] were able to activate C(sp^3)–F bonds of Ar-CF_3 compounds to afford the corresponding *trans*-difluorobenzyl Ni(II) fluoride complexes [NiF$(NHC)_2(CF_2Ar)$]. Activation of C(sp^3)–F bonds proceeded efficiently with the Ni complex bearing the sterically non-demanding carbene ligand I^{i}Pr (**142**), while the bulkier ICy produced **143** in lower yield (**Fig. 35**). However, complexes with more sterically demanding carbenes I^{t}Bu, IMes, and IDipp did not engage in C(sp^3)–F bond activation [94]. The group also tested the effect of different Ar groups on C(sp^3)–F bond activation, producing the series of complexes **144**–**148**. They found that the degree of electron deficiency of the arene ring significantly impacts reactivity, as does the position of the electron-withdrawing groups [94]. Soon after, the bond activation patterns were further extended to hydrofluoroolefins. Ni$(cod)_2$ reacted with IAd and 1,1-difluoroethylene to afford the dimeric compound **149**, while the same synthesis with the addition of DMAP afforded the monomeric compound **150** [95].

A planar cationic complex, **151** (**Fig. 36**), was obtained from the reaction of Ni$(cod)_2$ with an imidazolium salt. The crystal structure of the cationic complex also features square planar geometry with the phosphine ligands in *trans* positions [96]. The tetrabutylammonium salt of the anionic nickel fluoride **152** was prepared by reaction of the corresponding DMF complex with TBAF·$3H_2O$, which upon oxidation formed the corresponding neutral tetracoordinated Ni(III) complex **153** [97]. Formation of NHC-stabilized NiF complexes is also possible by fluorination of the corresponding chlorido complex. The chloride-fluoride exchange reaction quantitatively produced **154** using SCF_3-based reagents ($AgSCF_3$, $CuSCF_3$, NMe_4SCF_3) or AgF for fluorination [98].

Almost all known structures of NHC-stabilized Ni fluorides exhibit a square planar geometry at the metal center. The only exceptions are the recently published structures of **155** (CSD communication No. 2376667) and **156** (CSD communication No. 2214689) [99,100]. Generally, the NHC–Ni bond lengths range from 1.84 to 1.96 Å, while the Ni–F bond lengths are typically between 1.83 and 1.94 Å, except for the cationic complex **151** (2.12 Å) [96]. Among the wide variety of complexes with fluorinated aromatic ligands, it is notable that Ni–F bonds are slightly shorter with a higher degree of fluorination on the aromatic ligands [89].

4.7.2. Palladium

The first NHC-stabilized Pd fluoride compounds were prepared from the corresponding chloride or methyl analogues by exchanging ligands for a BF_4^- anion. The formation of fluoride-bridged complexes was confirmed by the crystal structure determination of **157** (**Fig. 37**). The structure of its IDipp counterpart, **158**, is presumably similar to **157** [101]. The group also attempted to prepare complexes with even weaker nucleophiles (PF_6 and AlR_4). Although the complexes formed by ligand exchange in solution, their X-ray single-crystal structures could not be determined [101].

Using a similar ligand exchange procedure, the Pd complex with bridging bonds to BF_4^-, **159** (**Fig. 38**), was prepared from the corresponding chloride analogue by adding $AgBF_4$. Compound **159** is a neutral complex in the solid state, but in solution it may be described as an inner-sphere ion pair [102].

Next, a series of Pd(II) fluoride complex cations stabilized by NHC-based pincer ligands **160**–**162** (**Fig. 38**) was prepared by fluorinating the corresponding chloride analogues with AgF in MeCN [103]. Electrophilic fluorination of a Pd(II) tetrafluoroborate salt with Selectfluor or NFSI enabled the formation of the Pd(IV) cationic complex **163** with octahedral coordination [104]. The compound was characterized by spectroscopy, mass spectrometry, and XPS analysis. Despite several attempts, suitable single crystals of **163** could not be obtained [104]. It is

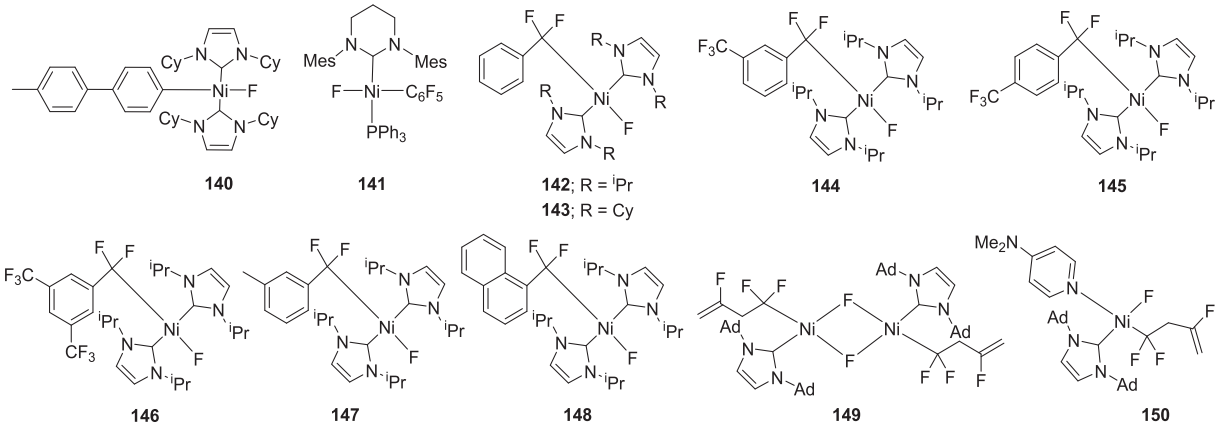

Fig. 35. Schematic representation of **140**–**150**.

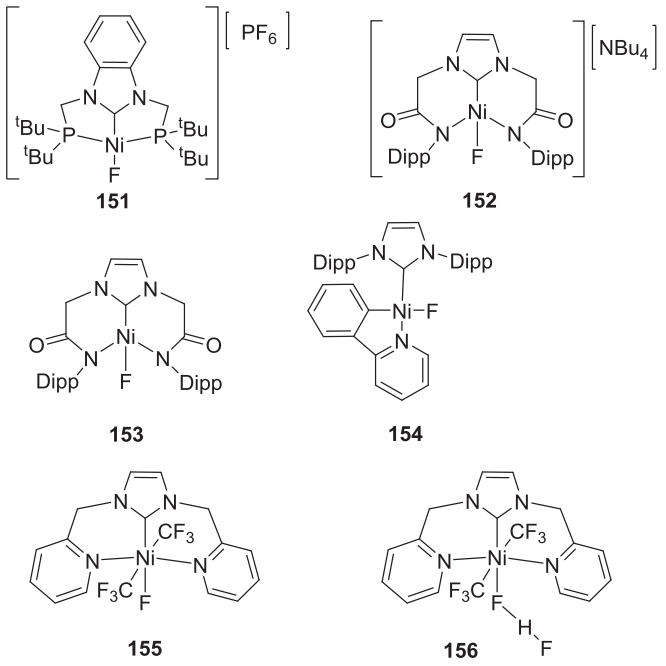

Fig. 36. Schematic representation of **151**–**156**.

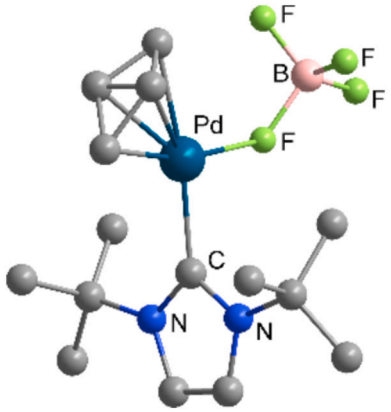

Fig. 37. View of the structures of **157**, redrawn from ref. [101].

worth mentioning that Pd(II) fluoride compounds are difficult to prepare due to excessive hard/soft mismatch. However, the group of Munz managed to prepare one from intermediate Pd imido complexes, which exhibit nitrene character, and C_6F_6. Activation of C_6F_6 led to the formation of compounds **164** and **165** [105]. These two compounds are the only Pd complexes featuring CAAC-based carbene ligands.

All known structures of neutral NHC-stabilized Pd fluorides, including the dimeric NHC-stabilized mixed Pd fluoride/chloride complex **166** (CSD communication No. 1031958) [106], adopt a square planar geometry at the metal center. The only exception is the octahedral complex **163** [104]. In general, the NHC–Pd bond lengths are between 1.94 and 2.07 Å, while the Pd–F bond lengths are typically in the range of 1.96–2.01 Å. Complexes with Pd–F bridging bonds exhibit longer bonds of 2.24 Å (**157**) [101] and 2.26 Å (**159**) [102].

4.8. GROUP XI

The NHC-stabilized Cu, Ag, and Au fluorides are mostly found in the +1 oxidation state. Only Au also forms compounds in the +3 oxidation state. The chemistry of these elements has been extensively studied because of their catalytic and biological properties.

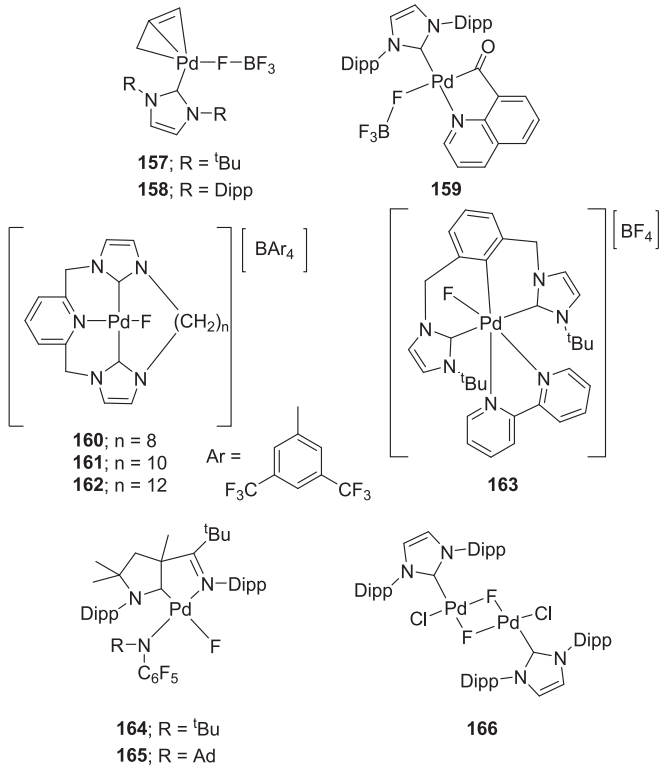

Fig. 38. Schematic representation of **157**–**166**.

4.8.1. Copper

A comprehensive review of various Cu-NHC complexes is available in ref. [29].

The first NHC-stabilized copper fluoride complex, [CuF(IDipp)] (**167**), was prepared by adding 0.33 equiv $Et_3N{\cdot}3HF$ to [Cu(OtBu)(IDipp)]. Initially, it was characterized only spectroscopically and used as a catalyst in further studies on the transmetalation reactions of organosilanes [107]. In 2020, its structural characterization revealed a linear arrangement at the Cu center, as shown in **Fig. 39** [108].

The same method was also used to synthesize [CuF(^{Cl2}IDipp)] (**168**), [CuF(SICy)] (**169**), [CuF(IMes)] (**170**), and the sterically demanding **171** (**Fig. 40**) [109–111]. Alternatively, the synthesis of **167** and **170** started from the corresponding chloride, which was first converted to the O^{t}Bu complex using NaO^{t}Bu and then to the fluoride using $Et_3N{\cdot}3HF$ [110,112]. However, when the reactions were carried out with 2 equiv of HF instead of 1, bifluoride complexes were formed. [Cu(F-HF)(IDipp)] (**172**) was structurally characterized, revealing a structure similar to **167** with an additional HF forming the bifluoride [113]. Bifluoride complexes can also be prepared directly from [CuCl(NHC)] using $AgHF_2$, which, in addition to complex **172**, also resulted in the synthesis of [CuF(SIDipp)] (**173**) and the two more sterically

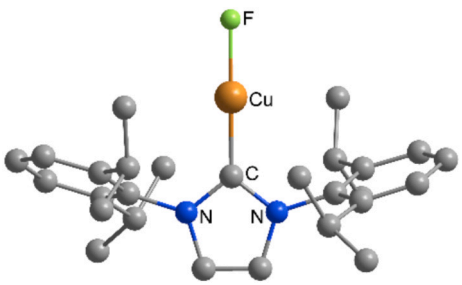

Fig. 39. View of the structure of [CuF(IDipp)] (**167**), redrawn from ref. [108].

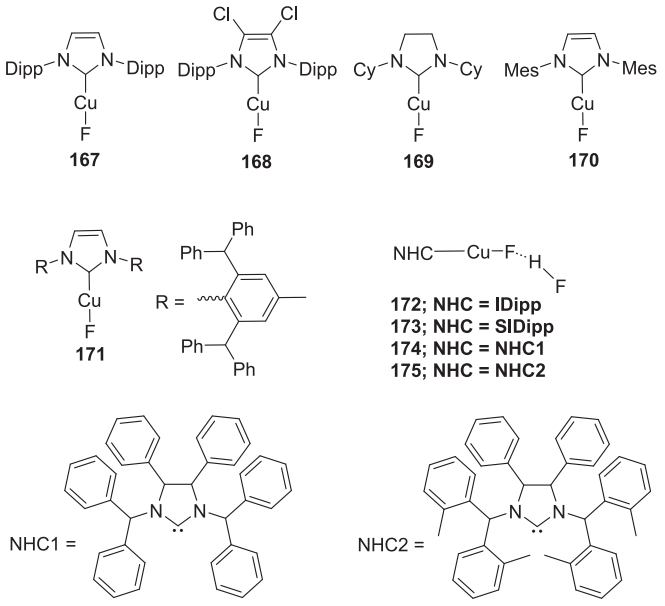

Fig. 40. Schematic representation of **167–175**.

encumbered variations **174** and **175** [113].

Fluorination of [Cu(Mes)(carbene)] complexes with 0.33 equiv $Et_3N{\cdot}3HF$ yielded various NHC- and CAAC-stabilized fluoride complexes: [CuF(6-Mes)] (**176**), [CuF(7-Mes)] (**177**), two more sterically encumbered carbene complexes **178** and **179**, and the CAAC counterpart **180** (Fig. 41) [114]. The same method was also used to prepare [CuF(NHC)] (NHC = IDipp **167**, SIDipp **181**, I^tBu **182**, ^{Me2}IMe **183**, $^{Me2}I^iPr$ **184**, and ^{Me}CAAC **185**) [115]. Alternatively, these complexes could be prepared from the corresponding chloride complex by reaction with NaO^tBu or KO^tBu, followed by fluorination with $Et_3N{\cdot}3HF$. In some cases, these conditions gave better yields [115]. Additionally, synthesis of [CuF(IAd)] (**186**) demonstrated that CuF complexes can also be prepared from the chloride counterpart using TMAF reagents [116], while fluorination of [Cu(O^tBu)(SIDipp)] with benzoyl fluoride also proved to be a feasible method for preparing terminal fluorides such as [CuF(SIDipp)] (**181**) [117]. Furthermore, when this compound subsequently reacts with $[Ph_3C][BF_4]$, it undergoes fluoride abstraction, forming a dinuclear fluoride-bridged cation in compound [(SIDipp)Cu-F-Cu(SIDipp)]$[BF_4]$ (**187**) [117]. The same cationic complex was also prepared by reacting [CuF(SIDipp)] with [Cu(OTf)(SIDipp)], resulting in the formation of the triflate salt **188**. In addition, the corresponding IDipp fluorine-bridged cationic compound **189** was also prepared [118].

Treatment of $CuSiF_6$ with an imidazolium salt led to in the formation of the Cu(II) NHC-stabilized complex **190** (Fig. 42). In its crystal structure, the compound adopts a pseudo-octahedral arrangement at the Cu(II) center, with a Cu–F contact of 2.56 Å [119]. This compound is a rare example of a Cu(II) NHC complex, which formed despite the unfavorable hard-soft interactions between carbon and Cu(II) [119]. Treatment of [CuBr(SIDipp)] with $AgSbF_6$ in the presence of carbon monoxide yielded the Cu(I) dicarbonyl complex $[Cu(CO)_2(IDipp)][SbF_6]$ (**191**). In its crystal structure, Cu forms a contact with F of 2.49 Å (Fig. 42). However, this contact is not strong enough to distort the Cu from the trigonal planar geometry of the $[Cu(CO)_2(SIDipp)]^+$ cation [120].

Based on the known structures of NHC-stabilized Cu fluorides, the NHC–Cu bond lengths in these complexes are usually between 1.85 and 1.96 Å, while the average Cu–F bond lengths are typically between 1.78 and 1.87 Å. The only exceptions are the Cu–F contact bond lengths in structures **190** and **191**, where SiF_6^{2-} and SbF_6^- are coordinated to Cu, respectively [119,120].

4.8.2. Silver

There are only a few NHC-stabilized AgF compounds. The first neutral complex, [AgF(SIDipp)] (**192**) (Fig. 43), was prepared by reacting [Ag(O^tBu)(IDipp)] with benzoyl fluoride, similar to the Cu compounds [117]. In this case, the subsequent reaction of **192** with $[Ph_3C][BF_4]$ led to fluoride abstraction and the formation of a dinuclear, fluoride-bridged cation in compound [(SIDipp)Ag-F-Ag(SIDipp)]$[BF_4]$ (**193**). The dinuclear complex is the only NHC-stabilized AgF compound that has also been structurally characterized. It features a linear arrangement at each Ag center and a bent arrangement at the fluoride. The average NHC–Ag bond distance is 2.05 Å, while the average Ag–F bond distance is 2.07 Å [117]. The structure is shown in Fig. 44.

Later, the benzoyl fluoride fluorination method was used by the same group to prepare the [AgF(6-Dipp)] (**194**) and [AgF(7-Dipp)] (**195**) complexes (Fig. 43) [121].

4.8.3. Gold

The properties of Au fluorides stabilized by NHC and other neutral ligands have been reviewed to some extent in ref. [26].

The first NHC-stabilized gold fluoride complex, [AuF(SIDipp)] (**196**) (Fig. 45), was prepared from the corresponding chloride compound. The chloride compound was first converted to the O^tBu derivative using NaO^tBu, which was then reacted with 0.33 equiv of $Et_3N{\cdot}3HF$ to form the fluoride complex **196**. Structural determination revealed a linear geometry at the Au center, similar to the related Cu complexes described above [122]. Complex **196** was also prepared by the benzoyl fluoride fluorination method from the corresponding O^tBu substrate [117]. Subsequently, reaction of **196** with $[Ph_3C][BF_4]$ resulted in the formation of a dinuclear fluoride-bridged cation in compound [(SIDipp)Au-F-

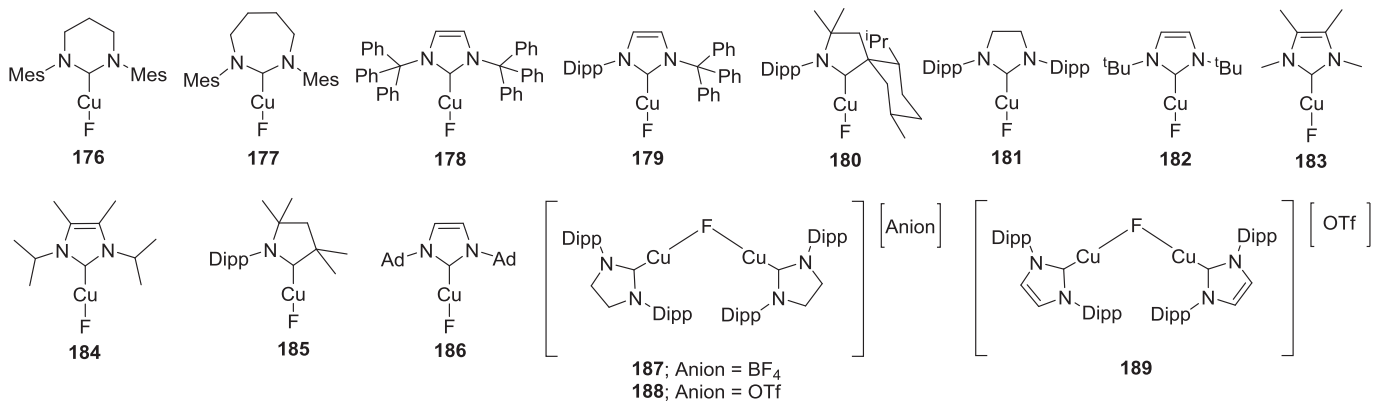

Fig. 41. Schematic representation of **176–189**.

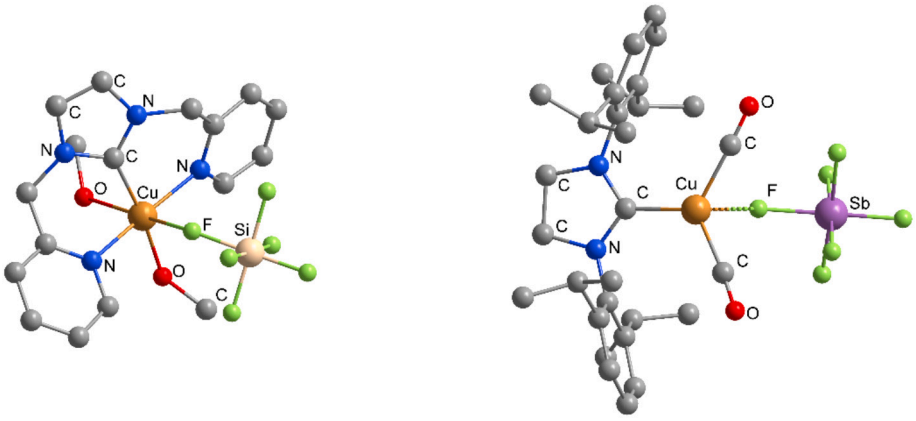

Fig. 42. View of the structures of **190** (left) and **191** (right), redrawn from ref. [119, 120].

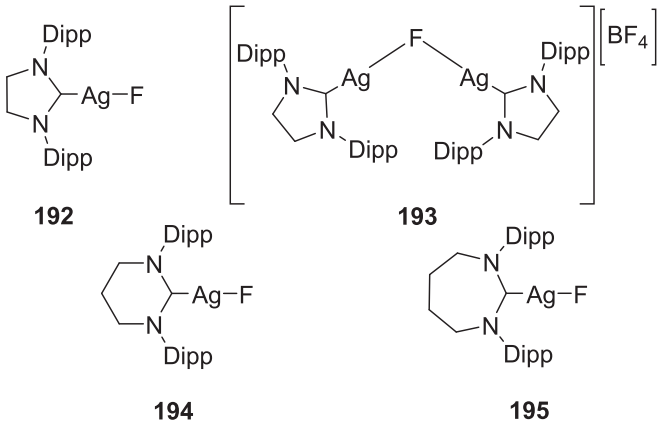

Fig. 43. Schematic representation of **192–195**.

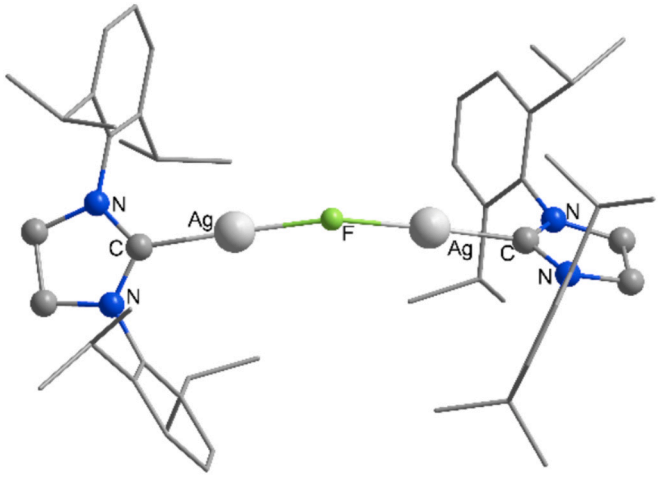

Fig. 44. View of the structures of the cationic complex in **193**, redrawn from ref. [117].

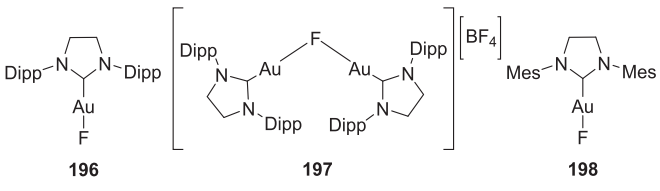

Fig. 45. Schematic representation of **196–198**.

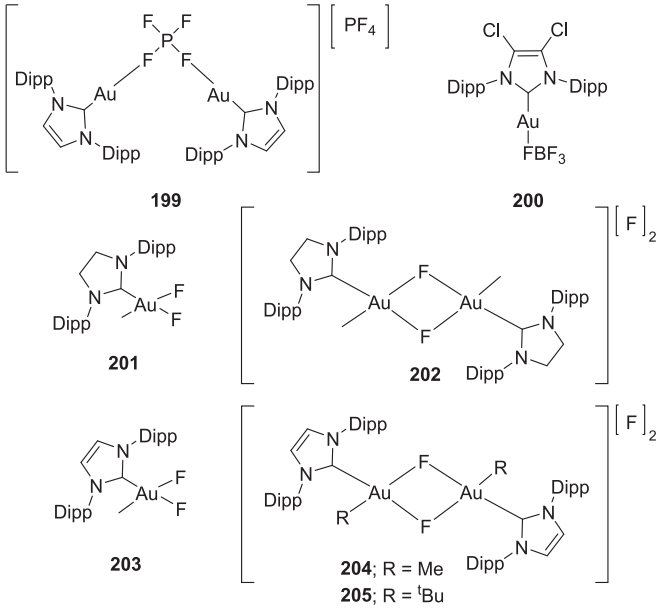

Fig. 46. Schematic representation of **199–205**.

Au(SIDipp)][BF_4] (**197**) [117]. The benzoyl fluoride method was also used to prepare [AuF(SIMes)] (**198**) from the corresponding alkoxide [123].

In 2009, Nolan's group prepared a rare compound featuring a bridging anionic PF_4 ligand bonded to two Au(IDipp) units in [(μ-PF_4)(Au(IDipp))$_2$][PF_4] (**199**) (Fig. 46). The complex formed as a result of decomposition during slow crystallization [124]. Metathesis of [AuCl(^{Cl2}IDipp)] with $AgBF_4$ led to the formation of [Au(F-BF_3)(^{Cl2}IDipp)] (**200**), which is best described as an inner-sphere complex [125]. Alternatively, **200** can be prepared from the corresponding acetonyl complex using $HBF_4{\cdot}OEt_2$. However, the bonding of BF_4 to Au is reversible. In $CDCl_3$, the BF_4 dissociates, forming the solvent-separated ion pair [Au(^{Cl2}IDipp)($CDCl_3$)][BF_4] [125].

Oxidation of [AuMe(SIDipp)] with XeF_2 led to the formation of the first Au(III) fluoride species. In solution, a mixture of [AuF_2(Me)(SIDipp)] (**201**) and the dimer **202** was observed (Fig. 46), while slow crystallization yielded only crystals of **202**, attributed to its lower solubility [126]. The same reaction with the IDipp analogue produced [AuF_2(Me)(IDipp)] (**203**) as the sole product, while slow crystallization again yielded the corresponding dimer **204**. In contrast, using [Au(^{t}Bu)(IDipp)] as the starting compound, which contains a more sterically

demanding group, resulted in the formation of dimer **205** as the only product [126]. Using the same fluorination procedure, the group identified a series of [AuF_2(R)(IDipp)] complexes **206**–**210** in solution (**Fig. 47**) [127,128]. However, these complexes tend to decompose in solution to form [AuF(IDipp)] (**211**) as the major product, along with other organic elimination products [127]. Later, **211** was quantitatively prepared by fluorination of the corresponding [Au(OH)(IDipp)] complex with KHF_2 [129]. Additionally, it formed as a side product during hydrofluorination of NHC-stabilized Au alkoxy complexes [129].

[AuF_3(SIMes)] (**212**) (**Fig. 47**) was obtained from [NMe_4][AuF_4] and SIMes carbene in DCM. At the same time, the ionic compound **213**, containing [$AuF_2(SIMes)_2]^+$ cations, was also formed. Compound **213** can be selectively prepared using two or more equiv of SIMes. It was characterized only spectroscopically and is most likely present as a chloride salt after Cl/F exchange in DCM [130]. Compound **212** is also the first structurally characterized NHC-stabilized AuF_3 species (**Fig. 48**). In its crystal structure, it features a square-planar coordinated Au center. Due to the *trans* influence, the length of the Au–F bond in the *trans* position (1.972(1) Å) is elongated compared with the *cis*-positioned bonds (1.916(1) and 1.921(1) Å) [130]. This feature enables subsequent substitution of the *trans*-F with other substituents. [AuF_2Cl(SIMes)] (**214**) was prepared by reacting **212** with Me_3SiCl, while [$AuF_2(OTeF_5)$(SIMes)] (**215**) was obtained using $Me_3Si(OTeF_5)$ [131]. Both complexes are more stable than **212**, and further replacement reactions were not observed [131]. In contrast, trifluoromethylation of **212** with Me_3SiCF_3 in the presence of CsF resulted in mixtures of compounds. According to ^{19}F NMR investigations in DCM, the reaction first leads to the formation of [$AuF_2(CF_3)$(SIMes)] (**216**), but over time [$AuF(CF_3)_2$(SIMes)] (**217**) is also formed. In THF, the reaction preferentially yields **217** and [$Au(CF_3)_3$(SIMes)], likely due to the better solubility of CsF in THF compared with DCM, which enhances activation of Me_3SiCF_3 [132]. The *trans*-F in [AuF_3(SIMes)] (**212**) was also substituted by several other ligands with different electronic properties. Monosubstitutions yielded alkynido, cyanido, azido, and a series of perfluoroalkoxido complexes **218**–**225** [133]. Upon close examination of complexes **212**–**225**, the group demonstrated that the electron-withdrawing nature of the ligand in the *trans* position influences the Lewis acidity of the Au(III) center. More electron-withdrawing groups lead to shorter and stronger NHC–Au bonds. This trend also correlates with the calculated SIMes affinities and the chemical shifts of the carbene carbon atom in ^{13}C NMR spectra. Finally, the ligands were classified by their *trans* influence, in the order $OTeF_5$<F<OCF_3≈OC_2F_5≈OC_3F_7≈OC_4F_9<Cl<CN ≈N_3<CCH≈$CCSiMe_3$<CF_3 [133].

The carbene complexes [AuF(SIDipp)] (**196**) and [AuF(IDipp)] (**211**) reacted with poly(4-vinylpyridinium poly(hydrogen fluoride)) to form [Au(F-HF)(IDipp)] (**226**) and [Au(F-HF)(SIDipp)] (**227**), respectively (**Fig. 49**). The formation of these two complexes was confirmed in solution by ^1H and ^{19}F NMR spectra [134]. Oxidation of the Au(I) complex stabilized by a bis(NHC)-carbazolide pincer ligand with Selectfluor reagent produced an ionic compound with an Au(III) center, **228**, in 37% yield [135]. Recently, the ionic compounds with Au(III) fluoride centers **229** and **230** were prepared by fluorination of the corresponding chloride salts with AgF [136].

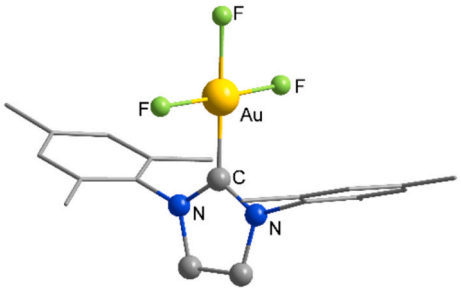

Fig. 48. View of the structure of [AuF_3(SIMes)] (**212**), redrawn from ref. [130].

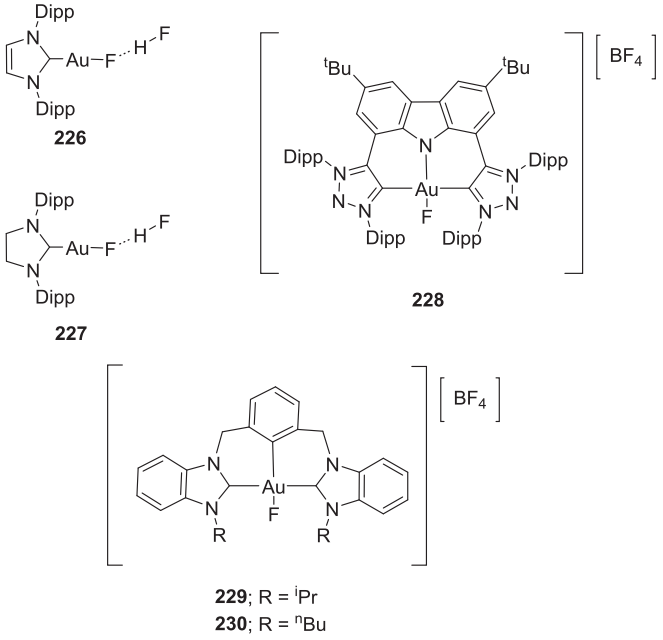

Fig. 49. Schematic representation of **226**–**230**.

Based on known crystal structures of NHC-stabilized Au fluorides, the NHC–Au bond lengths in these complexes are typically between 1.94 and 2.05 Å, while the Au–F bond lengths can vary significantly depending on the configuration. Au(III) complexes with square planar geometry generally have Au–F bond lengths in the range of 1.91–1.94 Å, whereas Au(I) complexes with linear geometry usually have Au–F bond lengths ranging from 1.97 to 2.08 Å. Notably, a *trans* arrangement of F relative to NHC usually results in longer Au–F bonds.

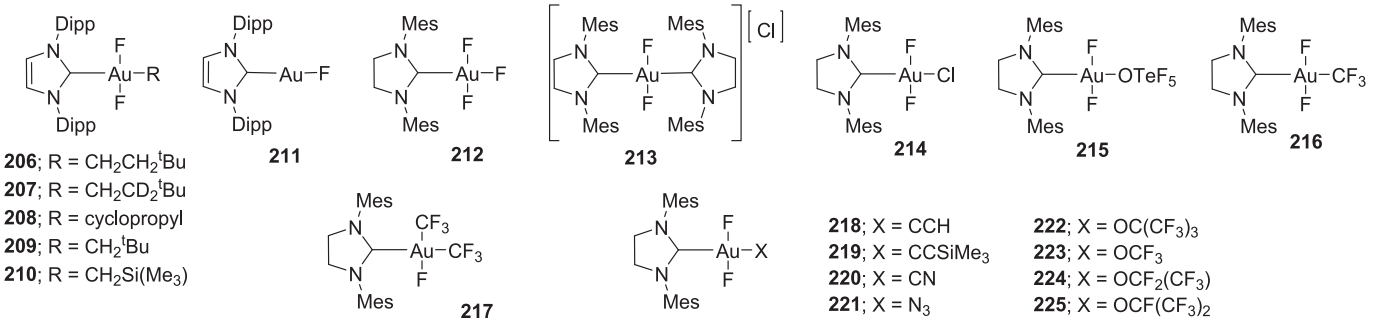

Fig. 47. Schematic representation of **206**–**225**.

5. p-block compounds

5.1. GROUP XIII

BF_3 is a gaseous compound and a reactive Lewis acid that promptly reacts with Lewis bases to form coordination compounds. In contrast, the heavier counterparts MF_3 (M = Al, Ga, In) are unreactive polymeric solids, with an octahedral environment at the metal center. Group XIII metal fluorides stabilized with NHC ligands are mostly found in the +3 oxidation state. Upon reduction, rare examples in the +1 oxidation state have been prepared.

5.1.1. Boron

NHC-stabilized B fluorides are widely studied. A broad variety of synthetic methods are used for their preparation.

The first [BF_3(NHC)] (NHC = ^{Me2}IMe **231**, ^{Me2}IEt **232**, ^{Me2}I^{i}Pr **233**) adducts (Fig. 50) were prepared by the direct reaction of the free NHC with $BF_3{\cdot}Et_2O$ in THF solution [137]. The adduct **231** was also structurally characterized, revealing a tetrahedral coordination at the B center [138].

The same method was also used to prepare the adducts [BF_3(IMes)] (**234**) [139], [BF_3(^{Cl2}IMes)] (**235**) [139], and [BF_3(IDipp)] (**236**) [140]. The latter was also prepared by reacting a free carbene with $NOBF_4$ [141]. The crystal structure of **236** is shown in Fig. 51 and represents a typical example of a tetrahedrally coordinated NHC-stabilized B fluoride adduct. The structure was reported in 2020 as a CSD Communication (No. 2010795) [142].

Adduct **236** was used as a precursor for further functionalization of the backbone. Deprotonation with n-BuLi enabled formation of the lithiated product **237** [140], which can subsequently be converted to **238** and **239** by addition of the electrophiles TMS or ethyloxirane, as shown in Scheme 6 [143]. The lithiated **237** also reacts with AgCl to form the lithium salt **240**, which was further functionalized by addition of [Ru(*p*-cymene)Cl_2]$_2$ to form the dimer **241**. This is a rare example of an abnormally bound Ru complex with two Ru centers connected by bridging chloride atoms [140]. Compound **241** was further reacted with Ag(Et_2O)[$B(C_6F_5)_4$] to give compound **242**, and with the monodentate ligands PPh_3 and CO to give the monomeric adducts **243** and **244**, respectively [140].

Using the free carbene route, a DAC-stabilized BF_3 adduct **245** (Fig. 52) was prepared from the DAC carbene and $BF_3{\cdot}Et_2O$ in benzene [144]. Similarly, [BF(I^tBu)$(Mes)_2$] was also synthesized. Although the carbene adduct is observed in solution, it quickly rearranges to the thermodynamically more favorable abnormal carbene adduct [BF(aI^tBu)$(Mes)_2$] (**246**) [145]. The crystal structure of **246** was first published by the authors in 2014, revealing the tetrahedral arrangement at the B center. Years later, the same group published the structure of **246** as a cocrystal and as a solvate in CSD communications (No. 2282956, and 2282952, respectively) [146,147]. The same group also published the crystal structures of the abnormally bonded aIDipp compound [BF(aIDipp)$(Mes)_2$] (**247**) (CSD No. 2282984) [148], [BF_3($^{Me2}I^tBu$)] (**248**) (CSD No. 2282987) [149], [BF_2($^{Me2}I^tBu$)OTf] (**249**) (CSD No. 2282989) [150], [BF_2(I^tBu)OTf] (**250**) (CSD No. 2282988) [151], and [BF_3($^{Cl2}I^tBu$)] (**251**) (CSD No. 2282996) [152].

The free carbene route was also used to synthesize various CAAC adducts. Reactions of CAAC carbenes with $BF_3{\cdot}Et_2O$ yielded adducts **252** and **253** (Fig. 52) [153], the BICAAC adduct **254** [154], and [BF_3(^{Me}CAAC)] (**255**) [17]. The latter reacted with 1 equiv of free ^{Me}CAAC and 2 equiv of KC_8 to give [BF(^{Me}CAAC)$_2$] (**256**), which subsequently underwent one-electron oxidation in reaction with $LiB(C_6F_5)_4$ to produce the ionic compound with the radical cation [BF(^{Me}CAAC)$_2$][$B(C_6F_5)_4$] (**257**) [17]. In their crystal structures, compound **256** and the radical cation of **257** adopt trigonal planar geometry at the B center, as shown in Fig. 53 [17].

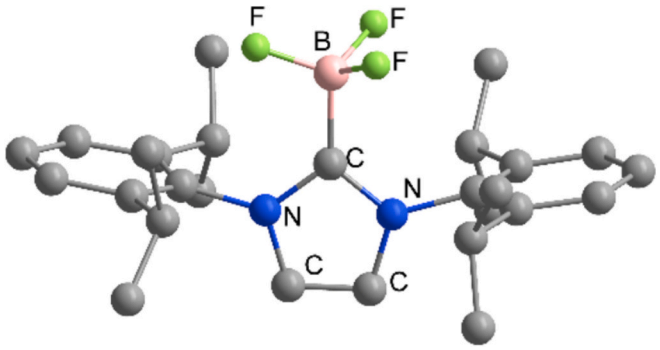

Fig. 51. View of the structure of **236**, redrawn from CSD No. 2010795 [142].

Instead of using free carbene, a carbene-transfer reagent [AgI(NHC)] was used to produce [BF_3(NHC)] (**258**) in combination with $BF_3{\cdot}Et_2O$, a BF_3 source [155]. The adduct **258** was subsequently functionalized to form adducts **259**–**261**, as shown in Scheme 7 [155].

In a similar experiment, the carbene-transfer reagent [$SiCl_4$(IMe)] was used to produce [BF_3(SIMe)] (**262**) (Fig. 54) [156], while [BEt_3(IMes)] was used to produce [BF_3(IMes)] (**234**) [157]. The NHC-stabilized Mg complex also acted as a carbene-transfer reagent in the reaction with $BF(Mes)_2$, resulting in the formation of [$BF(Mes)_2(I^iPr)$] (**263**) [158]. Carbene transfer was also observed in the formation of the bis-NHC-stabilized BF_3 adduct **264**. In this case, an Ag(I) NHC-stabilized salt with $[BF_4]^-$ anions was used as the starting compound, which formed **264** in combination with $ZnCl_4$. This reaction represents the first reported case of a $[BF_4]^-$ anion acting as a source of BF_3 [159].

Later, imidazolium-based tetrafluoroborate salts proved to be effective precursors for NHC-stabilized BF_3 adducts. At elevated temperatures, [(NHC)H][BF_4] undergoes dehydrofluorination to form [BF_3(NHC)] adducts. At temperatures above 227 °C, adducts **265** and **266** were obtained (Fig. 54) [160,161], while **267** was obtained at 300–400 °C [162]. [BF_3(SIDipp)] (**268**) formed at 120 °C from the corresponding tetrafluoroborate salt in the presence of [Fe{N($SiMe_3$)$_2$}$_2$], which presumably facilitated the dehydrofluorination reaction [163]. Trimethylsilyl-substituted triazaphospholenium tetrafluoroborate salts were converted to the corresponding carbene-stabilized BF_3 adducts **269** and **270** by heating the salt in DME at 60 °C [164]. The proposed mechanism involves elimination of $FSiMe_3$, which initially forms the carbene intermediate that subsequently reacts with the remaining BF_3 to form the adduct [164]. Similarly, the silylimidazolium tetrafluoroborate salt is converted to [BF_3(IMe)] (**271**) upon heating, offering an alternative route to existing methods [165]. Alternatively, **271** was also prepared by heating the imidazolium tetrafluoroborate salt at 200 °C [155]. Imidazolium-based tetrafluoroborate salts can also form [BF_3(NHC)] adducts upon deprotonation. Using LiHMDS, [BF_3(6-Mes)] (**272**) and the more sterically encumbered **273** were prepared [166], as well as [BF_3(IMes)] (**234**) and [BF_3(SIMes)] (**274**) [167]. The reaction proceeds *via in situ* generation of the free carbene and $LiBF_4$, which acts as a source of BF_3 [167]. In this way, a series of CAAC-stabilized adducts **275**–**280** was also prepared [167]. The KHMDS reagent was suitable for the preparation of **281** [168] and **282** [169]. Deprotonation using LDA afforded **283** from the corresponding tetrafluoroborate salt [170], while deprotonation of

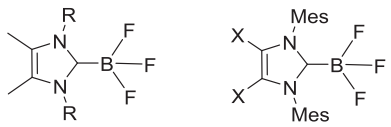

231; R = Me
232; R = Et
233; R = ^{i}Pr

234; X = H
235; X = Cl

Fig. 50. Schematic representation of **231**–**235**.

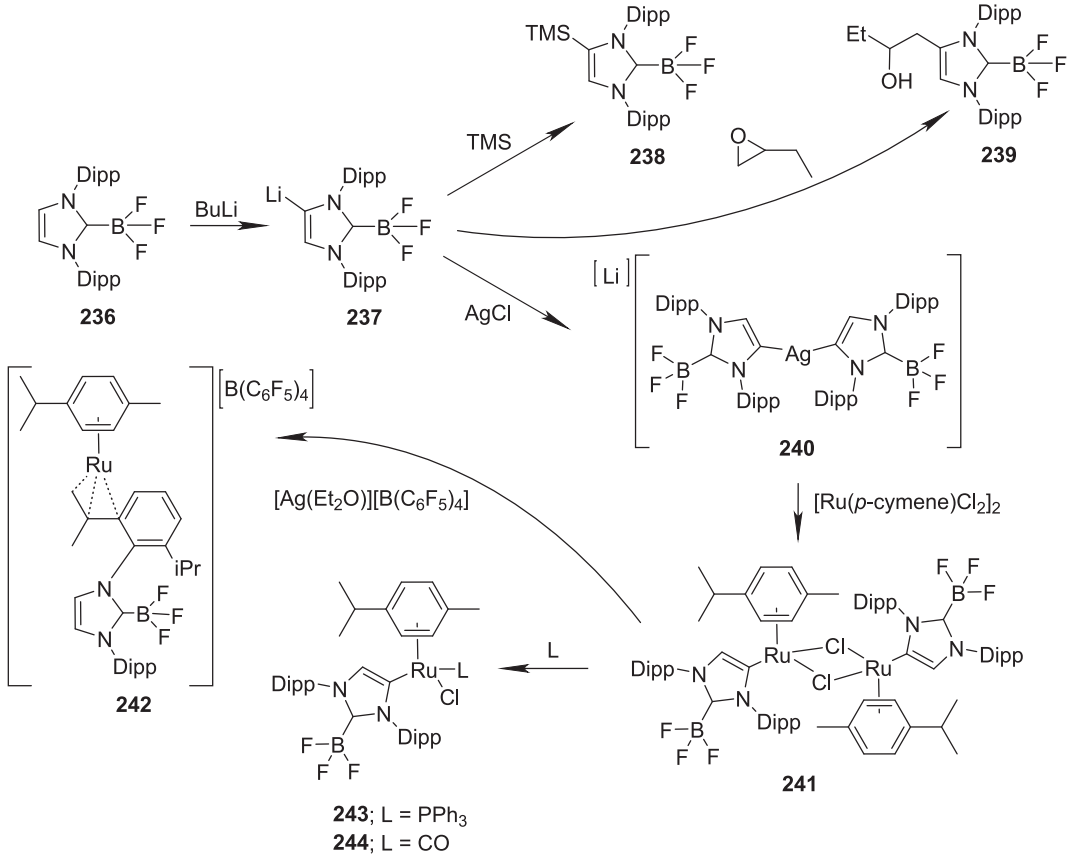

Scheme 6. Synthesis of **237**–**244**.

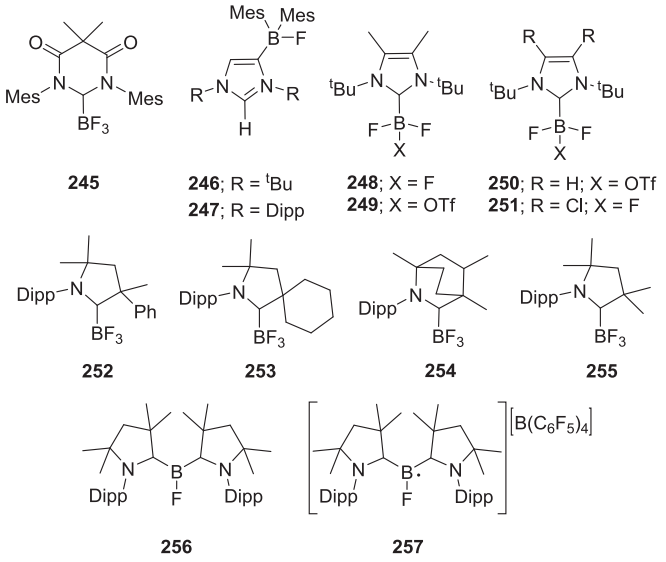

Fig. 52. Schematic representation of **245**–**257**.

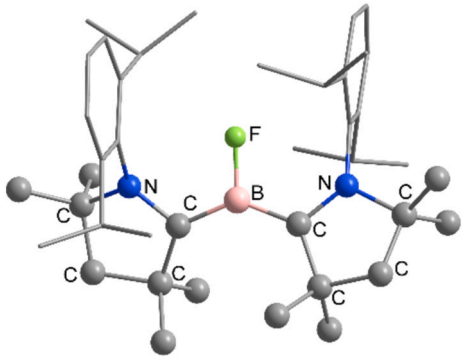

Fig. 53. View of the structure of **256**, redrawn from ref. [17].

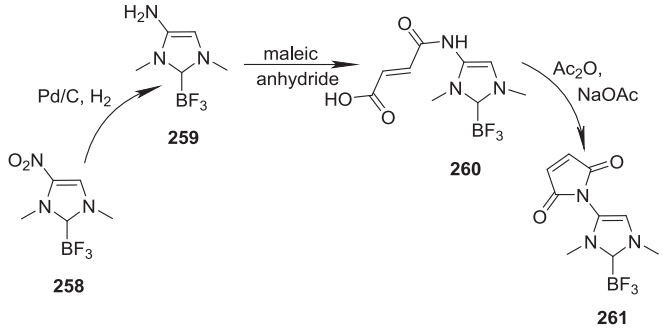

Scheme 7. Synthesis of **259**–**261**.

NHC-anilido tetrafluoroborate precursors with LDA and subsequent addition of $BF_3{\cdot}Et_2O$ allowed synthesis of **284**–**289** [171].

Another method that enabled the synthesis of a wide variety of NHC-stabilized B fluoride compounds is the fluorination of the corresponding hydrides [BH_3(NHC)]. One of the first experiments in this area was the fluorination of the dimeric carbene-borane adduct with $BF_3{\cdot}Et_2O$. The reaction produced a mixture of two products in a 95:5 ratio, with the major compound being the tetrafluoro-substituted **290** and the minor product being the partially fluorinated difluoro dihydro-substituted **291**

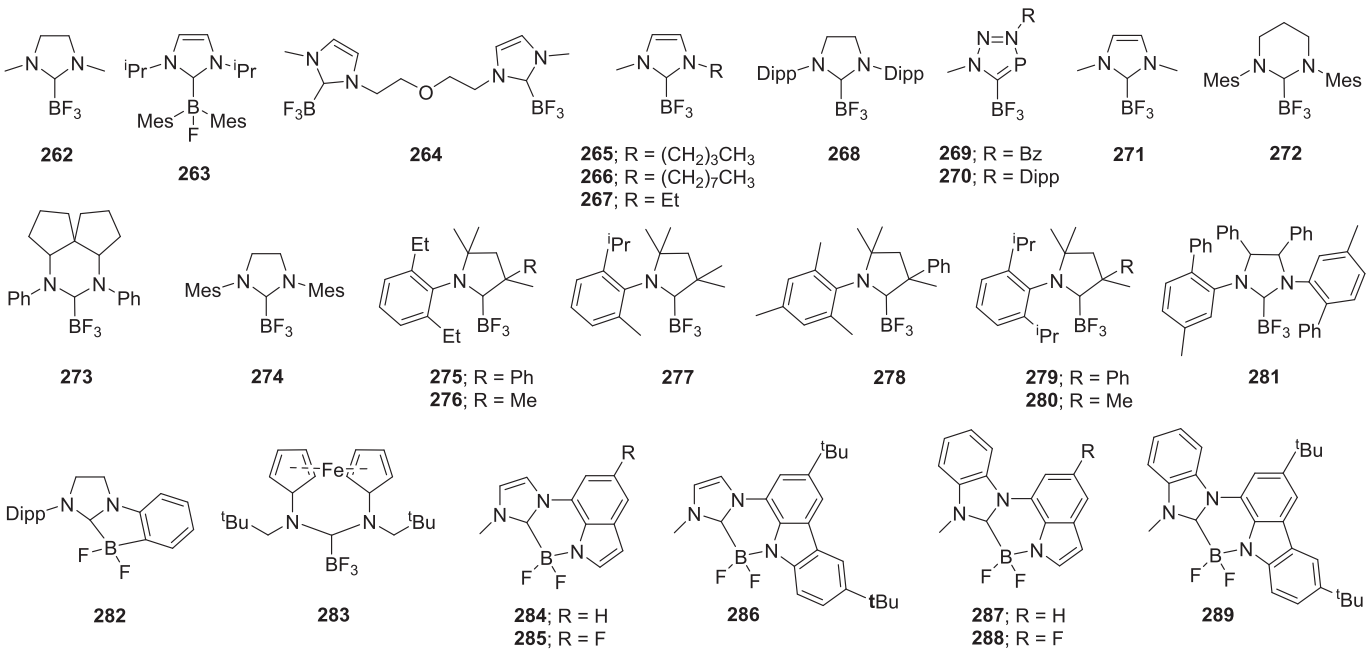

Fig. 54. Schematic representation of **262**–**289**.

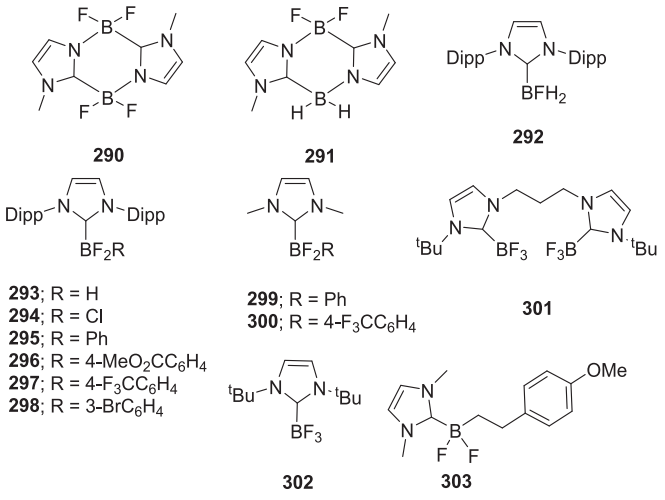

Fig. 55. Schematic representation of **290**–**303**.

(Fig. 55) [172]. Selective fluorination was later observed in a two-step synthesis of the monofluorinated [BFH_2(IDipp)] (**292**) and difluorinated [BF_2H(IDipp)] (**293**). The starting BH_3 adduct was first selectively converted to the mono- or disubstituted triflates using TfOH, and then to the corresponding fluorides **292** and **293** using Bu_4NF. During the fluorination reaction, the OTf substituent acted as a good leaving group, facilitating the formation of fluorinated adducts [173]. These partially fluorinated compounds were not structurally characterized. However, a mixed fluoride chloride counterpart [BF_2Cl(IDipp)] (**294**) was reported [174]. [CPh_3][BF_4] was used as a fluorination reagent for a series of [BH_2Ar(NHC)] compounds. The authors observed that product formation was highly dependent on the nature of the Ar substituents, yielding either [BF_2Ar(NHC)] adducts (**295**–**300**) or [BF_3(NHC)] (NHC = IDipp **236**, IMe **271**) adducts. The trifluorides were formed from the corresponding adducts with 4-$MeOC_6H_4$ and 2-thiophenyl Ar substituents [175]. Similarly, [CPh_3][PF_6] was used to fluorinate bis-NHC and NHC-stabilized BH_3 adducts to form the corresponding BF_3 compounds **301** and **302** [176]. The latter was structurally characterized a few years earlier, with its crystal structure published only as a CSD Communication (No. 2053984) [177]. An H/F rearrangement was also observed in the formation of adduct **303**, which was obtained by decomposition of the α-difluoroborane [178].

In the past decade, the use of Selectfluor in the fluorination of NHC-supported B hydrides has been extensively studied. Generally, reactions of [BH_2R(NHC)] with Selectfluor in MeCN produced difluorides [BF_2Ar(NHC)] in high yields. This pathway enabled the synthesis of aryl-substituted adducts **295**, **299**, **304**–**307** (Fig. 56) [179], **308** [180], **309** [181]; polyfluoroaryl-substituted adducts **310** [182], **311** [183], **312** [184,185], **313**, and **314** [186]; alkenyl-substituted adducts **315** [187], **316** [188], and **317** [189]; the benzothiazole **318** [190]; and alkyl-substituted adducts **319** [191], **320** [184], **321**, **322** [192], **323** [188], **324** [193], **325** [194], and **326** [195]. Compound **312** subsequently underwent defluoroborylation to form the diborylated compound **327** [185]. Only in one case did the fluorination of BH_2 compounds with Selectfluor result in a mixture of mono-, di-, and trifluorinated adducts **328**–**330** [196]. Furthermore, the monofluorinated adduct **331** was formed using the same procedure starting from the monohydride counterpart [197]. Finally, Selectfluor was also successfully used for the fluorination of diazaborolone, which was converted to the cationic derivative **332** [198].

[BF_2H(IMe)] (**333**) (Fig. 57) was also prepared from the corresponding BH_3 adduct and Selectfluor. However, the reaction was not sufficiently selective for the author's needs. High-purity **333** was obtained using an alternative one-pot, two-step reaction in which fluorine was introduced as a nucleophile. The parent BH_3 was first converted to diiodoborane by *in situ* addition of I_2, which then reacted with TBAF in THF to form **333** [199]. Subsequent hydrogen abstraction reactions of **333** with *tert*-butoxyl radical, prepared by photocleavage of di-*tert*-butyl peroxide with laser excitation at 355 nm, produced the difluoroboryl radical **334** [199]. B_2pin_2 reacted with free NHC in the presence of a fluoride ion (TMAF) in a 1:1:1 ratio to form a mixture of two products. The adducts [FB(NHC)(pin)] (NHC = I^iPr **335**, IMe **336**, I^iPrMe **337**, I^nPr **338**) formed together with [NMe_4][BF_2pin] salt and some unidentified side products [200]. While compounds **335**–**337** formed in very low yields, **338** was obtained as the main product in 91% yield [200]. TBAF also reacted with the fluoride-sensing molecule [B(Mes)(aIMe)][I], which was converted to the neutral fluorinated abnormal adduct [BF

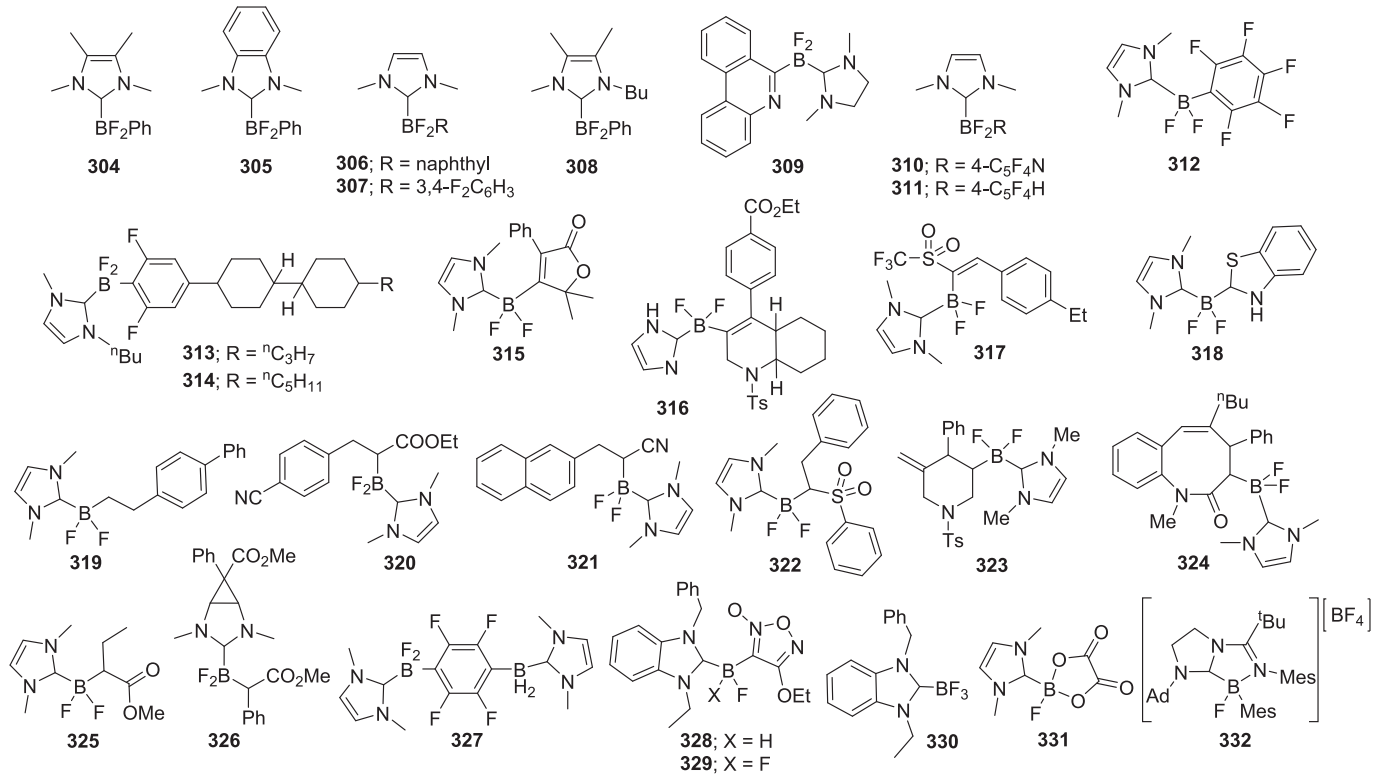

Fig. 56. Schematic representation of **304**–**332**.

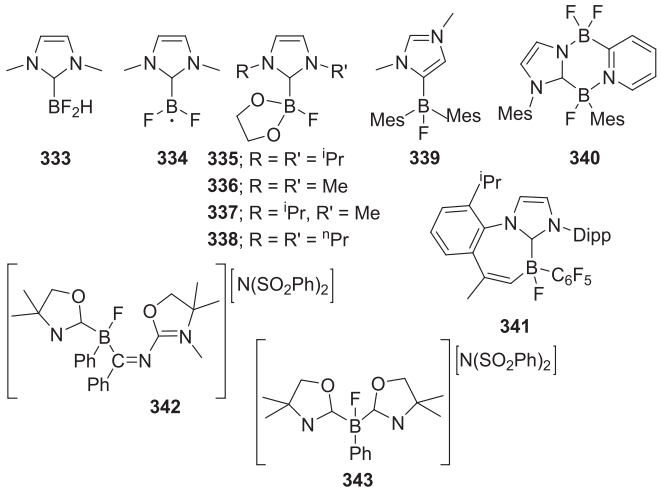

Fig. 57. Schematic representation of **333**–**343**.

(aIMe)(Mes)$_2$] (**339**) [201]. Fluorination of the bidentate pyridyl-carbene B(Mes) adduct with $BF_3{\cdot}Et_2O$ yielded the unprecedented example of a Lewis-acid-induced ring expansion $B_2C_2N_2$ heterocycle **340** [202]. An attempt to oxidize a boryl-nitroxide radical with $AgBF_4$ led to the formation of BF adduct **341** [203]. The reaction successfully oxidized the boryl NO radical to the boryl oxoammonium cation. However, the instability of the cation triggered a substitution reaction to **341**, which was characterized as the observable product [203]. The reactivity of the electron-rich B=C units in the adduct supported by strong σ-donating oxazol-2-ylidene was investigated toward NFSI. The reaction afforded the boronium fluoride species **342** [204].The same group also investigated the reactivity of borylene metal complexes with NFSI, which produced the ionic species **343** regardless of the metal complex used [205].

Based on the known crystal structures of NHC-stabilized B fluorides, including the crystal structure of compound **344** (Fig. 58), the NHC–B bond lengths in adducts are usually between 1.53 and 1.73 Å, while the B–F bond lengths are typically in the range of 1.32 to 1.46 Å.

5.1.2. *Aluminum*

The first NHC-stabilized Al fluoride adducts, [AlF_3(SIMes)] (**345**) and [$AlFMe_2$(SIMes)] (**346**) (Fig. 59), were prepared by treating the corresponding $AlMe_3$ adduct with SF_4 and SF_6, respectively. The formation of both compounds was determined only by spectroscopic methods [207]. Alternatively, compounds **345** and **346** were prepared by treating [$AlMe_3$(SIMes)] with 1.5 equiv or an excess of Me_3SnF, respectively. In contrast, the use of HF sources resulted in the formation of the salts [(SIMes)H][AlF_2Me_2] and [(SIMes)H][AlF_4] [207].

Later, Me_3SnF was also used to prepare the carbocyclic Al fluoride **347** by dehydrofluorination of the corresponding alane [208]. In its crystal structure, the Al center adopts a tetrahedral arrangement, with the two carbene ligands connected to the Al center by the backbone to form the C_4Al_2 core, as shown in Fig. 60 [208].

The NHC-stabilized Al fluoride adduct **348** (Fig. 59) was prepared

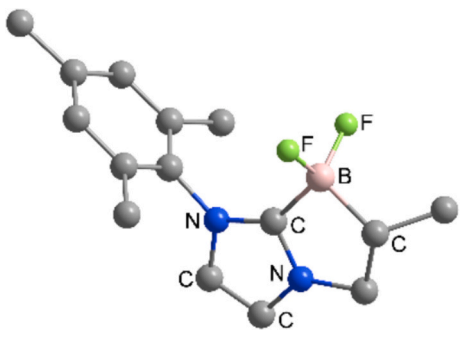

Fig. 58. View of the structure of **344**, redrawn from ref. [206].

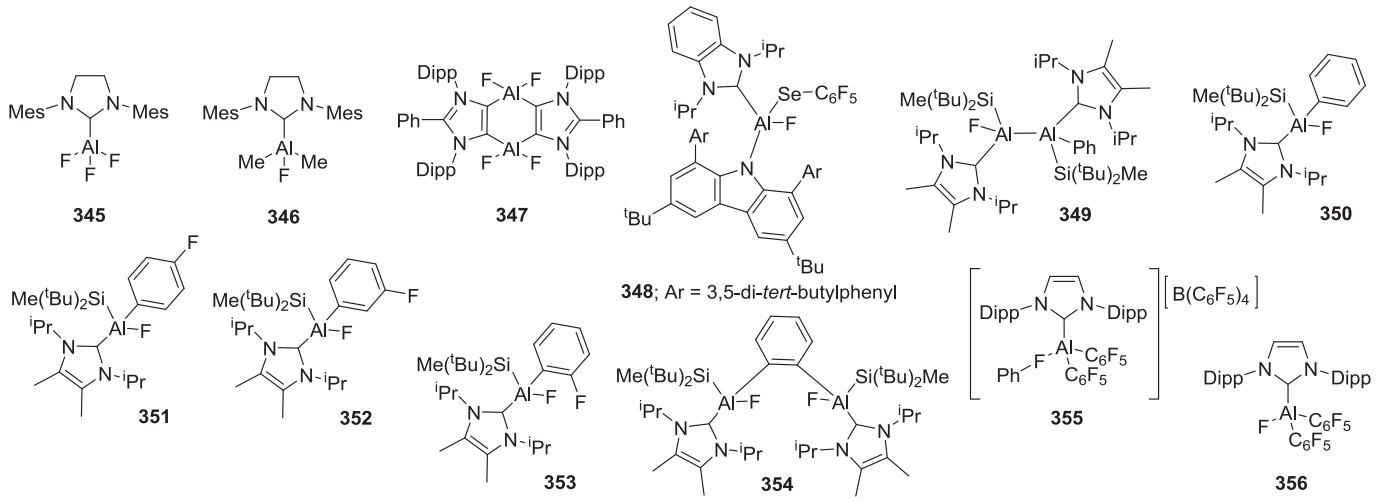

Fig. 59. Schematic representation of **345**–**356**.

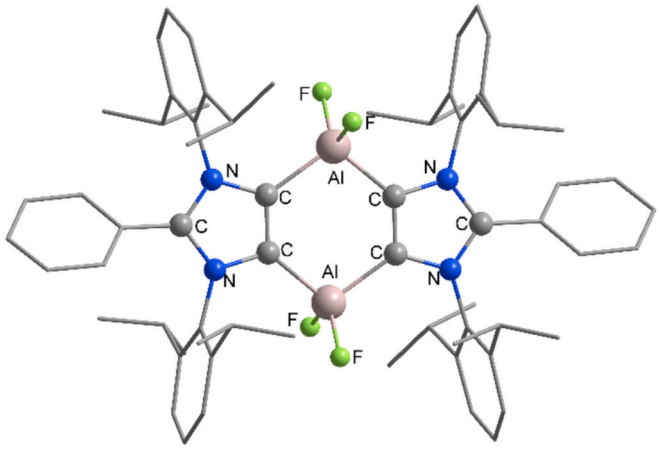

Fig. 60. View of the structure of **347,** redrawn from ref. [208].

from the corresponding Al=Se compound by treatment with C_6F_6. The Al–Se unit exhibited ambiphilic character, capable of cleaving σ C–F bonds in small molecules such as C_6F_6 [209]. The C–F bond of fluorobenzene is also cleaved by the dialumene [(^{Me2}I^{i}Pr)(Si(Me(^{t}Bu)$_2$))Al=Al(Si(Me(^{t}Bu)$_2$))(^{Me2}I^{i}Pr)] compound, enabling the synthesis of formal oxidative addition products at single or double Al centers. First, the Al–Al compound **349** formed as the major product, which over time converted to the monomeric Al(III) compound **350**. The dialumene also reacts with more activated difluorobenzenes, proceeding more rapidly than with fluorobenzene and leading to various Al(III) products. The use of 1,4-difluorobenzene resulted in the formation of **351**, 1,3-difluorobenzene produced **352**, while 1,2-difluorobenzene formed a mixture of **353** and **354** in a 2:1 ratio [210]. The reaction of [AlH(C_6F_5)$_2$(IDipp)] with fluorobenzene in the presence of [Ph_2C][B(C_6F_5)$_4$] led to nearly quantitative formation of the [Al(F-Ph)(C_6F_5)$_2$(IDipp)][B(C_6F_5)$_4$] salt (**355**). This compound can act as a Lewis superacid and abstract fluoride from [SbF_6]$^-$, forming [AlF(C_6F_5)$_2$(IDipp)] (**356**) [211]. Both compounds were structurally characterized, revealing a tetrahedral arrangement at the Al center, which is typical for Al(III) compounds [211]. Finally, the NHC-stabilized Al compound **357** was also characterized, where the Al atom is connected to F atoms of the anion. The structure of **357** is shown in **Fig. 61** [212].

Based on known crystal structures of NHC-stabilized Al fluorides, the NHC–Al bond lengths in adducts are usually between 1.99 and 2.11 Å, while the Al–F bond lengths typically range from 1.67 to 1.71 Å. The bridging Al–F bonds are generally longer, with a length of 1.88 Å for **355** [211] and 2.14 Å for **357** [212].

5.1.3. *Gallium*

The first NHC-stabilized Ga fluoride adduct, [GaF_3(IDipp)] (**358**), was prepared in 2014. Its crystal structure revealed a tetrahedral arrangement at the Ga center, which is typical for group XIII M(III) adducts (**Fig. 62**) [213]. Adduct **358** was formed by reacting the

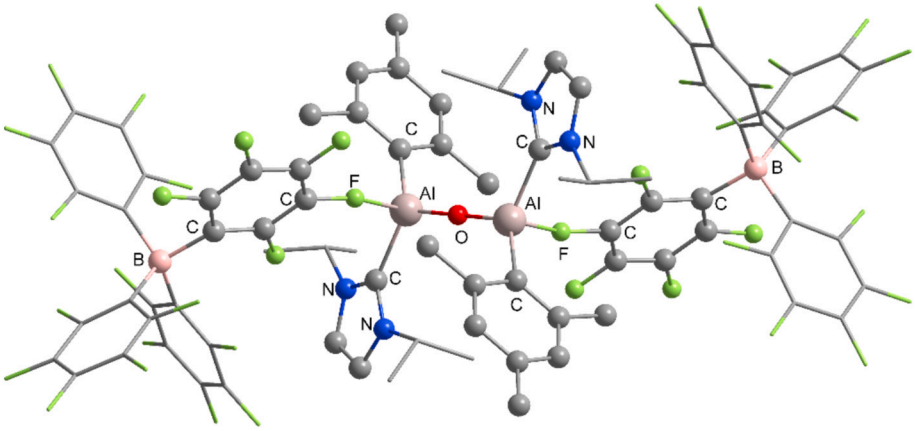

Fig. 61. View of the structure of **357**, redrawn from ref. [212].

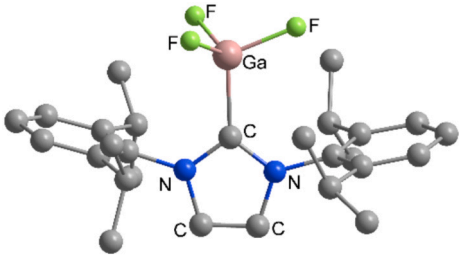

Fig. 62. View of the structure of **358**, redrawn from ref. [213].

corresponding chloride with 3 equiv of $AgBF_4$. The same reaction with 1 equiv of $AgBF_4$ led to the formation of [Ga(F-BF_3)Cl_2(IDipp)] (**359**), while the reaction with 1 equiv of $AgSbF_6$ resulted in [Ga(F-SbF_5)Cl_2(IDipp)] (**360**) (Fig. 63). Notably, the reaction of the free carbene with GaF_3 did not yield adduct **358**, but instead produced the corresponding [(IDipp)H][GaF_4] salt [213].

The Ga fluoride adduct **361** was obtained from the corresponding triflate by additing KF in the presence of 18-crown-6 [214], while the bis-gallylene reacted with aryl fluorides to give *cis*- and *trans*-Ga(III) compounds through C–F bond activation [215]. Compounds **362**–**365** adopt a tetrahedral arrangement at the Ga center, with two carbene ligands connected to Ga by the backbone to form the C_4Ga_2 cone, similar to the Al counterpart in Fig. 60 [215].

Based on known crystal structures of NHC-stabilized Ga fluorides, the NHC–Ga bond lengths in adducts are usually between 1.99 and 2.05 Å, while the Ga–F bond lengths are typically in the range of 1.79–1.84 Å. The bridging Ga–F bonds are usually longer, with lengths of 1.87 Å for **359**, and 1.92 Å for **360** [213].

5.1.4. Indium

Only one structure is known for an NHC-stabilized In fluoride. The fluorine-bridged compound [In(F-SbF_5)Br_2(IDipp)] (**366**) is formed by combining the corresponding NHC-stabilized $InBr_3$ with one equiv of $AgSbF_6$. Its crystal structure (Fig. 64) shows a tetrahedral arrangement at the In center, with an NHC–In bond distance of 2.178(2) Å and a bridging In–F bond distance of 2.189(2) Å [216].

5.2. GROUP XIV

The chemistry of Si and Ge halides with neutral electron-donating ligands is well developed and extensively reviewed in ref. [32]. Group XIV metal fluorides stabilized with NHC ligands are mostly found in the +4 oxidation state. Upon reduction, rare examples in the +2 state and only one in the +3 state have been prepared.

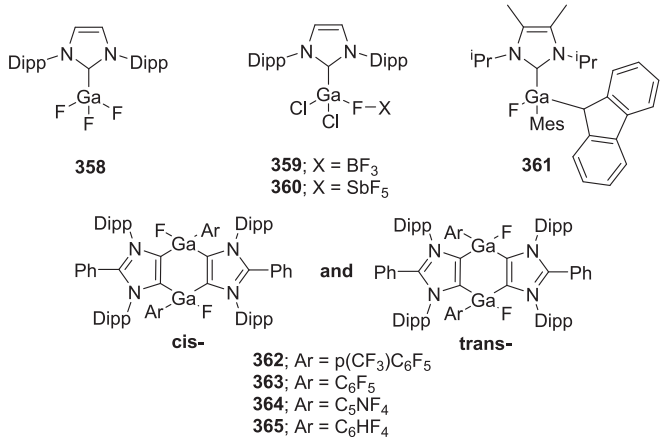

Fig. 63. Schematic representation of **358**–**365**.

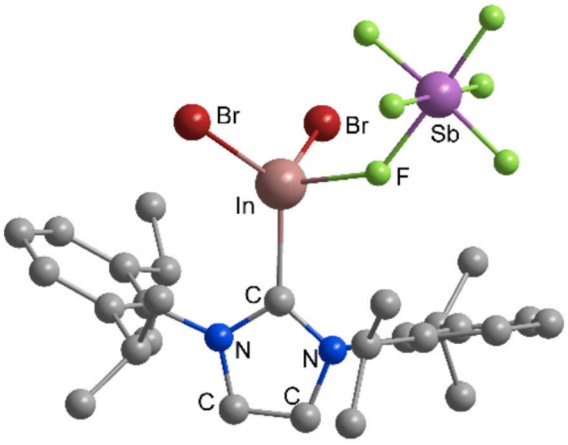

Fig. 64. View of the structure of **366**, redrawn from ref. [216].

5.2.1. Silicon

The first NHC-stabilized Si fluoride adducts were prepared by reacting a free carbene with SiF_4. Using 1 equiv of NHC afforded the pentacoordinated [SiF_4(IDipp)] (**367**), while using 2 equiv of NHC resulted in the formation of the hexacoordinated [SiF_4(IDipp)$_2$] (**368**) (Fig. 65) [217]. Using the same procedure, [SiF_4(I^iPr)$_2$] (**369**) was also prepared [218]. In the crystal structure, compound **367** adopts a trigonal bipyramidal arrangement at the Si center with the NHC ligand in the axial position, while compound **368** adopts an octahedral coordination at the Si center with both NHC ligands in *trans* positions [217]. The same octahedral arrangement was also observed in the crystal structure of [SiF_4(IMes)$_2$] (**370**), published as a CSD Communication (No. 611491) [219]. In contrast, a trigonal bipyramidal arrangement with the carbene ligand in the equatorial position was observed in the crystal structure of [SiF_3Ph(^{Me}CAAC)] (**371**), published as a CSD Communication (No. 2149531) [220].

By passing SiF_4 gas through a THF solution of ^{Me}CAAC carbene, [SiF_4(^{Me}CAAC)] (**372**) was prepared (Fig. 65). Subsequent reduction of **372** with 2 equiv of KC_8 in the presence of 1 equiv of free ^{Me}CAAC afforded [SiF_2(^{Me}CAAC)$_2$] (**373**) [16]. The same reduction starting from the [SiF_4(NHC)] adduct did not yield the [SiF_2(NHC)$_2$]. The different performance of the CAAC- and NHC-stabilized adducts was attributed to the stronger σ-donating and π-accepting abilities of CAAC carbenes compared to NHCs [16]. In addition, **372** reacted with 1 equiv of KC_8 in THF to form the monoradical product [SiF_3(^{Me}CAAC)] (**374**), which is stable at room temperature. In its crystal structure, the Si center adopts a distorted tetrahedral geometry, as shown in Fig. 66 [16].

Based on known crystal structures of NHC-stabilized Si fluorides, the NHC–Si bond lengths of adducts are usually between 1.80 and 2.03 Å, while the Si–F bond lengths typically range from 1.58 to 1.69 Å.

5.2.2. Germanium

The first NHC-stabilized Ge fluoride compound was the germylene derivative [GeF_2($^{Me2}I^iPr$)] (**375**) (Fig. 67). It was prepared from the

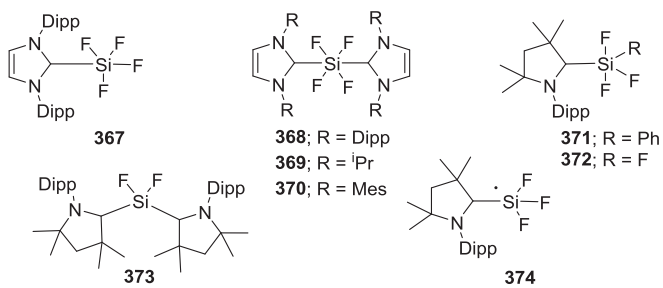

Fig. 65. Schematic representation of **367**–**374**.

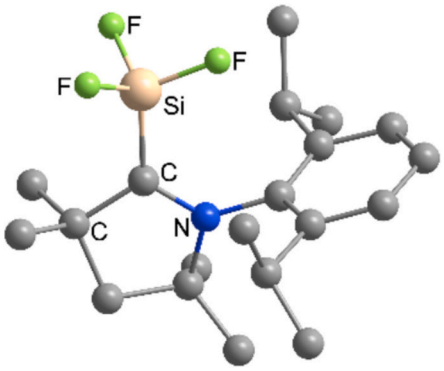

Fig. 66. View of the structure of **374**, redrawn from ref. [16].

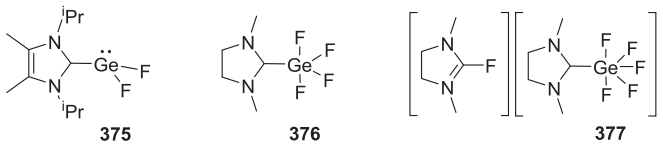

Fig. 67. Schematic representation of **375**–**377**.

corresponding chloride by fluorination with KF in the presence of 18-crown-6, and its structure was confirmed by single-crystal structural analysis [221]. Additionally, the NHC-stabilized Ge(IV) fluoride complex [GeF_4(SIMe)] (**376**) was synthesized by oxidative addition of 2,2-difluoro-1,3-dimethylimidazolidine to $GeCl_2$·dioxane. However, an excess of the difluoro reagent leads to the formation of the salt [(SIMe)F][GeF_5(SIMe)] (**377**) [222]. The structurally related acyclic analogue was obtained by the same procedure using bis(dimethylamino)difluoromethane as the reagent. The crystal structure of **376** revealed a trigonal bipyramidal geometry at the Ge center, with the NHC ligand in the equatorial position, as shown in Fig. 68, while the crystal structure of the NHC-stabilized anionic part of **377** adopts an octahedral geometry [222].

Based on the known crystal structures of NHC-stabilized Ge fluorides, the NHC–Ge bond lengths in neutral adducts are usually between 1.98 and 2.12 Å, while the Ge–F bond lengths are typically in the range of 1.78–1.83 Å.

5.2.3. Tin

The NHC-stabilized SnF_4 compound [SnF_4(^{Me2}I^{i}Pr)$_2$] (**378**) (Fig. 69) was prepared by reacting free NHC with SnF_4. In its crystal structure, the Sn atom adopts octahedral coordination, with the two NHC ligands in *trans* positions [223]. In contrast, SnF_2 reacts with 2,2-difluoro-1,3-dimethylimidazolidine to form the salt [(SIMe)F][SnF_5(SIMe)] (**379**) (Fig. 70) [222]. The structurally related acyclic analogue was also obtained by the same procedure using bis(dimethylamino)difluoromethane as the reagent [222].

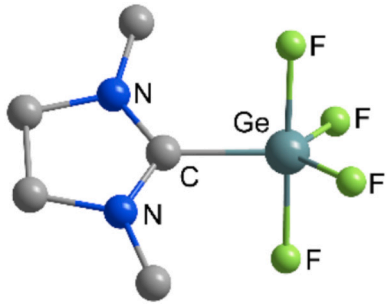

Fig. 68. View of the structure of **376**, redrawn from ref. [222].

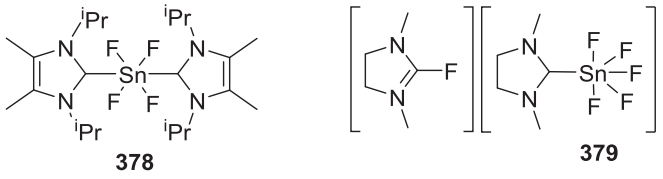

Fig. 69. Schematic representation of **378** and **379**.

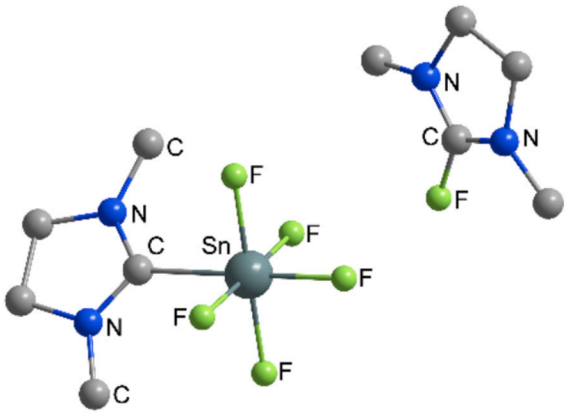

Fig. 70. View of the structure of **379**, redrawn from ref. [222].

Based on known crystal structures of NHC-stabilized Sn fluorides, the NHC–Sn bond lengths are usually between 1.97 and 1.98 Å, while the Sn–F bond lengths are typically in the range of 1.97–1.98 Å.

5.3. GROUP XV

The chemistry of P halides with neutral electron-donating ligands is well established and extensively reviewed in references [18, 30, 224]. Group XV metal fluorides stabilized with NHC ligands are mostly found in the +5 and +3 oxidation states. The latter possess one lone pair of electrons at the group XV element center, which may be stereochemically active.

5.3.1. Phosphorus

NHC-stabilized P(V) fluorides have been widely studied. A broad variety of synthetic methods are used for their preparation.

The first [PF_4(Ph)(IMes)] (**380**) adduct (Fig. 71) was prepared by the direct reaction of the free NHC with $PhPF_4$ in THF solution [225]. The adduct **380** was also structurally characterized, revealing octahedral coordination at the P center [225]. In contrast, PF_5 reacts with IMes to form a mixture of [PF_5(IMes)] (**381**) and the salt [(IMes)H][PF_6]. Product formation depends on the nucleophilic nature of the carbene. The more nucleophilic ^{Cl2}IMes reacts with PF_5 to form exclusively the [PF_5(^{Cl2}IMes)] (**382**) adduct [139]. [PF_5(IMe)] (**383**) was prepared using the same procedure, while the structurally related [PF_4(Ph)(IMe)] (**384**) was obtained by reacting K[PF_5(Ph)] with imidazolium iodide salt and n-BuLi [226]. In the second procedure, a free NHC is formed *in situ* and subsequently reacts with the phosphate anion to form adduct **384** [226]. Initially, the *cis*-**384** product was formed and characterized by NMR spectroscopy. Heating the compound to 66 °C triggered isomerization to the *trans*-**384** product, which was also structurally characterized [226].

Starting from $PF_2(C_2F_5)_3$ and free NHCs, a series of [$PF_2(C_2F_5)_3$(NHC)] adducts (NHC = IMe **385**, I^{n}Pr **386**, I^{i}Pr **387**, I^{i}PrMe **388**, ^{Me2}IMe **389**, ^{Me2}I^{n}Pr **390**, ^{Me2}I^{i}Pr **391**, ^{Me2}IEtMe **392**) (Fig. 71) were produced [227]. The use of more sterically demanding carbenes led to the slow formation of abnormal adducts [$PF_2(C_2F_5)_3$(aNHC)] (NHC = IDipp **393**, I^{t}Bu **394**, Mes **395**), although the synthesis of **395**

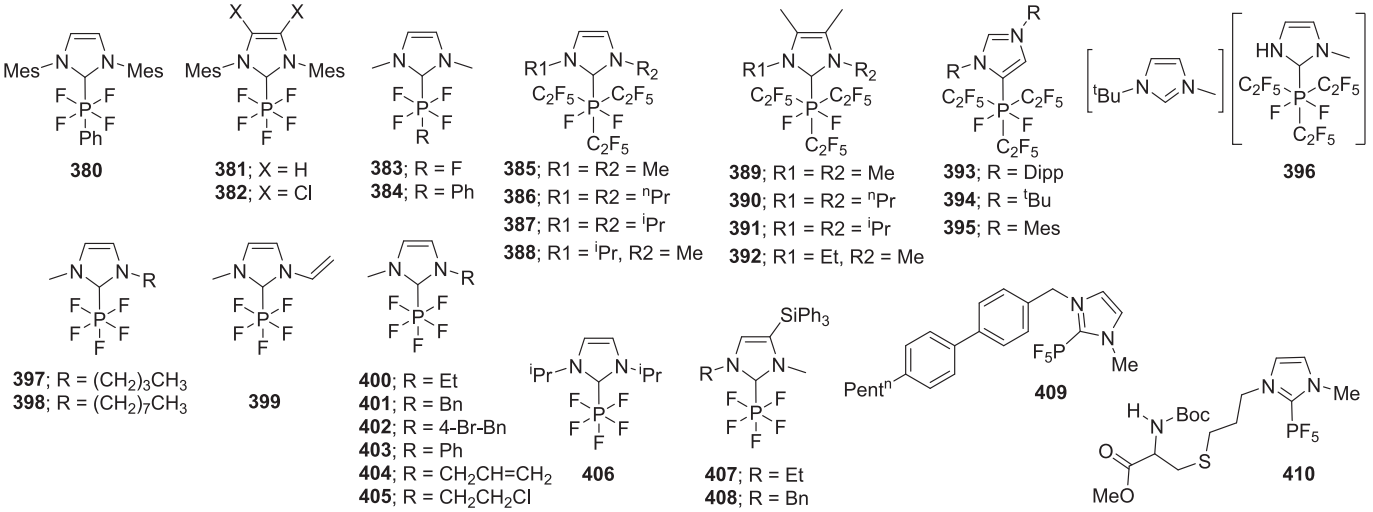

Fig. 71. Schematic representation of **380**–**410**.

did not result in clean adduct formation. In contrast, using the I^{t}BuMe NHC carbene resulted in the formation of salt **396** [227]. All compounds were crystallized and structurally characterized featuring octahedral coordination at the P center with the two fluorine atoms in a *trans* arrangement, as shown in Fig. 72 for compound **393** [227].

Imidazolium-based hexafluorophosphate salts have proven to be effective precursors for NHC-stabilized PF_5 adducts. At elevated temperatures, [(NHC)H][PF_6] undergoes dehydrofluorination to form [PF_5(NHC)] adducts. At temperatures above 327 °C, compounds **397** and **398** were obtained (Fig. 71) [161], while [PF_5(IMe)] (**383**) formed at 300–400 °C [162]. In contrast, heating the bis-imidazolium hexafluorophosphate salt at 300–400 °C resulted in thermolytic decomposition of the bis-imidazolium compound, producing a 1:1 mixture of [PF_5(NHC)] (**399**) and the imidazole N-stabilized PF_5 adduct [228]. Furthermore, the silylimidazolium hexafluorophosphate salt was converted to the corresponding NHC-stabilized PF_5 adducts **381**, **383**, **398**, and **400**–**406** by heating the salt at 190–200 °C in the presence of $LiPF_6$ [165]. The Lewis acidic nature of silanes enables the defluorinative decomposition of $[PF_6]^-$ to PF_5 by forming the fluorosilane byproduct. Desilylation of the silylimidazolium salts generated NHC and PF_5 *in situ*, which subsequently formed the [PF_5(NHC)] adduct in high yields. Using $LiPF_6$ in catalytic quantities ensured high conversion rates to the desired [PF_5(NHC)] adducts; otherwise, byproduct formation was observed. The silyl-NHC adducts **407** and **408**, as well as their corresponding imidazolium salts [(NHC)H][PF_6], formed by bimolecular proton transfer between the free NHC and silylimidazolium salt [165]. Additionally, adduct **401** was subsequently functionalized using a standard Suzuki–Miyaura cross-coupling reaction to yield **409**, while **404** was functionalized using a thiol-ene reaction to form **410** [165].

Oxidative addition of 2,2-difluoroimidazolidine reagents to P species is another widely used method to prepare NHC-stabilized P(V) fluorides. Using 2,2-difluoro-1,3-dimethylimidazolidine, [PF_4R(SIMe)] (R = F **411**, Me **412**, Ph **413**) (Fig. 73) were prepared from PF_3, PCl_2Me, and PCl_2Ph, respectively [229]. The structurally related acyclic PF_5 analogue was obtained by the same procedure using the bis(dimethylamino) difluoromethane reagent [229], and other (difluoroorganyl)dimethylamine reagents [230]. The 2,2-difluoro-1,3-dimethylimidazolidine also reacted with $PX_2(CF_3)$, $PX_2(C_2F_5)$, and $PX(C_2F_5)_2$ (X = F, Cl, Br) to form the corresponding NHC-stabilized $PF_4(CF_3)$ **414**, $PF_4(C_2F_5)$ **415**, and $PF_3(C_2F_5)_2$ **416** [231]. The structurally related acyclic analogues of **414**, **415**, and **416** were also prepared by the same method using acyclic bis(dimethylamino)difluoromethane [231]. Oxidative addition of 2,2-difluoroimidazolidines to PX_3 or PX_2R (X = F, Cl) was also used to obtain more sterically encumbered P(V) adducts **417**–**421** [232]. Fluorination of [PCl_3(SIMe)] with $Et_3N{\cdot}3HF$ in the presence of additional Et_3N resulted in the formation of [PF_4H(SIMe)] (**422**). During the reaction, chloride/fluoride metathesis occurs, followed by the addition of HF [233].

Oxidation of the corresponding precursors with XeF_2 led to the formation of various salts. The phosphine salts [PR_2(SIMes)][$B(C_6F_5)_4$] reacted with XeF_2 to yield salts containing $[PF_2R_2(SIMes)]^+$ cations (R = Ph **423**, Me **424**, Et **425**) (Fig. 74). Subsequent fluoride abstraction from

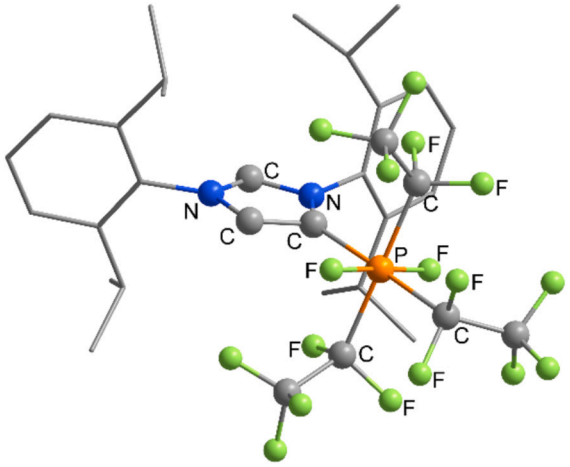

Fig. 72. View of the structure of **393**, redrawn from ref. [227].

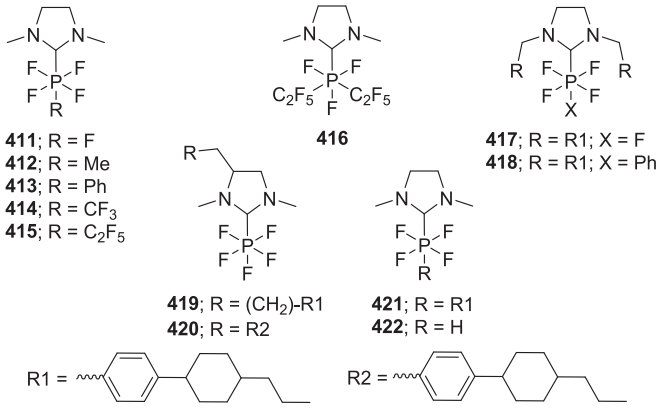

Fig. 73. Schematic representation of **411**–**422**.

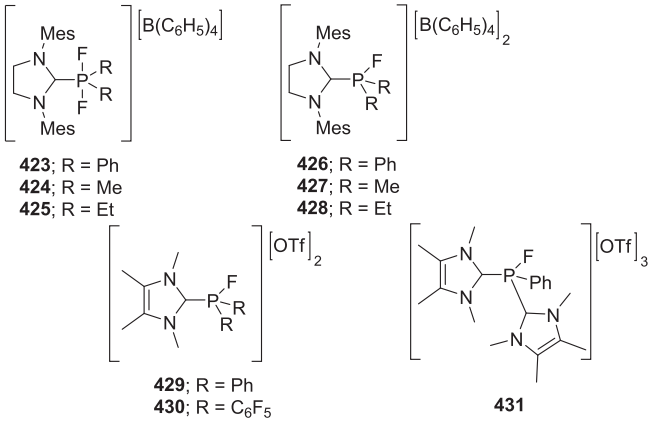

Fig. 74. Schematic representation of **423**–**431**.

these compounds produced salts with $[PFPh_2(SIMes)]^{2+}$ cations (R = Ph **426**, Me **427**, Et **428**) [234,235].

The molecular structure of $[PF_2Ph_2(SIMes)]^+$ in **423** exhibits a distorted trigonal bipyramidal geometry at the P center, with the two F atoms in axial positions. In contrast, the molecular structure of the dicationic $[PFPh_2(SIMes)]^{2+}$ in **426** displays a distorted tetrahedral geometry, as shown in Fig. 75 [234]. The same tetrahedral arrangement was also observed in the crystal structures of the $[PF(^{Me2}IMe)(Ph)_2]^{2+}$, $[PF(^{Me2}IMe)(C_6F_5)_2]^{2+}$, and $[PF(^{Me2}IMe)_2(Ph)]^{3+}$ cations in the corresponding triflate salts **429**, **430**, and **431**. These three compounds were published as part of the Thesis and can be found in the CSD database (No. 2051028, 2051030, and 2051040, respectively) [236–238].

By oxidation with XeF_2, other phosphine cations were converted to difluorophosphorane cations stabilized by imidazolylidene, CAAC, and triazolylidene ligands in compounds **432**–**435** (Fig. 76) [239]. Among these, only compound **434** was structurally characterized. It crystallized in the presence of AgCl, forming the $[AgCl_2]^-$ salt **435** [239]. The aNHC-stabilized PPh_2 cations were also oxidized by XeF_2 to the corresponding $[PF_2R_2(aNHC)]^+$ (R = Cy, Ph) in compounds **436** and **437**, which, upon fluoride abstraction, form the dicationic $[PFR_2(aNHC)]^{2+}$ (R = Cy, Ph) in compounds **438** and **439**, respectively [240]. The dicationic compound **439** further reacted with PPh_3 to form the chlorophosphonium

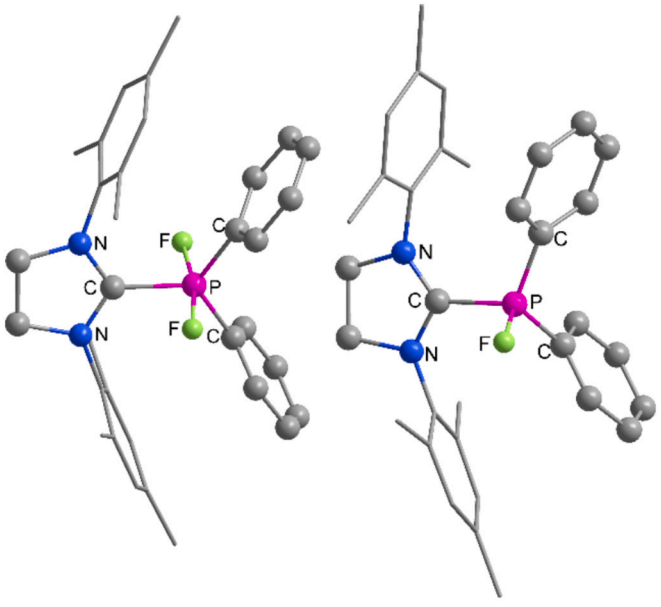

Fig. 75. View of the structure of the cationic $[PF_2Ph_2(SIMes)]^+$ in **423** (left) and the dicationic $[PFPh_2(SIMes)]^{2+}$ in **426** (right), redrawn from ref. [234].

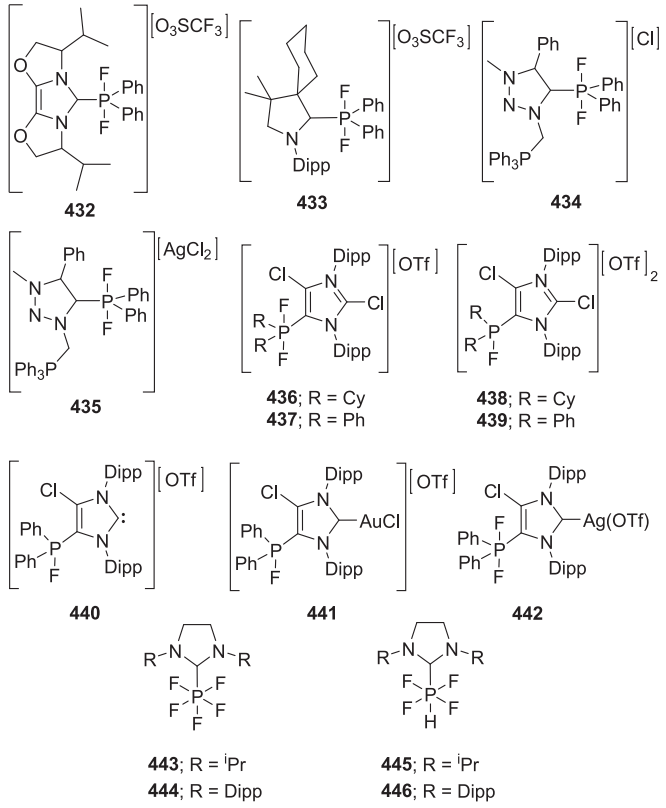

Fig. 76. Schematic representation of **432**–**446**.

salt [PClPh$_3$][OTf] and the NHC carbene **440**, which, upon addition of AuCl and AgF, formed complexes **441** and **442**, respectively [240]. In contrast, oxidation of the $[PI_2H(NHC)]$ compounds with XeF_2 was unselective. The authors suggested that the reaction with XeF_2 first proceeds *via* oxidative I/F and H/F exchange to afford cationic phosphines, which are then oxidized to phosphoranides **443**–**446** [241].

Based on the known crystal structures of NHC-stabilized P fluorides, the NHC–P bond lengths strongly depend on the charge of the NHC-stabilized P fluoride fragment. For neutral compounds, the NHC–P bond lengths are usually between 1.87 and 1.99 Å; for monocationic compounds, they range from 1.81 to 1.89 Å; and for dicationic compounds, from 1.77 to 1.85 Å. In contrast, the P–F bond lengths of all compounds are typically in the range of 1.53–1.66 Å. Notably, the dicationic compounds have slightly shorter P–F bond lengths (1.53–1.56 Å) compared to the monocationic and neutral compounds (1.59–1.66 Å).

5.3.2. *Arsenic & Antimony*

To date, only one NHC-stabilized As fluoride compound, [AsF$_5$(-^{Cl2}IMes)] (**447**), is known. It was synthesized by adding free carbene to AsF_5. The reaction was carried out in 1,3-bis(trifluoromethyl)benzene and resulted in a 65% yield. The complex was structurally characterized, revealing an octahedral geometry at the As center, with an NHC–As bond length of 2.00 Å, an average equatorial As–F bond length of 1.72 Å, and an axial As–F bond in the *trans* position relative to the NHC of 1.71 Å [139]. The structure of **447** is schematically presented in Fig. 77.

Using the same procedure, the group also prepared [SbF$_5$(^{Cl2}IMes)] (**448**) in 77% yield (Fig. 77) [139]. Recently, [SbF$_5$(IMe)] (**449**) was prepared from the silylimidazolium hexafluoroantimonate salt by heating at 180 °C. This method circumvents the use of SbF_5 as a reagent but still allows isolation of the carbene SbF_5 adduct [165]. The adduct **449** was also structurally characterized, revealing the octahedral coordination of Sb, as shown in Fig. 78 (left) [165]. In addition, adduct **450** was prepared by deprotonation of imidazolium hexafluoroantimonate

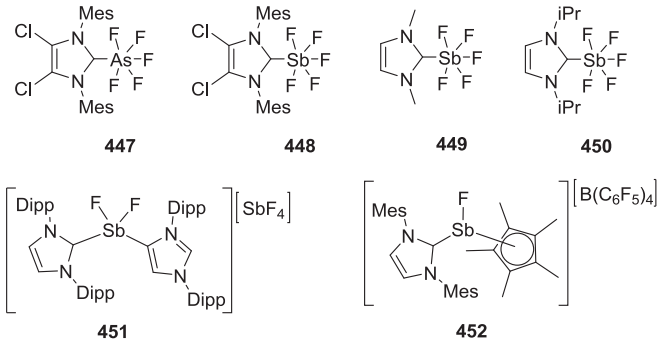

Fig. 77. Schematic representation of **447**–**452**.

salt with LiHMDS [242].

The NHC-stabilized SbF_3 compound [SbF_3(IDipp)] was detected in solution during the reaction of [SbF_3(tmen)] with IDipp carbene. However, this intermediate complex is unstable and undergoes autoionization, leading to the formation of [SbF_2(IDipp)(aIDipp)][SbF_4] (**451**). During autoionization, one of the IDipp ligands rearranges to the abnormal carbene [243]. The cationic complex is the first example in which a carbon-based ligand is coordinated to the SbF_2 moiety [243]. Its structure is shown in Fig. 78 (right). The NHC-stabilized Sb fluoride motif is also found in [SbF(Cp*)(IMes)][$B(C_6F_5)_4$] (**452**). The group attempted to trap the highly reactive [SbF(Cp*)]$^+$ fragment by stabilizing it with IMes carbene, which enabled the isolation of **452** [244].

Based on known crystal structures of NHC-stabilized Sb fluorides, the NHC–Sb and Sb–F bond lengths strongly depend on the geometry and charge of the NHC-stabilized Sb fluoride fragment. For neutral compounds with octahedral geometry, the NHC–Sb bond lengths are usually between 2.14 and 2.18 Å, while the Sb–F bond lengths range from 1.86 to 1.90 Å. In cationic species, the NHC–Sb bond lengths range from 2.17 to 2.41 Å, and the Sb–F bond lengths range from 1.89 to 2.03 Å.

5.4. GROUP XVI

Group XVI chalcogen fluorides stabilized with NHC ligands are extremely rare. To the best of our knowledge, only two references in the literature describe complexes in the +2 and +4 oxidation states.

5.4.1. Sulfur, Selenium, & Tellurium

Reaction of NHC-stabilized SCl_2 with AgF led to the isolation of the first [SF_2(^{Me2}I^{i}Pr)] (**453**) complex (Fig. 79) [245]. Compound **453** was characterized only by spectroscopic methods [245].

In 2022, Beckmann's group systematically tested the reactivity of group XVI NHC complexes. Oxidation of IDipp=S and IDipp=Se with XeF_2 resulted in the formation of S(II) and Se(II) compounds, [SF_2(IDipp)] (**454**) and [SeF_2(IDipp)] (**455**) (Fig. 79), respectively. The Se analogue could be further oxidized with another equiv of XeF_2 to form the Se(IV) adduct [SeF_4(IDipp)] (**456**). Alternatively, **456** could be prepared by direct reaction of SeF_4 with free carbene. However, in the presence of excess XeF_2 or at elevated temperature (80 °C), **456** decomposes to the [(IDipp)F][SeF_5] salt [246]. In contrast, the chemistry of Te differs from that of its lighter congeners. The Te(II) fluoride complex could not be prepared from NHC=Te and 1 equiv of XeF_2. Instead, the reaction led to the formation of [TeF_3(IDipp)$_2$][TeF_5] (**457**), whether 1 or 2 equiv of XeF_2 were used. Alternatively, **457** could be prepared by direct reaction of TeF_4 with free carbene. Over time, compound **457** converted to the mesoionic complex **458** following a normal-to-abnormal coordination switch [246]. Compounds **454**–**458** were structurally characterized. The M(II) complexes adopt a T-shaped geometry in the solid state, while the M(IV) compounds adopt a square pyramidal arrangement. Selected structures are presented in Fig. 80 [246].

Based on known crystal structures of NHC-stabilized S, Se, and Te fluorides, the NHC–M bond length is 1.73 Å for S, between 1.88 and 1.97 Å for Se, and ranges from 2.12 to 2.29 Å for Te. In contrast, the M–F bond length is 1.82 Å for S, between 1.85 and 1.94 Å for Se, and ranges from 1.94 to 1.98 Å for Te.

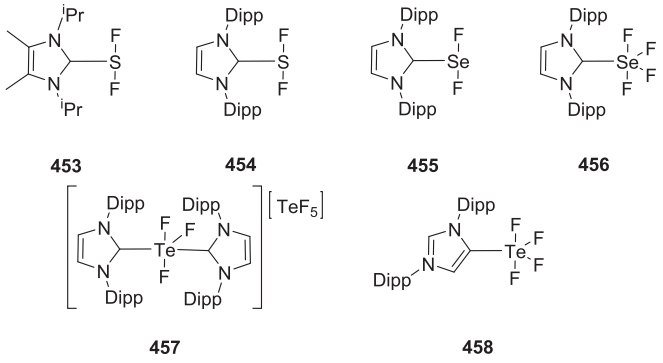

Fig. 79. Schematic representation of **453**–**458**.

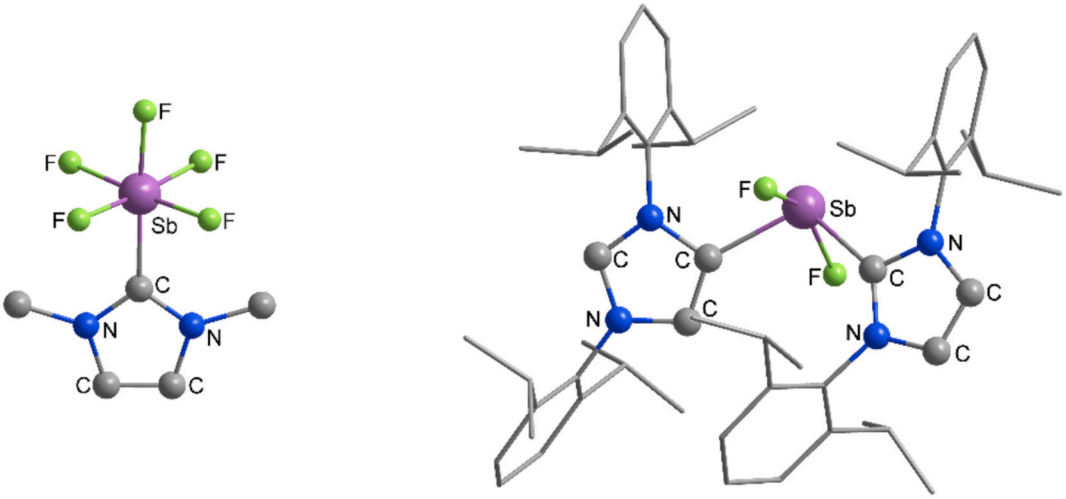

Fig. 78. View of the structure of **449** (left) and the cationic [SbF_2(IDipp)(aIDipp)]$^+$ in **451**, redrawn from ref. [165, 243].

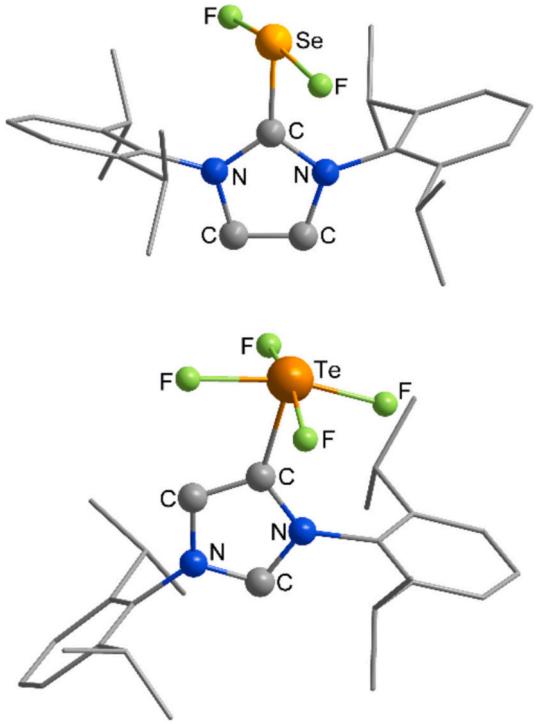

Fig. 80. View of the structure of **455** (above) and the cationic **458** (below), redrawn from ref. [246].

6. Conclusions

Despite a slow start, N-heterocyclic carbene (NHC) coordination chemistry with metal and non-metal fluorides has become an increasingly active and promising research area. A search of the CCDC crystal-structure database returns only 255 fluoride coordination compounds bearing NHC ligands, 17 with abnormal NHCs, and 11 with cyclic (alkyl)(amino)carbenes (CAACs), compared to roughly 8,650 NHC–halide structures overall (CCDC). This pronounced disparity largely reflects the intrinsic challenges of fluorides: many are poorly soluble, poorly reactive toward direct ligand substitution, and can be highly lattice-stabilized, all of which impede straightforward preparation of NHC–fluoride complexes.

Recent methodological advances, however, have begun to overcome these obstacles. Two-step or "precoordination–fluorination" strategies are now widely used: an NHC is first coordinated to a more labile halide or an organic precursor (e.g., silyl, alkyl, aryl, or pseudohalide), and this complex is then converted to the fluoride by a targeted fluorination step (Selectfluor, NFSI, XeF_2, $Et_3N{\cdot}3HF$, CsF with electrophilic activation, etc.). Alternative approaches include metathesis from soluble fluoride sources (e.g., tetraalkylammonium fluoride), fluoride abstraction or transfer from strong Lewis acids or fluorinating agents, and use of soluble fluoride surrogates (e.g., SF_4 derivatives, nucleophilic fluoride in polar aprotic solvents) or ionic liquid media to improve solubility and reactivity. Careful choice of solvent, counterion, and fluorinating reagent, combined with steric and electronic tuning of the carbene, has enabled isolation and crystallographic characterization of many previously inaccessible species.

Opportunities for expansion remain significant. Excluding transient intermediates in catalytic cycles, many elemental fluorides and their NHC complexes have yet to be reported; examples include late-row transition metals (e.g. Pt), group 12 metals (Zn, Cd, Hg), and others. The oxyfluoride domain is particularly underexplored since only two coordination-compound crystal structures are currently cataloged despite oxyfluorides' unique bonding and electronic properties, which could yield new structural motifs and reactivity. Exploration of mixed halide/oxide or fluoride-bridged architectures also promises novel multinuclear assemblies and catalytic behavior.

Ligand design offers another promising avenue for progress. CAACs, abnormal NHCs, and strongly donating or bulky variants can significantly alter metal-fluoride bonding, stabilize low-coordinate or high-oxidation-state centers, and affect reactivity toward migratory insertion or fluoride transfer. For example, CAACs have been implicated in the stabilization of SiF_2 and SiF_3 species and could enable the isolation of small, highly electrophilic fluorinated fragments that are otherwise elusive with classical NHCs. Redox-active carbene frameworks and multifunctional ligands (hemilabile donors, pendant Lewis bases/acids) may further enable cooperative stabilization and activation of fluoride ligands.

Advances in synthetic techniques, choice of fluorinating reagents, and ligand design have begun to close the gap between NHC–fluoride and NHC–halide chemistry, but substantial unexplored territory remains. Focused efforts on underrepresented elements, oxyfluorides, and nonclassical carbene ligands should yield new structures, bonding motifs, and catalytic applications.

Declaration of competing interest

The authors declare the following financial interests/personal relationships which may be considered as potential competing interests: Gasper Tavcar reports financial support was provided by Slovenian Research and Innovation Agency. If there are other authors, they declare that they have no known competing financial interests or personal relationships that could have appeared to influence the work reported in this paper.

Acknowledgements

The authors would like to thank the Slovenian Research and Innovation Agency (ARIS) for financial support of the Research Program P1-0045 (Inorganic Chemistry and Technology).

Appendix A. Supplementary data

Supplementary data to this article can be found online at https://doi.org/10.1016/j.ccr.2026.217604.

Data availability

No data was used for the research described in the article.

References

[1] A.J. Arduengo, R.L. Harlow, M. Kline, A stable crystalline carbene, J. Am. Chem. Soc. 113 (1991) 361–363, https://doi.org/10.1021/ja00001a054.
[2] R.H. Crabtree, NHC ligands versus cyclopentadienyls and phosphines as spectator ligands in organometallic catalysis, J. Organomet. Chem. 690 (2005) 5451–5457, https://doi.org/10.1016/j.jorganchem.2005.07.099.
[3] N. Holzmann, A. Stasch, C. Jones, G. Frenking, Comparative Study of Phosphine and N-Heterocyclic Carbene Stabilized Group 13 Adducts [L(EH_3)] and [$L_2(E_2H_n)$], Chem. Eur. J. 19 (2013) 6467–6479, https://doi.org/10.1002/chem.201203679.
[4] M.N. Hopkinson, C. Richter, M. Schedler, F. Glorius, An overview of N-heterocyclic carbenes, Nature 510 (2014) 485–496, https://doi.org/10.1038/nature13384.
[5] O. Hollóczki, L. Nyulászi, Stability and Structure of Carbene-Derived Neutral Penta- and Hexacoordinate Silicon Complexes, Organometallics 28 (2009) 4159–4164, https://doi.org/10.1021/om9002768.
[6] K. George, A.L. Hector, W. Levason, G. Reid, G. Sanderson, M. Webster, W. Zhang, Hypervalent neutral O-donor ligand complexes of silicon tetrafluoride, comparisons with other group 14 tetrafluorides and a search for soft donor ligand complexes, Dalton Trans. 40 (2011) 1584, https://doi.org/10.1039/c0dt01115k.
[7] S.L. Benjamin, W. Levason, G. Reid, Medium and high oxidation state metal/non-metal fluoride and oxide–fluoride complexes with neutral donor ligands, Chem. Soc. Rev. 42 (2013) 1460–1499, https://doi.org/10.1039/C2CS35263J.
[8] R.H. Crabtree, Abnormal, mesoionic and remote N-heterocyclic carbene complexes, Coord. Chem. Rev. 257 (2013) 755–766, https://doi.org/10.1016/j.ccr.2012.09.006.

[9] M. Melaimi, M. Soleilhavoup, G. Bertrand, Stable cyclic carbenes and related species beyond diaminocarbenes, Angew. Chem. Int. Ed. 49 (2010) 8810–8849, https://doi.org/10.1002/anie.201000165.

[10] H.V. Huynh, Electronic Properties of N-Heterocyclic Carbenes and Their Experimental Determination, Chem. Rev. 118 (2018) 9457–9492, https://doi.org/10.1021/acs.chemrev.8b00067.

[11] M. Soleilhavoup, G. Bertrand, Cyclic (Alkyl)(Amino)Carbenes (CAACs): Stable Carbenes on the Rise, Acc. Chem. Res. 48 (2015) 256–266, https://doi.org/10.1021/ar5003494.

[12] R.S. Ghadwal, 1,3-Imidazole-Based Mesoionic Carbenes and Anionic Dicarbenes: Pushing the Limit of Classical N-Heterocyclic Carbenes, Angew. Chem. Int. Ed. 62 (2023) e202304665, https://doi.org/10.1002/anie.202304665.

[13] P. Bellotti, M. Koy, M.N. Hopkinson, F. Glorius, Recent advances in the chemistry and applications of N-heterocyclic carbenes, Nat. Rev. Chem. 5 (2021) 711–725, https://doi.org/10.1038/s41570-021-00321-1.

[14] S.C. Sau, P.K. Hota, S.K. Mandal, M. Soleilhavoup, G. Bertrand, Stable abnormal N-heterocyclic carbenes and their applications, Chem. Soc. Rev. 49 (2020) 1233–1252, https://doi.org/10.1039/C9CS00866G.

[15] M. Riethmann, L. Eyßelein, I. Krummenacher, R. Bertermann, H. Braunschweig, M. Gerken, M. Finze, U. Radius, A Joyful Journey: Tungsten(VI) and Tungsten(V) Fluorides Meet *N*-Heterocyclic Carbenes and Cyclic (Alkyl)(Amino)Carbenes, Angew. Chem. Int. Ed. 64 (2025), https://doi.org/10.1002/anie.202504498.

[16] S. Sinhababu, S. Kundu, A.N. Paesch, R. Herbst-Irmer, D. Stalke, I. Fernández, G. Frenking, A.C. Stückl, B. Schwederski, W. Kaim, H.W. Roesky, A Route to Base Coordinate Silicon Difluoride and the Silicon Trifluoride Radical, Chem. Eur. J. 24 (2018) 1264–1268, https://doi.org/10.1002/chem.201705773.

[17] S.K. Sarkar, M.M. Siddiqui, S. Kundu, M. Ghosh, J. Kretsch, P. Stollberg, R. Herbst-Irmer, D. Stalke, A.C. Stückl, B. Schwederski, W. Kaim, S. Ghorai, E. D. Jemmis, H.W. Roesky, Isolation of base stabilized fluoroborylene and its radical cation, Dalton Trans. 48 (2019) 8551–8555, https://doi.org/10.1039/C9DT01899A.

[18] V. Nesterov, D. Reiter, P. Bag, P. Frisch, R. Holzner, A. Porzelt, S. Inoue, NHCs in Main Group Chemistry, Chem. Rev. 118 (2018) 9678–9842, https://doi.org/10.1021/acs.chemrev.8b00079.

[19] R.K. Singh, T.K. Khan, S. Misra, A.K. Singh, CAACs as efficient ancillary ligands for the synthesis of robust catalysts, J. Organomet. Chem. 956 (2021) 122133, https://doi.org/10.1016/j.jorganchem.2021.122133.

[20] A. Röther, R. Kretschmer, Syntheses of Bis(N-heterocyclic carbene)s and their application in main-group chemistry, J. Organomet. Chem. 918 (2020) 121289, https://doi.org/10.1016/j.jorganchem.2020.121289.

[21] Á. Vivancos, C. Segarra, M. Albrecht, Mesoionic and Related Less Heteroatom-Stabilized N-Heterocyclic Carbene Complexes: Synthesis, Catalysis, and Other Applications, Chem. Rev. 118 (2018) 9493–9586, https://doi.org/10.1021/acs.chemrev.8b00148.

[22] V.A. Voloshkin, N.V. Tzouras, S.P. Nolan, Recent advances in the synthesis and derivatization of N-heterocyclic carbene metal complexes, Dalton Trans. 50 (2021) 12058–12068, https://doi.org/10.1039/D1DT01847G.

[23] A. Doddi, M. Peters, M. Tamm, N-Heterocyclic Carbene Adducts of Main Group Elements and Their Use as Ligands in Transition Metal Chemistry, Chem. Rev. 119 (2019) 6994–7112, https://doi.org/10.1021/acs.chemrev.8b00791.

[24] E.A. Martynova, N.V. Tzouras, G. Pisanò, C.S.J. Cazin, S.P. Nolan, The "weak base route" leading to transition metal–N-heterocyclic carbene complexes, Chem. Commun. 57 (2021) 3836–3856, https://doi.org/10.1039/D0CC08149C.

[25] A.A. Tsygankov, A.S. Kozlov, S. Liao, D. Chusov, Application of transition metal fluorides in catalysis, Coord. Chem. Rev. 519 (2024) 216114, https://doi.org/10.1016/j.ccr.2024.216114.

[26] J. Miró, C. del Pozo, Fluorine and Gold: A Fruitful Partnership, Chem. Rev. 116 (2016) 11924–11966, https://doi.org/10.1021/acs.chemrev.6b00203.

[27] G.B. Nikiforov, H.W. Roesky, D. Koley, A survey of titanium fluoride complexes, their preparation, reactivity, and applications, Coord. Chem. Rev. 258–259 (2014) 16–57, https://doi.org/10.1016/j.ccr.2013.09.002.

[28] W. Levason, F.M. Monzittu, G. Reid, Coordination chemistry and applications of medium/high oxidation state metal and non-metal fluoride and oxide-fluoride complexes with neutral donor ligands, Coord. Chem. Rev. 391 (2019) 90–130, https://doi.org/10.1016/j.ccr.2019.04.005.

[29] A.A. Danopoulos, T. Simler, P. Braunstein, N-Heterocyclic Carbene Complexes of Copper, Nickel, and Cobalt, Chem. Rev. 119 (2019) 3730–3961, https://doi.org/10.1021/acs.chemrev.8b00505.

[30] T. Böttcher, G.-V. Röschenthaler, Highly reactive carbenes as ligands for main group element fluorides. Syntheses and applications, J. Fluorine Chem. 171 (2015) 4–11, https://doi.org/10.1016/j.jfluchem.2014.10.018.

[31] R. Deka, A. Orthaber, Carbene chemistry of arsenic, antimony, and bismuth: origin, evolution and future prospects, Dalton Trans. 51 (2022) 8540–8556, https://doi.org/10.1039/D2DT00755J.

[32] W. Levason, G. Reid, W. Zhang, Coordination complexes of silicon and germanium halides with neutral ligands, Coord. Chem. Rev. 255 (2011) 1319–1341, https://doi.org/10.1016/j.ccr.2010.11.019.

[33] C.R. Groom, I.J. Bruno, M.P. Lightfoot, S.C. Ward, The Cambridge Structural Database, Acta, Crystallogr. B Struct. Sci. Cryst. Eng. Mater. 72 (2016) 171–179, https://doi.org/10.1107/S2052520616003954.

[34] M. Brendel, J. Wenz, I.V. Shishkov, F. Rominger, P. Hofmann, Lithium Complexes of Neutral Bis-NHC Ligands, Organometallics 34 (2015) 669–672, https://doi.org/10.1021/om501229b.

[35] K.S. Flaig, B. Raible, V. Mormul, N. Denninger, C. Maichle-Mössmer, D. Kunz, Generation of Annelated Dicarbenes and Their Alkali-Metal Chelate Complexes in Solution: Equilibrium between Hetero- and Homoleptic NHC Lithium Complexes, Organometallics 37 (2018) 1291–1303, https://doi.org/10.1021/acs.organomet.8b00053.

[36] C. Röhr, R. Kniep, Die Kristallstrukturen von Li[PF_6] und Li[AsF_6]: Zur Kristallchemie von Verbindungen A[E^VF_6] / The Crystal Structures of Li[PF_6] and Li[AsF_6]: On the Crystal Chemistry of Compounds A[E^VF_6], Z. Naturforsch. B. 49 (1994) 650–654, https://doi.org/10.1515/znb-1994-0514.

[37] L. Zapf, U. Radius, M. Finze, Anionic N-heterocyclic carbenes featuring weakly coordinating perfluoroalkylphosphorane moieties, Dalton Trans. 52 (2023) 9553–9561, https://doi.org/10.1039/D3DT01249B.

[38] P.L. Arnold, Z.R. Turner, N. Kaltsoyannis, P. Pelekanaki, R.M. Bellabarba, R. P. Tooze, Covalency in Ce^{IV} and U^{IV} Halide and N-Heterocyclic Carbene Bonds, Chem. Eur. J. 16 (2010) 9623–9629, https://doi.org/10.1002/chem.201001471.

[39] A. Doddi, C. Gemel, R.W. Seidel, M. Winter, R.A. Fischer, Coordination complexes of TiX_4 (X=F, Cl) with a bulky N-heterocyclic carbene: Syntheses, characterization and molecular structures, Polyhedron 52 (2013) 1103–1108, https://doi.org/10.1016/j.poly.2012.06.067.

[40] G.B. Nikiforov, H.W. Roesky, P.G. Jones, J. Magull, A. Ringe, R.B. Oswald, Preparation of Ti(IV) Fluoride *N*-Heterocyclic Carbene Complexes, Inorg. Chem. 47 (2008) 2171–2179, https://doi.org/10.1021/ic701751r.

[41] R.L. Davidovich, D.V. Marinin, V. Stavila, K.H. Whitmire, Stereochemistry of fluoride and mixed-ligand fluoride complexes of zirconium and hafnium, Coord. Chem. Rev. 257 (2013) 3074–3088, https://doi.org/10.1016/j.ccr.2013.06.016.

[42] S.L. Benjamin, W. Levason, D. Pugh, G. Reid, W. Zhang, Preparation and structures of coordination complexes of the very hard Lewis acids ZrF_4 and HfF_4, Dalton Trans. 41 (2012) 12548, https://doi.org/10.1039/c2dt31501g.

[43] Ž. Zupanek, M. Tramšek, A. Kokalj, G. Tavčar, Reactivity of VOF_3 with N-Heterocyclic Carbene and Imidazolium Fluoride: Analysis of Ligand–VOF_3 Bonding with Evidence of a Minute π Back-Donation of Fluoride, Inorg. Chem. 57 (2018) 13866–13879, https://doi.org/10.1021/acs.inorgchem.8b02377.

[44] M.F. Davis, M. Jura, A. Leung, W. Levason, B. Littlefield, G. Reid, M. Webster, Synthesis, chemistry and structures of complexes of the dioxovanadium(v) halides VO_2F and VO_2Cl, Dalton Trans. (2008) 6265, https://doi.org/10.1039/b811422f.

[45] M. Bortoluzzi, E. Ferretti, F. Marchetti, G. Pampaloni, S. Zacchini, Coordination complexes of niobium and tantalum pentahalides with a bulky NHC ligand, Dalton Trans. 45 (2016) 6939–6948, https://doi.org/10.1039/C6DT00533K.

[46] Ž. Zupanek, M. Tramšek, A. Kokalj, G. Tavčar, The peculiar case of conformations in coordination compounds of group V pentahalides with N-heterocyclic carbene and synthesis of their imidazolium salts, J. Fluorine Chem. 227 (2019) 109373, https://doi.org/10.1016/j.jfluchem.2019.109373.

[47] M. Bortoluzzi, E. Ferretti, F. Marchetti, G. Pampaloni, S. Zacchini, A crystallographic and DFT study on a NHC complex of niobium oxide trifluoride, J. Coord. Chem. 69 (2016) 2766–2774, https://doi.org/10.1080/00958972.2016.1214950.

[48] P.A. Petrov, E.A. Golubitskaya, N.B. Kompankov, I.V. Eltsov, T.S. Sukhikh, M. N. Sokolov, Binuclear Niobium Complex with Coordinated N-Heterocyclic Carbene, J. Struct. Chem. 60 (2019) 1989–1994, https://doi.org/10.1134/S0022476619120151.

[49] P.A. Petrov, T.S. Sukhikh, M.N. Sokolov, NHC adducts of tantalum amidohalides: the first example of NHC abnormally coordinated to an early transition metal, Dalton Trans. 46 (2017) 4902–4906, https://doi.org/10.1039/C7DT00748E.

[50] C.M. Acosta, D.S. Belov, A.H. Lamur, C.L. Brantley, X. Solans-Monfort, K.L. Rue, G. Christou, K.V. Bukhryakov, Mononuclear Four-Coordinate Bis-Fluoride Bis-NHC Complexes of Chromium(II), Iron(II), and Cobalt(II), Inorg. Chem. 62 (2023) 18108–18115, https://doi.org/10.1021/acs.inorgchem.3c02442.

[51] H. Kropp, A. Scheurer, F.W. Heinemann, J. Bendix, K. Meyer, Coordination-Induced Spin-State Change in Manganese(V) Complexes: The Electronic Structure of Manganese(V) Nitrides, Inorg. Chem. 54 (2015) 3562–3572, https://doi.org/10.1021/acs.inorgchem.5b00112.

[52] Q. Zhang, L. Xiang, L. Deng, Dinuclear Iron–imido complexes with *n*-heterocyclic carbene ligation: synthesis, structure, and redox reactivity, Organometallics 31 (2012) 4537–4543, https://doi.org/10.1021/om300319n.

[53] J.A. Valdez-Moreira, A.E. Thorarinsdottir, J.A. DeGayner, S.A. Lutz, C.-H. Chen, Y. Losovyj, M. Pink, T.D. Harris, J.M. Smith, Strong π-backbonding enables record magnetic exchange coupling through cyanide, J. Am. Chem. Soc. 141 (2019) 17092–17097, https://doi.org/10.1021/jacs.9b09445.

[54] A.D. Chivington, S. Squire, N. Yamamoto, M. Pink, M.D. Griffith, J. Fletcher, Y. Gao, J.M. Zadrozny, J.M. Smith, Trimethylsilyldiazomethane disassembly at a three-fold symmetric iron site, Inorg. Chem. 63 (2024) 10221–10229, https://doi.org/10.1021/acs.inorgchem.4c00604.

[55] M. Keilwerth, W. Mao, M. Malischewski, S.A.V. Jannuzzi, K. Breitwieser, F. W. Heinemann, A. Scheurer, S. DeBeer, D. Munz, E. Bill, K. Meyer, The synthesis and characterization of an iron(VII) nitrido complex, Nat. Chem. 16 (2024) 514–520, https://doi.org/10.1038/s41557-023-01418-4.

[56] S.L. Chatwin, M.G. Davidson, C. Doherty, S.M. Donald, R.F.R. Jazzar, S. A. Macgregor, G.J. McIntyre, M.F. Mahon, M.K. Whittlesey, H−X bond activation via hydrogen transfer to hydride in ruthenium N-heterocyclic carbene complexes: density functional and synthetic studies, Organometallics 25 (2006) 99–110, https://doi.org/10.1021/om0507427.

[57] S.P. Reade, M.F. Mahon, M.K. Whittlesey, Catalytic Hydrodefluorination of Aromatic Fluorocarbons by Ruthenium N-Heterocyclic Carbene Complexes, J. Am. Chem. Soc. 131 (2009) 1847–1861, https://doi.org/10.1021/ja806545e.

[58] R. Armstrong, C. Ecott, E. Mas-Marzá, M.J. Page, M.F. Mahon, M.K. Whittlesey, Ring-Expanded N-Heterocyclic Carbene Complexes of Ruthenium, Organometallics 29 (2010) 991–997, https://doi.org/10.1021/om901044u.

[59] S.P. Reade, A.L. Acton, M.F. Mahon, T.A. Martin, M.K. Whittlesey, Synthesis and Reactivity of Ru(NHC)(dppp)(CO)H_2 and Ru(NHC)(dppp)(CO)HF Complexes: C–H and C–F Activation, Eur. J. Inorg. Chem. 2009 (2009) 1774–1785, https://doi.org/10.1002/ejic.200801105.

[60] S.P. Reade, D. Nama, M.F. Mahon, P.S. Pregosin, M.K. Whittlesey, Synthesis and Reactivity of Ru$(PPh_3)_3$(CO)HF and the N-Heterocyclic Carbene Derivatives Ru(NHC)$(PPh_3)_2$(CO)HF, Organometallics 26 (2007) 3484–3491, https://doi.org/10.1021/om070164p.

[61] L.M. Guard, A.E.W. Ledger, S.P. Reade, C.E. Ellul, M.F. Mahon, M.K. Whittlesey, [Ru(NHC)(P–P)(CO)HF] (NHC = N-heterocyclic carbene; P–P = xantphos, dppf) complexes: Efforts to prepare new hydrodefluorination catalysts, J. Organomet. Chem. 696 (2011) 780–786, https://doi.org/10.1016/j.jorganchem.2010.09.077.

[62] M.K. Cybulski, I.M. Riddlestone, M.F. Mahon, T.J. Woodman, M.K. Whittlesey, Stoichiometric and catalytic C–F bond activation by the *trans*-dihydride NHC complex [Ru$(IEt_2Me_2)_2(PPh_3)_2H_2$] ($IEt_2Me_2$ = 1,3-diethyl-4,5-dimethylimidazol-2-ylidene), Dalton Trans. 44 (2015) 19597–19605, https://doi.org/10.1039/C5DT01996F.

[63] M.K. Cybulski, J.E. Nicholls, J.P. Lowe, M.F. Mahon, M.K. Whittlesey, Catalytic Hydrodefluorination of Fluoroarenes Using Ru$(IMe_4)_2L_2H_2$ (IMe_4 = 1,3,4,5-Tetramethylimidazol-2-ylidene; L_2 = $(PPh_3)_2$, dppe, dppp, dppm) Complexes, Organometallics 36 (2017) 2308–2316, https://doi.org/10.1021/acs.organomet.7b00243.

[64] M.K. Cybulski, D. McKay, S.A. Macgregor, M.F. Mahon, M.K. Whittlesey, Room Temperature Regioselective Catalytic Hydrodefluorination of Fluoroarenes with *trans*-[Ru(NHC)$_4H_2$] through a Concerted Nucleophilic Ru−H Attack Pathway, Angew. Chem. Int. Ed. 56 (2017) 1515–1519, https://doi.org/10.1002/anie.201610820.

[65] J. Fawcett, D.A.J. Harding, E.G. Hope, K. Singh, G.A. Solan, *N*-Heterocyclic carbene-containing ruthenium difluoro complexes and their reactivity towards BF_3, Dalton Trans. (2009) 6861, https://doi.org/10.1039/b906321h.

[66] K.S. Coleman, J. Fawcett, D.A.J. Harding, E.G. Hope, K. Singh, G.A. Solan, Routes to Ruthenium–Fluoro Cations of the Type $[RuL_2(CO)_nF]^+$ (n = 2,3; L = PR_3, NHC): A Play-Off between Solvent, L and Weakly Coordinating Anion, Eur. J. Inorg. Chem. 2010 (2010) 4130–4138, https://doi.org/10.1002/ejic.201000410.

[67] S. Guidone, O. Songis, L. Falivene, F. Nahra, A.M.Z. Slawin, H. Jacobsen, L. Cavallo, C.S.J. Cazin, Ruthenium Olefin Metathesis Catalysts Containing Fluoride, ACS Catal. 5 (2015) 3932–3939, https://doi.org/10.1021/acscatal.5b00219.

[68] S.S. Bera, M. Szostak, Cobalt–N-Heterocyclic Carbene Complexes in Catalysis, ACS Catal. 12 (2022) 3111–3137, https://doi.org/10.1021/acscatal.1c05869.

[69] M. Iglesias, L.A. Oro, A leap forward in iridium–NHC catalysis: new horizons and mechanistic insights, Chem. Soc. Rev. 47 (2018) 2772–2808, https://doi.org/10.1039/C7CS00743D.

[70] S. Medici, M. Peana, A. Pelucelli, M.A. Zoroddu, Rh(I) Complexes in Catalysis: A Five-Year Trend, Molecules 26 (2021) 2553, https://doi.org/10.3390/molecules26092553.

[71] G. Sipos, R. Dorta, Iridium complexes with monodentate N-heterocyclic carbene ligands, Coord. Chem. Rev. 375 (2018) 13–68, https://doi.org/10.1016/j.ccr.2017.10.019.

[72] W. Mao, Z. Zhang, D. Fehn, S.A.V. Jannuzzi, F.W. Heinemann, A. Scheurer, M. van Gastel, S. DeBeer, D. Munz, K. Meyer, Synthesis and Reactivity of a Cobalt-Supported Singlet Nitrene, J. Am. Chem. Soc. 145 (2023) 13650–13662, https://doi.org/10.1021/jacs.3c01478.

[73] F. Ismael, C.L. Fleming, T.D. Christopher, T. Söhnel, Y. Zhou, E.H. Krenske, L. R. Gahan, A.G. Blackman, Co(III) complexes of the pentadentate NHC ligand PY4Im: carbene-induced *trans* influences and the non-disappearing ^{13}C NMR peak, Dalton Trans. 53 (2024) 12688–12697, https://doi.org/10.1039/D4DT01579G.

[74] C. Segarra, E. Mas-Marzá, J.P. Lowe, M.F. Mahon, R.C. Poulten, M.K. Whittlesey, Ring-Expanded N-Heterocyclic Carbene Complexes of Rhodium with Bifluoride, Fluoride, and Fluoroaryl Ligands, Organometallics 31 (2012) 8584–8590, https://doi.org/10.1021/om300984v.

[75] N. Bramananthan, M. Carmona, J.P. Lowe, M.F. Mahon, R.C. Poulten, M. K. Whittlesey, Rh–FHF and Rh–F Complexes Containing Small *N*-Alkyl Substituted Six-Membered Ring N-Heterocyclic Carbenes, Organometallics 33 (2014) 1986–1995, https://doi.org/10.1021/om500122e.

[76] L. Schwartsburd, M.F. Mahon, R.C. Poulten, M.R. Warren, M.K. Whittlesey, Mechanistic Studies of the Rhodium NHC Catalyzed Hydrodefluorination of Polyfluorotoluenes, Organometallics 33 (2014) 6165–6170, https://doi.org/10.1021/om500827d.

[77] B.J. Truscott, F. Nahra, A.M.Z. Slawin, D.B. Cordes, S.P. Nolan, Fluoride, bifluoride and trifluoromethyl complexes of iridium(I) and rhodium(I), Chem. Commun. 51 (2015) 62–65, https://doi.org/10.1039/C4CC07772E.

[78] R. Jaeger, M. Talavera, T. Braun, Studies on the reactivity of Rh(I) complexes towards SF_5Cl, J. Fluorine Chem. 247 (2021) 109803, https://doi.org/10.1016/j.jfluchem.2021.109803.

[79] J. Cabanes, M. Odnoroh, C. Duhayon, C. Bijani, A. Sournia-Saquet, R. Polia, A. Labande, Oxidation-promoted synthesis of ferrocenyl planar chiral rhodium (iii) complexes for C–H functionalization catalysis, Mendeleev Commun. 31 (2021) 620–623, https://doi.org/10.1016/j.mencom.2021.09.010.

[80] J. Fawcett, D.A.J. Harding, E.G. Hope, K. Singh, G.A. Solan, Stabilisation of iridium(iii) fluoride complexes with NHCs, Dalton Trans. 39 (2010) 10781, https://doi.org/10.1039/c0dt00857e.

[81] Z.N. Gafurov, A.O. Kantyukov, A.A. Kagilev, A.A. Balabayev, O.G. Sinyashin, D. G. Yakhvarov, Nickel and palladium *N*-heterocyclic carbene complexes. Synthesis and application in cross-coupling reactions, Russ. Chem. Bull.n 66 (2017) 1529–1535, https://doi.org/10.1007/s11172-017-1920-7.

[82] T. Schaub, U. Radius, Efficient C−F and C−C Activation by a Novel N-Heterocyclic Carbene–Nickel(0) Complex, Chem. Eur. J. 11 (2005) 5024–5030, https://doi.org/10.1002/chem.200500231.

[83] T. Schaub, P. Fischer, A. Steffen, T. Braun, U. Radius, A. Mix, C−F Activation of Fluorinated Arenes using NHC-Stabilized Nickel(0) Complexes: Selectivity and Mechanistic Investigations, J. Am. Chem. Soc. 130 (2008) 9304–9317, https://doi.org/10.1021/ja074640e.

[84] T. Schaub, M. Backes, U. Radius, Square-Planar (Pentafluorophenyl)nickel(II) Complexes by Derivatization of a C–F Activation Product, Eur. J. Inorg. Chem. 2008 (2008) 2680–2690, https://doi.org/10.1002/ejic.200800213.

[85] T. Schaub, M. Backes, U. Radius, Catalytic C−C Bond Formation Accomplished by Selective C−F Activation of Perfluorinated Arenes, J. Am. Chem. Soc. 128 (2006) 15964–15965, https://doi.org/10.1021/ja064068b.

[86] T. Schaub, P. Fischer, T. Meins, U. Radius, Consecutive C–F Bond Activation of Hexafluorobenzene and Decafluorobiphenyl, Eur. J. Inorg. Chem. 2011 (2011) 3122–3126, https://doi.org/10.1002/ejic.201100323.

[87] P. Fischer, K. Götz, A. Eichhorn, U. Radius, Decisive Steps of the Hydrodefluorination of Fluoroaromatics using [Ni(NHC)$_2$], Organometallics 31 (2012) 1374–1383, https://doi.org/10.1021/om2009815.

[88] J. Zhou, M.W. Kuntze-Fechner, R. Bertermann, U.S.D. Paul, J.H.J. Berthel, A. Friedrich, Z. Du, T.B. Marder, U. Radius, Preparing (Multi)Fluoroarenes as Building Blocks for Synthesis: Nickel-Catalyzed Borylation of Polyfluoroarenes via C–F Bond Cleavage, J. Am. Chem. Soc. 138 (2016) 5250–5253, https://doi.org/10.1021/jacs.6b02337.

[89] M.W. Kuntze-Fechner, H. Verplancke, L. Tendera, M. Diefenbach, I. Krummenacher, H. Braunschweig, T.B. Marder, M.C. Holthausen, U. Radius, Coligand role in the NHC nickel catalyzed C–F bond activation: investigations on the insertion of bis(NHC) nickel into the C–F bond of hexafluorobenzene, Chem. Sci. 11 (2020) 11009–11023, https://doi.org/10.1039/D0SC04237D.

[90] S.S. Wills, C. Bailly, M.J. Chetcuti, Towards Nickel–NHC Fluoro Complexes—Synthesis of Imidazolium Fluorides and Their Reactions with Nickelocene, Molecules 29 (2024) 4493, https://doi.org/10.3390/molecules29184493.

[91] V.G. Thangavadivale, L. Tendera, R. Bertermann, U. Radius, T. Beweries, R. N. Perutz, Solution and solid-state studies of hydrogen and halogen bonding with N-heterocyclic carbene supported nickel(II) fluoride complexes, Faraday Discuss. 244 (2023) 62–76, https://doi.org/10.1039/D2FD00171C.

[92] D.-Y. Wang, M. Kawahata, Z.-K. Yang, K. Miyamoto, S. Komagawa, K. Yamaguchi, C. Wang, M. Uchiyama, Stille coupling via C–N bond cleavage, Nat. Commun. 7 (2016) 12937, https://doi.org/10.1038/ncomms12937.

[93] S. Sabater, M.J. Page, M.F. Mahon, M.K. Whittlesey, Stoichiometric and Catalytic Reactivity of Ni(6-Mes)$(PPh_3)_2$, Organometallics 36 (2017) 1776–1783, https://doi.org/10.1021/acs.organomet.7b00129.

[94] H. Iwamoto, H. Imiya, M. Ohashi, S. Ogoshi, Cleavage of C(sp^3)–F Bonds in Trifluoromethylarenes Using a Bis(NHC)nickel(0) Complex, J. Am. Chem. Soc. 142 (2020) 19360–19367, https://doi.org/10.1021/jacs.0c09639.

[95] A.J. Sicard, B. Ghaffari, B.M. Gabidullin, J.S. Ovens, R.P. Hughes, R.T. Baker, Nickel-Catalyzed Homologation of Vinylidene Difluoride (CH_2═CF_2): Selective β-F *vs* β-H Elimination, J. Am. Chem. Soc. 144 (2022) 22713–22721, https://doi.org/10.1021/jacs.2c10448.

[96] F. He, C. Gourlaouen, H. Pang, P. Braunstein, Influence of the Flexibility of Nickel PCP-Pincer Complexes on C−H and P−C Bond Activation and Ethylene Reactivity: A Combined Experimental and Theoretical Investigation, Chem. Eur. J. 28 (2022), https://doi.org/10.1002/chem.202104234.

[97] A. Sarkar, S. Das, P. Mondal, B. Maiti, S. Sen Gupta, Synthesis, Characterization, and Reactivity of High-Valent Carbene Dicarboxamide-Based Nickel Pincer Complexes, Inorg. Chem. 62 (2023) 20439–20449, https://doi.org/10.1021/acs.inorgchem.3c03465.

[98] W. Chiu, B.E. Nadeau, B.O. Patrick, J.A. Love, Investigating the mechanism of Ni-mediated trifluoromethylthiolation of aryl halides using $AgSCF_3$, Dalton Trans. 52 (2023) 3738–3745, https://doi.org/10.1039/D2DT03758K.

[99] S. Schaefer, CCDC 2376667: Experimental Crystal Structure Determination, CSD Commun. (2024), https://doi.org/10.5517/ccdc.csd.cc2ks3p5.

[100] S. Schäfer, CCDC 2214689: Experimental Crystal Structure Determination, CSD Commun. (2024), https://doi.org/10.5517/ccdc.csd.cc2dbklx.

[101] E.S. Chernyshova, R. Goddard, K.-R. Pörschke, Mononuclear NHC−Pd−π-Allyl Complexes Containing Weakly Coordinating Ligands, Organometallics 26 (2007) 3236–3251, https://doi.org/10.1021/om0702274.

[102] D.I. Wozniak, W.A. Sabbers, K.C. Weerasiri, L.V. Dinh, J.L. Quenzer, A.J. Hicks, G. E. Dobereiner, Comparing Interactions of a Three-Coordinate Pd Cation with Common Weakly Coordinating Anions, Organometallics 37 (2018) 2376–2385, https://doi.org/10.1021/acs.organomet.8b00356.

[103] R.E. Andrew, A.B. Chaplin, Synthesis, structure and dynamics of NHC-based palladium macrocycles, Dalton Trans. 43 (2014) 1413–1423, https://doi.org/10.1039/C3DT52578C.

[104] H. Li, B. Zhang, R. Feng, S. Guo, An N-heterocyclic carbene-based pincer system of palladium and its versatile reactivity under oxidizing conditions, Dalton Trans. 53 (2024) 11470–11480, https://doi.org/10.1039/D4DT00980K.

[105] A. Grünwald, B. Goswami, K. Breitwieser, B. Morgenstern, M. Gimferrer, F. W. Heinemann, D.M. Momper, C.W.M. Kay, D. Munz, Palladium Terminal Imido Complexes with Nitrene Character, J. Am. Chem. Soc. 144 (2022) 8897–8901, https://doi.org/10.1021/jacs.2c02818.

[106] C. Pietraszuk, M. Kubicki, CCDC 1031958: Experimental Crystal Structure Determination, CSD Commun. (2018), https://doi.org/10.5517/ccdc.csd.cc13mtzj.
[107] J.R. Herron, Z.T. Ball, Synthesis and Reactivity of Functionalized Arylcopper Compounds by Transmetalation of Organosilanes, J. Am. Chem. Soc. 130 (2008) 16486–16487, https://doi.org/10.1021/ja8070804.
[108] L. Kuehn, A.F. Eichhorn, D. Schmidt, T.B. Marder, U. Radius, NHC-stabilized copper(I) aryl complexes and their transmetalation reaction with aryl halides, J. Organomet. Chem. 919 (2020) 121249, https://doi.org/10.1016/j.jorganchem.2020.121249.
[109] J.R. Herron, V. Russo, E.J. Valente, Z.T. Ball, Catalytic Organocopper Chemistry from Organosiloxane Reagents, Chem. Eur. J. 15 (2009) 8713–8716, https://doi.org/10.1002/chem.200901438.
[110] T. Fujihara, T. Xu, K. Semba, J. Terao, Y. Tsuji, Copper-Catalyzed Hydrocarboxylation of Alkynes Using Carbon Dioxide and Hydrosilanes, Angew. Chem. Int. Ed. 50 (2011) 523–527, https://doi.org/10.1002/anie.201006292.
[111] J. Zhai, A.S. Filatov, G.L. Hillhouse, M.D. Hopkins, Synthesis, structure, and reactions of a copper–sulfido cluster comprised of the parent Cu_2S unit: {(NHC)Cu}$_2$(μ-S), Chem. Sci. 7 (2016) 589–595, https://doi.org/10.1039/C5SC03258J.
[112] S. Wu, W. Zeng, Q. Wang, F.-X. Chen, Asymmetric trifluoromethylation of aromatic aldehydes by cooperative catalysis with (IPr)CuF and quinidine-derived quaternary ammonium salt, Org. Biomol. Chem. 10 (2012) 9334, https://doi.org/10.1039/c2ob26827b.
[113] T. Vergote, F. Nahra, A. Welle, M. Luhmer, J. Wouters, N. Mager, O. Riant, T. Leyssens, Unprecedented Copper(I) Bifluoride Complexes: Synthesis, Characterization and Reactivity, Chem. Eur. J. 18 (2012) 793–798, https://doi.org/10.1002/chem.201102655.
[114] J.W. Hall, F. Seeberger, M.F. Mahon, M.K. Whittlesey, (carbene)CuF Complexes Featuring Bulky Arduengo-Type, Ring-Expanded, and Cyclic (Alkyl)(amino) carbenes: Applications in Catalytic Aldehyde Allylation, Organometallics 39 (2020) 227–233, https://doi.org/10.1021/acs.organomet.9b00772.
[115] M. Riethmann, S.A. Föhrenbacher, H. Keiling, N.V. Ignat'ev, M. Finze, U. Radius, Fluoride Abstraction Induced by Tris(pentafluoroethyl)difluorophosphorane: A Convenient Way to Synthesize Cationic *N*-Heterocyclic Carbene- and Cyclic (Alkyl) (amino)carbene-Ligated Copper Alkyne and Arene Complexes, Inorg. Chem. 63 (2024) 8351–8365, https://doi.org/10.1021/acs.inorgchem.4c00750.
[116] L.S. Sharninghausen, A.F. Brooks, W.P. Winton, K.J. Makaravage, P.J.H. Scott, M. S. Sanford, NHC-Copper Mediated Ligand-Directed Radiofluorination of Aryl Halides, J. Am. Chem. Soc. 142 (2020) 7362–7367, https://doi.org/10.1021/jacs.0c02637.
[117] C.M. Wyss, B.K. Tate, J. Bacsa, M. Wieliczko, J.P. Sadighi, Dinuclear μ-fluoro cations of copper, silver and gold, Polyhedron 84 (2014) 87–95, https://doi.org/10.1016/j.poly.2014.06.039.
[118] A.M. Suess, M.R. Uehling, W. Kaminsky, G. Lalic, Mechanism of Copper-Catalyzed Hydroalkylation of Alkynes: An Unexpected Role of Dinuclear Copper Complexes, J. Am. Chem. Soc. 137 (2015) 7747–7753, https://doi.org/10.1021/jacs.5b03086.
[119] D.J. O'Hearn, R.D. Singer, Direct Synthesis of a Copper(II) N-Heterocyclic Carbene Complex in Air, Organometallics 36 (2017) 3175–3177, https://doi.org/10.1021/acs.organomet.7b00489.
[120] C. Dash, A. Das, M. Yousufuddin, H.V.R. Dias, Isolable, Copper(I) Dicarbonyl Complexes Supported by *N*-Heterocyclic Carbenes, Inorg. Chem. 52 (2013) 1584–1590, https://doi.org/10.1021/ic302455y.
[121] B.K. Tate, J.T. Nguyen, J. Bacsa, J.P. Sadighi, Heterolysis of Dihydrogen by Silver Alkoxides and Fluorides, Chem. Eur. J. 21 (2015) 10160–10169, https://doi.org/10.1002/chem.201500870.
[122] D.S. Laitar, P. Müller, T.G. Gray, J.P. Sadighi, A Carbene-Stabilized Gold(I) Fluoride: Synthesis and Theory, Organometallics 24 (2005) 4503–4505, https://doi.org/10.1021/om050619f.
[123] N.T. Daugherty, T.J. Robilotto, J. Bacsa, T.G. Gray, J.P. Sadighi, A trigold carbide cation stabilized as a labile pyridine adduct, Polyhedron 181 (2020) 114464, https://doi.org/10.1016/j.poly.2020.114464.
[124] P. de Frémont, N. Marion, S.P. Nolan, Cationic NHC–gold(I) complexes: Synthesis, isolation, and catalytic activity, J. Organomet. Chem. 694 (2009) 551–560, https://doi.org/10.1016/j.jorganchem.2008.10.047.
[125] R.M.P. Veenboer, A. Collado, S. Dupuy, T. Lebl, L. Falivene, L. Cavallo, D. B. Cordes, A.M.Z. Slawin, C.S.J. Cazin, S.P. Nolan, Inner-Sphere versus Outer-Sphere Coordination of BF_4^- in a NHC-Gold(I) Complex, Organometallics 36 (2017) 2861–2869, https://doi.org/10.1021/acs.organomet.7b00345.
[126] N.P. Mankad, F.D. Toste, C−C Coupling Reactivity of an Alkylgold(III) Fluoride Complex with Arylboronic Acids, J. Am. Chem. Soc. 132 (2010) 12859–12861, https://doi.org/10.1021/ja106257n.
[127] N.P. Mankad, F.D. Toste, C(sp^3)–F reductive elimination from alkylgold(III) fluoride complexes, Chem. Sci. 3 (2012) 72–76, https://doi.org/10.1039/C1SC00515D.
[128] E. Tkatchouk, N.P. Mankad, D. Benitez, W.A. Goddard, F.D. Toste, Two Metals Are Better Than One in the Gold Catalyzed Oxidative Heteroarylation of Alkenes, J. Am. Chem. Soc. 133 (2011) 14293–14300, https://doi.org/10.1021/ja2012627.
[129] F. Nahra, S.R. Patrick, D. Bello, M. Brill, A. Obled, D.B. Cordes, A.M.Z. Slawin, D. O'Hagan, S.P. Nolan, Hydrofluorination of Alkynes Catalysed by Gold Bifluorides, ChemCatChem 7 (2015) 240–244, https://doi.org/10.1002/cctc.201402891.
[130] M.A. Ellwanger, S. Steinhauer, P. Golz, T. Braun, S. Riedel, Stabilization of Lewis Acidic AuF_3 as an N-Heterocyclic Carbene Complex: Preparation and Characterization of [AuF_3(SIMes)], Angew. Chem. Int. Ed. 57 (2018) 7210–7214, https://doi.org/10.1002/anie.201802952.
[131] M.A. Ellwanger, C. von Randow, S. Steinhauer, Y. Zhou, A. Wiesner, H. Beckers, T. Braun, S. Riedel, Tuning the Lewis acidity of difluorido gold(III) complexes: the synthesis of [$AuClF_2$(SIMes)] and [AuF_2($OTeF_5$)(SIMes)], Chem. Commun. 54 (2018) 9301–9304, https://doi.org/10.1039/C8CC05233F.
[132] M. Winter, N. Limberg, M.A. Ellwanger, A. Pérez-Bitrián, K. Sonnenberg, S. Steinhauer, S. Riedel, Trifluoromethylation of [AuF_3(SIMes)]: Preparation and Characterization of [$Au(CF_3)_xF_{3-x}$(SIMes)] (x= 1–3) Complexes, Chem. Eur. J. 26 (2020) 16089–16097, https://doi.org/10.1002/chem.202002940.
[133] M. Winter, M.A. Ellwanger, N. Limberg, A. Pérez-Bitrián, P. Voßnacker, S. Steinhauer, S. Riedel, Reactivity of [AuF_3(SIMes)]: Pathway to Unprecedented Structural Motifs, Chem. Eur. J. 29 (2023), https://doi.org/10.1002/chem.202301684.
[134] S.G. Rachor, R. Müller, M. Kaupp, T. Braun, Hydrogen and Halogen Bonding to Au (I) Fluorido Complexes, Eur. J. Inorg. Chem. 26 (2023), https://doi.org/10.1002/ejic.202200668.
[135] G. Kleinhans, A.K.-W. Chan, M.-Y. Leung, D.C. Liles, M.A. Fernandes, V.W.-W. Yam, I. Fernández, D.I. Bezuidenhout, Synthesis and Photophysical Properties of T-Shaped Coinage-Metal Complexes, Chem. Eur. J. 26 (2020) 6993–6998, https://doi.org/10.1002/chem.202000726.
[136] H. Valdés, N. Alpuente, P. Salvador, A.S.K. Hashmi, X. Ribas, CCC-NHC Au(III) pincer complexes as a reliable platform for isolating elusive species, Chem. Sci. 15 (2024) 17618–17628, https://doi.org/10.1039/D4SC02999B.
[137] N. Kuhn, G. Henkel, T. Kratz, J. Kreutzberg, R. Boese, A.H. Maulitz, Derivate des Imidazols, VI. Stabile Carben-Borane, Chem. Ber. 126 (1993) 2041–2045, https://doi.org/10.1002/cber.19931260913.
[138] N. Kuhn, R. Fawzi, H. Kotowski, M. Steimann, Crystal structure of the di(2,3,4,5-tetramethylimidazol-2-ylidene trifluoroborane) toluene solvate, 2($C_7H_{12}BF_3N_2$)·$C_6H_5CH_3$, Z. fur Krist, New Cryst. Struct. 212 (1997) 259–260, https://doi.org/10.1524/ncrs.1997.212.1.259.
[139] A.J. Arduengo III, F. Davidson, R. Krafczyk, W.J. Marshall, R. Schmutzler, Carbene Complexes of Pnictogen Pentafluorides and Boron Trifluoride, Monatsh. Chem. 131 (2000) 0251–0265, https://doi.org/10.1007/s007060070101.
[140] C. Pranckevicius, D.W. Stephan, Ruthenium Complexes of an Abnormally Bound, Anionic N-Heterocyclic Carbene, Chem. Eur. J. 20 (2014) 6597–6602, https://doi.org/10.1002/chem.201402080.
[141] N. Parvin, N. Sen, P.V. Muhasina, S. Tothadi, P. Parameswaran, S. Khan, The diverse reactivity of $NOBF_4$ towards silylene, disilene, germylene and stannylene, Chem. Commun. 57 (2021) 5008–5011, https://doi.org/10.1039/D1CC01034D.
[142] M. Bolte, F. Schödel, H.-W. Lerner, CCDC 2010795: Experimental Crystal Structure Determination, CSD Commun. (2020), https://doi.org/10.5517/ccdc.csd.cc25hdcg.
[143] A. Solovyev, E. Lacôte, D.P. Curran, Ring Lithiation and Functionalization of Imidazol-2-ylidene-boranes, Org. Lett. 13 (2011) 6042–6045, https://doi.org/10.1021/ol202516c.
[144] D.N. Lastovickova, C.W. Bielawski, Diamidocarbene Induced B–H Activation: A New Class of Initiator-Free Olefin Hydroboration Reagents, Organometallics 35 (2016) 706–712, https://doi.org/10.1021/acs.organomet.5b00997.
[145] A. Winkler, M. Freytag, P.G. Jones, M. Tamm, Preparation and reactivity of an isolable *N*-heterocyclic carbene–borane, J. Organomet. Chem. 775 (2015) 164–168, https://doi.org/10.1016/j.jorganchem.2014.04.037.
[146] P.G. Jones, M. Freytag, A. Winkler, M. Tamm, CCDC 2282956: Experimental Crystal Structure Determination, CSD Commun. (2023), https://doi.org/10.5517/ccdc.csd.cc2gmlrg.
[147] P.G. Jones, M. Freytag, A. Winkler, M. Tamm, CCDC 2282952: Experimental Crystal Structure Determination, CSD Commun. (2023), https://doi.org/10.5517/ccdc.csd.cc2gmlmb.
[148] P.G. Jones, M. Freytag, M. Silva Valverde, M. Tamm, CCDC 2282984: Experimental Crystal Structure Determination, CSD Commun, 2023, https://doi.org/10.5517/ccdc.csd.cc2gmmnd.
[149] P.G. Jones, M. Freytag, M. Silva Valverde, M. Tamm, CCDC 2282987: Experimental Crystal Structure Determination, CSD Commun, 2023, https://doi.org/10.5517/ccdc.csd.cc2gmmrh.
[150] P.G. Jones, M. Freytag, M. Silva Valverde, M. Tamm, CCDC 2282989: Experimental Crystal Structure Determination, CSD Commun, 2023, https://doi.org/10.5517/ccdc.csd.cc2gmmtk.
[151] P.G. Jones, M. Freytag, M. Silva Valverde, M. Tamm, CCDC 2282988: Experimental Crystal Structure Determination, CSD Commun, 2023, https://doi.org/10.5517/ccdc.csd.cc2gmmsj.
[152] P.G. Jones, M. Freytag, M. Silva Valverde, M. Tamm, CCDC 2282996: Experimental Crystal Structure Determination, CSD Commun, 2023, https://doi.org/10.5517/ccdc.csd.cc2gmn1t.
[153] J. Monot, L. Fensterbank, M. Malacria, E. Lacôte, S.J. Geib, D.P. Curran, CAAC Boranes Synthesis and characterization of cyclic (alkyl) (amino) carbene borane complexes from BF_3 and BH_3, Beilstein J. Org. Chem. 6 (2010) 709–712, https://doi.org/10.3762/bjoc.6.82.
[154] K.K. Manar, V.K. Porwal, R.S. Kamte, M. Adhikari, S.K. Thakur, D. Bawari, A. R. Choudhury, S. Singh, Reactions of a BICAAC with hydroboranes: propensity for Lewis adduct formation and carbene insertion into the B–H bond, Dalton Trans. 48 (2019) 17472–17478, https://doi.org/10.1039/C9DT03382C.
[155] K. Chansaenpak, M. Wang, Z. Wu, R. Zaman, Z. Li, F.P. Gabbaï, [^{18}F]–NHC–BF_3 adducts as water stable radio-prosthetic groups for PET imaging, Chem. Commun. 51 (2015) 12439–12442, https://doi.org/10.1039/C5CC04545B.
[156] T. Böttcher, S. Steinhauer, L.C. Lewis-Alleyne, B. Neumann, H. Stammler, B. S. Bassil, G.-V. Röschenthaler, B. Hoge, NHC→$SiCl_4$: An Ambivalent Carbene-

Transfer Reagent, Chem. Eur. J. 21 (2015) 893–899, https://doi.org/10.1002/chem.201404628.
[157] Y. Yamaguchi, T. Kashiwabara, K. Ogata, Y. Miura, Y. Nakamura, K. Kobayashi, T. Ito, Synthesis and reactivity of triethylborane adduct of *N*-heterocyclic carbene: versatile synthons for synthesis of *N*-heterocyclic carbene complexes, Chem. Commun. (2004) 2160, https://doi.org/10.1039/b405459h.
[158] A.-F. Pécharman, M.S. Hill, C.L. McMullin, M.F. Mahon, $[BO_2]^-$ as a Synthon for the Generation of Boron-Centered Carbamate and Carboxylate Isosteres, Angew. Chem. Int. Ed. 59 (2020) 13628–13632, https://doi.org/10.1002/anie.202005674.
[159] D.J. Nielsen, K.J. Cavell, B.W. Skelton, A.H. White, Tetrafluoroborate anion B−F bond activation—unusual formation of a nucleophilic heterocyclic carbene:BF_3 adduct, Inorg. Chim. Acta. 352 (2003) 143–150, https://doi.org/10.1016/S0020-1693(03)00143-9.
[160] A.W. Taylor, K.R.J. Lovelock, R.G. Jones, P. Licence, Borane-substituted imidazol-2-ylidenes: syntheses *in vacuo*, Dalton Trans. 40 (2011) 1463, https://doi.org/10.1039/c0dt01240h.
[161] C.J. Clarke, S. Puttick, T.J. Sanderson, A.W. Taylor, R.A. Bourne, K.R.J. Lovelock, P. Licence, Thermal stability of dialkylimidazolium tetrafluoroborate and hexafluorophosphate ionic liquids: *ex situ* bulk heating to complement *in situ* mass spectrometry, Phys. Chem. Chem. Phys. 20 (2018) 16786–16800, https://doi.org/10.1039/C8CP01090K.
[162] C. Tian, W. Nie, M.V. Borzov, P. Su, High-Yield Thermolytic Conversion of Imidazolium Salts into Arduengo Carbene Adducts with BF_3 and PF_5, Organometallics 31 (2012) 1751–1760, https://doi.org/10.1021/om201086d.
[163] A.A. Danopoulos, P. Braunstein, N. Stylianides, M. Wesolek, Aminolysis of Bis[bis (trimethylsilyl)amido]iron and -cobalt as a Versatile Route to N-Heterocyclic Carbene Complexes, Organometallics 30 (2011) 6514–6517, https://doi.org/10.1021/om200951m.
[164] L. Dettling, N. Limberg, R. Küppers, D. Frost, M. Weber, N.T. Coles, D.M. Andrada, C. Müller, Phosphorus derivatives of mesoionic carbenes: synthesis and characterization of triazaphosphole-5-ylidene → BF_3 adducts, Chem. Commun. 59 (2023) 10243–10246, https://doi.org/10.1039/D3CC03268J.
[165] R.A. Rowsey, J.D. Hilgar, N.A. Romero, Silylimidazolium Hexafluorophosphate Salts as Synthetic Precursors to N-Heterocyclic Carbene Pentafluorophosphorus Adducts, Org. Lett. 26 (2024) 4750–4755, https://doi.org/10.1021/acs.orglett.4c01549.
[166] B.-M. Yang, K. Xiang, Y.-Q. Tu, S.-H. Zhang, D.-T. Yang, S.-H. Wang, F.-M. Zhang, Spiro-fused six-membered N-heterocyclic carbene: a new scaffold toward unique properties and activities, Chem. Commun. 50 (2014) 7163–7165, https://doi.org/10.1039/C4CC01627K.
[167] E.-J.Y. Boisvert, R. Ramos Castellanos, M.J. Ferguson, D.E. Fogg, Abstraction of Trifluoroborane from Tetrafluoroborate: Li^+-Assisted Borylation of Nucleophilic Carbenes, ChemCatChem 16 (2024), https://doi.org/10.1002/cctc.202401003.
[168] H. Wu, J.M. Garcia, F. Haeffner, S. Radomkit, A.R. Zhugralin, A.H. Hoveyda, Mechanism of NHC-Catalyzed Conjugate Additions of Diboron and Borosilane Reagents to *α,β*-Unsaturated Carbonyl Compounds, J. Am. Chem. Soc. 137 (2015) 10585–10602, https://doi.org/10.1021/jacs.5b06745.
[169] A.L. Gott, W.E. Piers, R. McDonald, M. Parvez, Synthesis of trifluoroborate functionalised imidazolium salts as precursors to weakly coordinating bidentate NHC ligands, Inorg. Chim. Acta. 369 (2011) 180–189, https://doi.org/10.1016/j.ica.2010.12.030.
[170] U. Siemeling, C. Färber, C. Bruhn, S. Fürmeier, T. Schulz, M. Kurlemann, S. Tripp, Group 10 Metal Complexes of a Ferrocene-Based N-Heterocyclic Carbene: Syntheses, Structures and Catalytic Applications, Eur. J. Inorg. Chem. 2012 (2012) 1413–1422, https://doi.org/10.1002/ejic.201100856.
[171] J. He, S. Wang, X.-F. Song, X. Chang, C. Zou, W. Lu, K. Li, Tetradentate carbene–anilido boron complexes: highly fluorescent dyes with larger Stokes shifts than BODIPY analogues, Chem. Commun. 60 (2024) 11524–11527, https://doi.org/10.1039/D4CC03944K.
[172] I.I. Padilla-Martínez, F.J. Martínez-Martínez, A. López-Sandoval, K.I. Girón-Castillo, M.A. Brito, R. Contreras, New Imidazabole Derivatives: Dimers of Carbene–Borane Adducts, Eur. J. Inorg. Chem. 1998 (1998) 1547–1553, https://doi.org/10.1002/(SICI)1099-0682(199810)1998:10<1547::AID-EJIC1547>3.3.CO;2-X.
[173] A. Solovyev, Q. Chu, S.J. Geib, L. Fensterbank, M. Malacria, E. Lacôte, D. P. Curran, Substitution Reactions at Tetracoordinate Boron: Synthesis of N-Heterocyclic Carbene Boranes with Boron−Heteroatom Bonds, J. Am. Chem. Soc. 132 (2010) 15072–15080, https://doi.org/10.1021/ja107025y.
[174] S. Aldridge, S.K. Callear, M.B. Hursthause, $C_{27}H_{36}BClF_2N_2$, University of Southampton, Crystal Structure Report, 2008, https://doi.org/10.5258/ecrystals/618.
[175] M. Makhlouf Brahmi, M. Malacria, D. Curran, L. Fensterbank, E. Lacôte, Substituent Effects in NHC-Boranes: Reactivity Switch in the Nucleophilic Fluorination of NHC-Boranes, Synlett 24 (2013) 1260–1262, https://doi.org/10.1055/s-0033-1338847.
[176] A. Röther, J.C. Farmer, F.L. Portwich, H. Görls, R. Kretschmer, Anion-Dependent Reactivity of Mono- and Dinuclear Boron Cations, Chem. Eur. J. 29 (2023), https://doi.org/10.1002/chem.202302544.
[177] P.G. Jones, C.-G. Daniliuc, A. Winkler, M. Tamm, CCDC 2053984: Experimental Crystal Structure Determination, CSD Commun. (2021), https://doi.org/10.5517/ccdc.csd.cc26ybk2.
[178] J.-K. Jin, W.-X. Zheng, H.-M. Xia, F.-L. Zhang, Y.-F. Wang, Regioselective Radical Hydroboration of *gem*-Difluoroalkenes: Synthesis of *α*-Borylated Organofluorines, Org. Lett. 21 (2019) 8414–8418, https://doi.org/10.1021/acs.orglett.9b03173.
[179] S. Nerkar, D.P. Curran, Synthesis and Suzuki Reactions of N-Heterocyclic Carbene Difluoro(aryl)-boranes, Org. Lett. 17 (2015) 3394–3397, https://doi.org/10.1021/acs.orglett.5b01101.
[180] D.A. Bolt, D.P. Curran, 1-Butyl-3-methylimidazol-2-ylidene Borane: A Readily Available, Liquid N-Heterocyclic Carbene Borane Reagent, J. Org. Chem. 82 (2017) 13746–13750, https://doi.org/10.1021/acs.joc.7b02730.
[181] Y. Liu, J.-L. Li, X.-G. Liu, J.-Q. Wu, Z.-S. Huang, Q. Li, H. Wang, Radical Borylative Cyclization of Isocyanoarenes with N-Heterocyclic Carbene Borane: Synthesis of Borylated Aza-arenes, Org. Lett. 23 (2021) 1891–1897, https://doi.org/10.1021/acs.orglett.1c00309.
[182] P.-J. Xia, Z.-P. Ye, Y.-Z. Hu, J.-A. Xiao, K. Chen, H.-Y. Xiang, X.-Q. Chen, H. Yang, Photocatalytic C–F Bond Borylation of Polyfluoroarenes with NHC-boranes, Org. Lett. 22 (2020) 1742–1747, https://doi.org/10.1021/acs.orglett.0c00020.
[183] Q.-J. Pan, Y.-Q. Miao, H.-J. Cao, Z. Liu, X. Chen, Visible Light-Induced 1,2-Diphenyldisulfane-Mediated Defluoroborylation of Polyfluoroarenes, J. Org. Chem. 89 (2024) 5049–5059, https://doi.org/10.1021/acs.joc.4c00286.
[184] F. Xie, Z. Mao, D.P. Curran, H. Liang, W. Dai, Facile Borylation of Alkenes, Alkynes, Imines, Arenes and Heteroarenes with *N*-Heterocyclic Carbene-Boranes and a Heterogeneous Semiconductor Photocatalyst, Angew. Chem. Int. Ed. 62 (2023), https://doi.org/10.1002/anie.202306846.
[185] W. Xu, H. Jiang, J. Leng, H.-W. Ong, J. Wu, Visible-Light-Induced Selective Defluoroborylation of Polyfluoroarenes, *gem*-Difluoroalkenes, and Trifluoromethylalkenes, Angew. Chem. Int. Ed. 59 (2020) 4009–4016, https://doi.org/10.1002/anie.201911819.
[186] K. Takahashi, M. Shimoi, T. Watanabe, K. Maeda, S.J. Geib, D.P. Curran, T. Taniguchi, Revisiting Polyfluoroarenes as Radical Acceptors: Radical C–F Bond Borylation of Polyfluoroarenes with N-Heterocyclic Carbene Boranes and Synthesis of Borane-Containing Liquid Crystals, Org. Lett. 22 (2020) 2054–2059, https://doi.org/10.1021/acs.orglett.0c00481.
[187] M. Shimoi, K. Maeda, S.J. Geib, D.P. Curran, T. Taniguchi, Esters as Radical Acceptors: β-NHC-Borylalkenyl Radicals Induce Lactonization by C−C Bond Formation/Cleavage on Esters, Angew. Chem. Int. Ed. 58 (2019) 6357–6361, https://doi.org/10.1002/anie.201902001.
[188] S.-C. Ren, F.-L. Zhang, J. Qi, Y.-S. Huang, A.-Q. Xu, H.-Y. Yan, Y.-F. Wang, Radical Borylation/Cyclization Cascade of 1,6-Enynes for the Synthesis of Boron-Handled Hetero- and Carbocycles, J. Am. Chem. Soc. 139 (2017) 6050–6053, https://doi.org/10.1021/jacs.7b01889.
[189] Y. Duan, Z. Zheng, Z. Yu, S. Sun, B. Lin, X. Liu, P. Liu, Catalyst-Free *α-trans*-Selective Hydroboration and (*E*)-Selective Deuterated Semihydrogenation of Alkynyl Sulfones, J. Org. Chem. 89 (2024) 8326–8333, https://doi.org/10.1021/acs.joc.3c02833.
[190] Z.-L. Chen, C. Empel, Y. Xie, R.M. Koenigs, J. Xuan, Photocatalytic Direct Borylation of Benzothiazole Heterocycles via a Triplet Activation Strategy, Org. Lett. 27 (2025) 892–897, https://doi.org/10.1021/acs.orglett.4c04667.
[191] X. Wu, Y. Wang, M.-X. Zhou, Z. Chen, X. Peng, Z. Wang, Y.-F. Zeng, Switchable Access to Mono- and Di-Alkylated Boranes via Visible-Light-Induced Hydroboration of Alkenes with NHC-Borane, Adv. Synth. Catal. 365 (2023) 3824–3829, https://doi.org/10.1002/adsc.202300863.
[192] Y.-S. Huang, J. Wang, W.-X. Zheng, F.-L. Zhang, Y.-J. Yu, M. Zheng, X. Zhou, Y.-F. Wang, Regioselective radical hydroboration of electron-deficient alkenes: synthesis of α-boryl functionalized molecules, Chem. Commun. 55 (2019) 11904–11907, https://doi.org/10.1039/C9CC06506G.
[193] S.-C. Ren, F.-L. Zhang, A.-Q. Xu, Y. Yang, M. Zheng, X. Zhou, Y. Fu, Y.-F. Wang, Regioselective radical α-borylation of α,β-unsaturated carbonyl compounds for direct synthesis of α-borylcarbonyl molecules, Nat. Commun. 10 (2019) 1934, https://doi.org/10.1038/s41467-019-09825-3.
[194] J.E. Radcliffe, V. Fasano, R.W. Adams, P. You, M.J. Ingleson, Reductive α-borylation of α,β-unsaturated esters using NHC–BH_3 activated by I_2 as a metal-free route to α-boryl esters, Chem. Sci. 10 (2019) 1434–1441, https://doi.org/10.1039/C8SC04305A.
[195] Z.-L. Chen, C. Empel, K. Wang, P.-P. Wu, B.-G. Cai, L. Li, R.M. Koenigs, J. Xuan, Enabling Cyclopropanation Reactions of Imidazole Heterocycles via Chemoselective Photochemical Carbene Transfer Reactions of NHC-Boranes, Org. Lett. 24 (2022) 2232–2237, https://doi.org/10.1021/acs.orglett.2c00609.
[196] W. Xie, M. Hayashi, R. Matsubara, Borylfuroxans: Synthesis and Applications, Org. Lett. 23 (2021) 4317–4321, https://doi.org/10.1021/acs.orglett.1c01250.
[197] D.A. Bolt, S.J. Geib, D.P. Curran, Synthesis and characterization of N-heterocyclic carbene complexes of 1,3,2-dioxaborolane-4,5-dione (NHC-boryl oxalates), Tetrahedron 74 (2018) 6961–6965, https://doi.org/10.1016/j.tet.2018.10.031.
[198] B. Su, Y. Li, R. Ganguly, J. Lim, R. Kinjo, Isolation and Reactivity of 1,4,2-Diazaborole, J. Am. Chem. Soc. 137 (2015) 11274–11277, https://doi.org/10.1021/jacs.5b07823.
[199] D. Subervie, B. Graff, S. Nerkar, D.P. Curran, J. Lalevée, E. Lacôte, Difluorination at Boron Leads to the First Electrophilic Ligated Boryl Radical (NHC-BF_2), Angew. Chem. Int. Ed. 57 (2018) 10251–10256, https://doi.org/10.1002/anie.201806476.
[200] L. Kuehn, M. Stang, S. Würtemberger-Pietsch, A. Friedrich, H. Schneider, U. Radius, T.B. Marder, FBpin and its adducts and their role in catalytic borylations, Faraday Discuss. 220 (2019) 350–363, https://doi.org/10.1039/C9FD00053D.
[201] I. Avinash, S. Parveen, G. Anantharaman, Backbone Boron-Functionalized Imidazoles/Imidazolium Salts: Synthesis, Structure, Metalation Studies, and Fluoride Sensing Properties, Inorg. Chem. 59 (2020) 5646–5661, https://doi.org/10.1021/acs.inorgchem.0c00348.

[202] V. Pattathil, C. Pranckevicius, Aromaticity transfer in an annulated 1,4,2-diazaborole: facile access to C_s symmetric 1,4,2,5-diazadiborinines, Chem. Commun. 60 (2024) 7705–7708, https://doi.org/10.1039/D4CC02414A.
[203] C. Chen, C.G. Daniliuc, S. Klabunde, M.R. Hansen, G. Kehr, G. Erker, Generation of boryl-nitroxide radicals from a boraalkene *via* the nitroso ene reaction, Chem. Sci. 13 (2022) 10891–10896, https://doi.org/10.1039/D2SC02485C.
[204] L. Kong, W. Lu, Y. Li, R. Ganguly, R. Kinjo, Azaborabutadienes: Synthesis by Metal-Free Carboboration of Nitriles and Utility as Building Blocks for B,N-Heterocycles, Angew. Chem. Int. Ed. 55 (2016) 14718–14722, https://doi.org/10.1002/anie.201608994.
[205] L. Kong, W. Lu, L. Yongxin, R. Ganguly, R. Kinjo, Formation of Boron–Main-Group Element Bonds by Reactions with a Tricoordinate Organoboron L_2PhB: (L = Oxazol-2-ylidene), Inorg. Chem. 56 (2017) 5586–5593, https://doi.org/10.1021/acs.inorgchem.6b02993.
[206] O. Chuzel, CCDC 1871388: Experimental Crystal Structure Determination, CSD Commun. (2018), https://doi.org/10.5517/ccdc.csd.cc20tbck.
[207] P. Tomar, T. Braun, E. Kemnitz, Preparation of NHC Stabilized Al(III)fluorides: Fluorination of [(SIMes)$AlMe_3$] with SF_4 or Me_3SnF, Eur. J. Inorg. Chem. 2019 (2019) 4735–4739, https://doi.org/10.1002/ejic.201900921.
[208] A. Merschel, Y.V. Vishnevskiy, B. Neumann, H.-G. Stammler, R.S. Ghadwal, Access to a *peri* -Annulated Aluminium Compound via C−H Bond Activation by a Cyclic Bis-Aluminylene, Chem. Eur. J. 30 (2024), https://doi.org/10.1002/chem.202400293.
[209] X. Zhang, L.L. Liu, Crystalline Neutral Aluminum Selenide/Telluride: Isoelectronic Aluminum Analogues of Carbonyls, J. Am. Chem. Soc. 145 (2023) 15729–15734, https://doi.org/10.1021/jacs.3c05954.
[210] X. Liu, S. Dong, J. Zhu, S. Inoue, Dialumene as a Dimeric or Monomeric Al Synthon for C–F Activation in Monofluorobenzene, J. Am. Chem. Soc. 146 (2024) 23591–23597, https://doi.org/10.1021/jacs.4c08171.
[211] S. Ju, C. Zhang, B. Tang, L.L. Liu, D.W. Stephan, Y. Wu, The Lewis superacidic aluminium cation: $[(NHC)Al(C_6F_5)_2]^+$, Chem. Commun. 60 (2024) 698–701, https://doi.org/10.1039/D3CC05440C.
[212] L. Werner, J. Hagn, J. Walpuski, U. Radius, Aluminum(III) Cations [(NHC)·$AlMes_2]^+$: Synthesis, Characterization, and Application in FLP-Chemistry, Angew. Chem. Int. Ed. 62 (2023), https://doi.org/10.1002/anie.202312111.
[213] C. Bour, J. Monot, S. Tang, R. Guillot, J. Farjon, V. Gandon, Structure, Stability, and Catalytic Activity of Fluorine-Bridged Complexes IPr·$GaCl_2(\mu$-F)EF_{n-1} (EF_n^- = SbF_6^-, PF_6^-, or BF_4^-), Organometallics 33 (2014) 594–599, https://doi.org/10.1021/om4012054.
[214] J.L. Bourque, K.M. Baines, Synthesis of Donor-Stabilized Organogallium Complexes En Route to a Gallene, Z. Anorg. Allg. Chem. 649 (2023), https://doi.org/10.1002/zaac.202200360.
[215] A. Merschel, S. Heda, Y.V. Vishnevskiy, B. Neumann, H.-G. Stammler, R. S. Ghadwal, Annulated carbocyclic gallylene and bis-gallylene with two-coordinated Ga(I) atoms, Chem. Sci. 16 (2025) 2222–2230, https://doi.org/10.1039/D4SC06782G.
[216] B. Michelet, J.-R. Colard-Itté, G. Thiery, R. Guillot, C. Bour, V. Gandon, Dibromoindium(III) cations as a π-Lewis acid: characterization of [IPr·$InBr_2$][SbF_6] and its catalytic activity towards alkynes and alkenes, Chem. Commun. 51 (2015) 7401–7404, https://doi.org/10.1039/C5CC00740B.
[217] R.S. Ghadwal, S.S. Sen, H.W. Roesky, G. Tavcar, S. Merkel, D. Stalke, Neutral Penta- and Hexacoordinate N-Heterocyclic Carbene Complexes Derived from SiX_4 (X = F, Br), Organometallics 28 (2009) 6374–6377, https://doi.org/10.1021/om9007696.
[218] F. Uhlemann, R. Köppe, A. Schnepf, Synthesis of Metastable $Si^{II}X_2$ Solutions (X = F, Cl). A Novel Binary Halide for Synthesis, Z, Anorg. Allg. Chem. 640 (2014) 1658–1664, https://doi.org/10.1002/zaac.201400122.
[219] P.G. Jones, H. Thonnessen, CCDC 611491: Experimental Crystal Structure Determination, CSD Commun. (2006), https://doi.org/10.5517/ccnj9jz.
[220] N. Graw, CCDC 2149531: Experimental Crystal Structure Determination, CSD Commun. (2022), https://doi.org/10.5517/ccdc.csd.cc2b4rqz.
[221] P.A. Rupar, M.C. Jennings, K.M. Baines, Synthesis and Structure of N-Heterocyclic Carbene Complexes of Germanium(II), Organometallics 27 (2008) 5043–5051, https://doi.org/10.1021/om800368d.
[222] T. Böttcher, B.S. Bassil, G.-V. Röschenthaler, Complexes of Ge(IV)- and Sn(IV)-Fluorides with Cyclic and Acyclic Carbenes: Bis(dialkylamino)-difluoromethylenes as Carbene Sources, Inorg. Chem. 51 (2012) 763–765, https://doi.org/10.1021/ic202008m.
[223] M. Göhner, F. Herrmann, N. Kuhn, M. Ströbele, $(Carb)_2SnF_4$ (Carb = 2, 3-Dihydro-1, 3-diisopropyl-4, 5-dimethylimidazol-2-yliden – ein Carbenkomplex des vierwertigen Zinns), Z. Anorg. Allg. Chem. 638 (2012) 2196–2199, https://doi.org/10.1002/zaac.201200353.
[224] P.A. Gray, N. Burford, Coordination complexes of pnictogen(V) cations, Coord. Chem. Rev. 324 (2016) 1–16, https://doi.org/10.1016/j.ccr.2016.05.010.
[225] A.J. Arduengo, R. Krafczyk, W.J. Marshall, R. Schmutzler, A Carbene−Phosphorus(V) Adduct, J. Am. Chem. Soc. 119 (1997) 3381–3382, https://doi.org/10.1021/ja964094h.
[226] B. Vabre, K. Chansaenpak, M. Wang, H. Wang, Z. Li, F.P. Gabbaï, Radiofluorination of a NHC–PF_5 adduct: toward new probes for ^{18}F PET imaging, Chem. Commun. 53 (2017) 8657–8659, https://doi.org/10.1039/C7CC04402J.
[227] S.A. Föhrenbacher, V. Zeh, M.J. Krahfuss, N.V. Ignat'ev, M. Finze, U. Radius, Tris (pentafluoroethyl)difluorophosphorane and *N* -Heterocyclic Carbenes: Adduct Formation and Frustrated *Lewis* Pair Reactivity, Eur. J. Inorg. Chem. 2021 (2021) 1941–1960, https://doi.org/10.1002/ejic.202100183.
[228] C. Tian, W. Nie, Q. Chen, G. Sun, J. Hu, M.V. Borzov, *C*- and *N*-Adducts of *N*-alkenyl substituted Arduengo carbene and *N*-alkyl substituted imidazole with PF_5: synthesis and structural investigation, Russ. Chem. Bull. 63 (2014) 2668–2674, https://doi.org/10.1007/s11172-014-0796-z.
[229] T. Böttcher, O. Shyshkov, M. Bremer, B.S. Bassil, G.-V. Röschenthaler, Carbene Complexes of Phosphorus(V) Fluorides by Oxidative Addition of 2,2-Difluorobis (dialkylamines) to Phosphorus(III) Halides, Organometallics 31 (2012) 1278–1280, https://doi.org/10.1021/om2009827.
[230] T. Böttcher, B.S. Bassil, L. Zhechkov, G.-V. Röschenthaler, Phosphorus(V) Complexes with Acyclic Monoaminocarbene Ligands via Oxidative Addition, Inorg. Chem. 52 (2013) 5651–5653, https://doi.org/10.1021/ic400756z.
[231] T. Böttcher, S. Steinhauer, N. Allefeld, B. Hoge, B. Neumann, H.G. Stammler, B. S. Bassil, M. Winter, N.W. Mitzel, G.-V. Röschenthaler, Carbene complexes of phosphorus(V) fluorides substituted with perfluoroalkyl-groups synthesized by oxidative addition. Cleavage of the complexes reveals a new synthetic protocol for ionic liquids, Dalton Trans. 43 (2014) 2979–2987, https://doi.org/10.1039/C3DT53043D.
[232] R. Pajkert, T. Böttcher, M. Ponomarenko, M. Bremer, G.-V. Röschenthaler, Synthesis and characterization of novel carbene complexes of phosphorus(V) fluorides with potential liquid-crystalline properties, Tetrahedron 69 (2013) 8943–8951, https://doi.org/10.1016/j.tet.2013.07.062.
[233] T. Böttcher, B.S. Bassil, L. Zhechkov, T. Heine, G.-V. Röschenthaler, (NHC^{Me})$SiCl_4$: a versatile carbene transfer reagent – synthesis from silicochloroform, Chem. Sci. 4 (2013) 77–83, https://doi.org/10.1039/C2SC21214E.
[234] M.H. Holthausen, M. Mehta, D.W. Stephan, The Highly Lewis Acidic Dicationic Phosphonium Salt: [(SIMes)$PFPh_2$][$B(C_6F_5)_4]_2$, Angew. Chem. Int. Ed. 53 (2014) 6538–6541, https://doi.org/10.1002/anie.201403693.
[235] M. Mehta, M.H. Holthausen, I. Mallov, M. Pérez, Z.-W. Qu, S. Grimme, D. W. Stephan, Catalytic Ketone Hydrodeoxygenation Mediated by Highly Electrophilic Phosphonium Cations, Angew. Chem. Int. Ed. 54 (2015) 8250–8254, https://doi.org/10.1002/anie.201502579.
[236] C.-X. Guo, J.J. Weigand, T.A.M. Gulder, CCDC 2051028: Experimental Crystal Structure Determination, Thesis (2021), https://doi.org/10.5517/ccdc.csd.cc26v86k.
[237] C.-X. Guo, J.J. Weigand, T.A.M. Gulder, CCDC 2051030: Experimental Crystal Structure Determination, Thesis (2021), https://doi.org/10.5517/ccdc.csd.cc26v88m.
[238] C.-X. Guo, J.J. Weigand, T.A.M. Gulder, CCDC 2051040: Experimental Crystal Structure Determination, Thesis (2021), https://doi.org/10.5517/ccdc.csd.cc26v8ly.
[239] M. Mehta, T.C. Johnstone, J. Lam, B. Bagh, A. Hermannsdorfer, M. Driess, D. W. Stephan, Synthesis and oxidation of phosphine cations, Dalton Trans. 46 (2017) 14149–14157, https://doi.org/10.1039/C7DT03175K.
[240] K. Schwedtmann, R. Schoemaker, F. Hennersdorf, A. Bauzá, A. Frontera, R. Weiss, J.J. Weigand, Cationic 5-phosphonio-substituted N-heterocyclic carbenes, Dalton Trans. 45 (2016) 11384–11396, https://doi.org/10.1039/C6DT01871H.
[241] M. Cicač-Hudi, S.H. Schlindwein, C.M. Feil, M. Nieger, D. Gudat, Isolable N-heterocyclic carbene adducts of the elusive diiodophosphine, Chem. Commun. 54 (2018) 7645–7648, https://doi.org/10.1039/C8CC03972K.
[242] U. Monkowius, M. Jachs Née Kriechbaum, G. Redhammer, R.F.J. Berger, The hare and the hedgehog – Similar thermal expansion of argento- and aurophilic contacts for different reasons, Z, Naturforsch. B 79 (2024) 723–728, https://doi.org/10.1515/znb-2024-0094.
[243] B. Ališ, A. Štefančič, G. Tavčar, Small molecule activation: SbF_3 auto-ionization supported by transfer and mesoionic NHC rearrangement, Dalton Trans. 46 (2017) 3338–3346, https://doi.org/10.1039/C6DT04909E.
[244] O. Coughlin, T. Krämer, S.L. Benjamin, Diverse structure and reactivity of pentamethylcyclopentadienyl antimony(III) cations, Dalton Trans. 49 (2020) 1726–1730, https://doi.org/10.1039/D0DT00024H.
[245] N. Kuhn, H. Bohnen, J. Fahl, D. Bläser, R. Boese, Derivate des Imidazols, XIX. Koordination oder Reduktion? Zur Reaktion von 1,3-Diisopropyl-4,5-dimethylimidazol-2-yliden mit Schwefelhalogeniden und Schwefeloxidhalogeniden, Chem. Ber. 129 (1996) 1579–1586, https://doi.org/10.1002/cber.19961291228.
[246] P. Komorr, M. Olaru, E. Hupf, S. Mebs, J. Beckmann, Donor Acceptor Complexes between the Chalcogen Fluorides SF_2, SeF_2, SeF_4 and TeF_4 and an N-Heterocyclic Carbene, Chem. Eur. J. 28 (2022), https://doi.org/10.1002/chem.202201023.